On the contribution of Tau phosphorylation to nuclear and cytoplasmic changes in human neuroblastoma cells

By

Parisa Tabeshmehr

A Thesis submitted to the Faculty of Graduate Studies of The University of Manitoba
in partial fulfilment of the requirements of the degree of

MASTER OF SCIENCE

Department of Physiology and Pathophysiology

Rady Faculty of Health Sciences

University of Manitoba

Winnipeg

Canada

Abstract

Human tauopathies are characterized by intracellular aggregation of hyperphosphorylated tau protein in neurons. Tau is involved in many cellular functions through its association with microtubules and actin filaments. In tauopathies overstabilization of filamentous actin (f-actin) leads to invagination of nuclear envelope. An intricate protein layer known as Nuclear Lamina (NL) is located at the interface of inner layers of nuclear envelope and chromatin. NL is degraded after nuclear envelope invagination, resulting in aberrant gene expression and re-emergence of ancient retroviruses. It is not clear if inhibition of kinases involved in tau pathology can prevent NL invagination and its downstream events.

In this study, we first established that overexpression of full-length tau (FL-Tau) and the 35kDa C-terminal fragment (Tau35) in differentiated human neuroblastoma (dSH-SY5Y) cell lines enhanced nuclear lamina invagination and overstabilization of filamentous actin; however, these changes were significantly exacerbated in Tau35-overexpressing cells.

Application of two small molecule inhibitors of c-Jun N-terminal kinase (JNK) and glycogen synthase kinase-3β (GSK-3β) reduced the extent of damages in tau-overexpressing cells. JNK inhibitor significantly decreased NL invagination in dSH-SY5Y-FL-Tau and -Tau35 cells. Furthermore, GSK-3β inhibition alleviated f-actin overstabilization in dSH-SY5Y-FL-Tau cells. In conclusion, we identified that NL invagination and f-actin overstabilization could be modulated by inhibition of involving kinases in tauopathies.

Keywords: Tau, Tauopathy, Neurodegeneration, Alzheimer's disease, Dementia, Aging, MAPT, Cytoskeleton.

Acknowledgements

This thesis, along with my entire MSc journey, has been one of the most considerable steps of my career, and it could not have been completed without the support of my mentor and my family.

I would like to thank my supervisor for shaping me scientifically into the person who I am today. To Dr. Eftekhar Eftekharpour, it was a great pleasure and opportunity to work in your laboratory. Thank you for the details you have taught me, for arousing my curiosity about hidden parts of the project, for being understanding and for motivating me to keep going even when the project did not go according to the plan. I have learned that even those unexpected negative results or insurmountable problems are exactly the bright pathway to a new experience and knowledge.

I would like to thank my advisory committee, Prof. Soheila Karimi and Dr. Benjamin Lindsey. Thank you for your questions which allowed me to think critically and accurately. Thank you for your guidance and constructive feedbacks which helped me deal with the challenges much easier.

A huge thank you to my better half, my spouse, Dr. Mojtaba Hosseini. Thank you for constantly motivating me to pursue my career and go after what I want, no matter what. You were always there to console me when times were really tough. Thank you for keeping our beautiful life a peaceful and happy environment even with all those ups and downs you have had in your personal career. I could not be more appreciative.

I would like to thank my entire family. To my incredibly nurturing parents, you have always been my strength and inspiration. To my lovely mother who is the only one who knows what my heart sounds like from the inside. To my father, my rock, few people possess the considerate, unselfish,

loving heart that you have and even fewer are willing to give so much of themselves. To my brothers, Amir and Mohamad, thank you for always being my number-one cheerleaders.

I would additionally like to acknowledge my colleagues, Dr. Md Imamul Islam and Shakila Sultana for teaching me the new techniques and their incredible ideas in troubleshooting the experiments. Another thanks to Tetiana Shcholok for her help around the lab. Thank you to all past and present members of "Neuroredoxin Lab".

This MSc program as a unique academic journey allowed me to discover my capabilities and expand my comfort zone. I learned how to abide by the common principles of research and deal with challenges that had no obvious solutions. I also learned, to succeed you must be consistent in your approach, have a plan and stick to it. As a team player, your research team needs to rely on you and plan accordingly. It has been well stated by John Green, the American author in explanation of science "What I love about science is that as you learn, you don't really get answers. You just get better questions."

Dedication

This thesis is wholeheartedly dedicated to my spouse, Mojtaba, who has been a constant source of support and encouragement since the very first day we met.

The person who has been the source of inspiration for his perseverance, dedication and consistency in his research.

The real supporter who has been always there for me
especially during the challenges of graduate
school and immigration.

I am truly thankful for having you in my life.

.

Table of contents

Abstract ii

Acknowledgements iii

Dedication v

Abbreviations xii

Contribution xiv

1 Chapter I: Introduction 1

1.1 Tauopathies, Types and Importance 1

1.2 Tau 2

1.3 Physiologic Tau 4

1.4 Pathologic tau 7

1.4.1 One protein and various conformers 8

1.4.2 Abnormal post-translational modifications of tau 9

1.4.3 Inducers of pathologic tau, upstream mechanisms of tau dysfunction 12

1.4.4 Pathologic tau and cell toxicity, downstream events of tau dysfunction 14

1.5 Diagnosis and therapeutic strategies for tauopathies 17

1.6 Summary and Conclusion 23

1.7 Study rational, hypothesis and research objectives 24

1.7.1 Study Rational 24

1.7.2 Hypothesis 25

1.7.3 Research Objectives 25

2 Chapter II: Materials & Methods 27

2.1 Materials 27

2.2 Methods 32

2.2.1 Plasmids 32

2.2.2 Generation of stable tau-expressing SH-SY5Y cell line 33

2.2.3 Cell culture 34

2.2.4 Neuronal differentiation of stable SH-SY5Y cells (dSH-SY5Y) 35

2.2.5 Cell treatments and determination of cell viability 35

2.2.6 Inhibition of protein kinases 35

2.2.7 Immunoblotting 36

2.2.8 Immunocytochemistry 37

2.2.9 DNA Methylation Assessment 38

2.2.9.2 LINE-1 Bisulfate Pyrosequencing 38
2.2.10 Data Analysis 39
2.2.10.2 Image Analysis 41
2.2.10.3 Statistical Analysis 42
3 Chapter III: Results 43
3.1 Retinoic Acid treatment induces neuronal-like phenotypes in SH-SY5Y cells. 43
3.2 SH-SY5Y cells can express high levels of FL-Tau and Tau35 by transient transfection 45
3.3 Tau phosphorylation levels did not increase significantly in this cellular model of tauopathy. 49
3.4 Autophagy-lysosomal pathway was unaffected in pSH-SY5Y and dSH-SY5Y tauopathy model 51
3.5 Tau35 overexpression is associated with exacerbated cytoskeletal and nucleoskeletal alterations. 54
3.5.1 Overexpression of Tau35 in dSH-SY5Y neurons exacerbates nuclear lamina invagination. 54
3.5.2 Nuclear lamina invagination after FL-Tau and Tau35 overexpression is not associated with nuclear Lamin-B protein degradation. 56
3.5.3 FL-Tau and Tau35 overexpression adversely affects f-actin distribution in dSH-SY5Y cells 57
3.6 Nuclear lamina invagination in tau constructs overexpressing cells is not associated with chromatin changes. 60
3.6.1 FL-Tau and Tau35 overexpression did not correlate with double-strand breakage in DNA 60
3.6.2 FL-Tau and Tau35 overexpression did not epigenetically affect SH-SY5Y cells 61
3.7 Pharmacological interventions to inhibit tauopathy-related characteristics in SH-SY5Y-derived model of tauopathy 63
3.8 Administration of inhibitors did not alter tau phosphorylation significantly. 64
3.9 JNK inhibition can reduce nuclear envelope invagination in dSH-SY5Y cells. 67
3.10 JNK and GSK-3β inhibition significantly attenuated f-actin distribution in FL-dSH-SY5Y cells. 70
4 Chapter IV: Discussion 73
4.1 Inducing overexpression of FL-Tau and Tau35 in neuroblastoma cells may mimic some characteristics of tau pathology. 73
4.2 Overexpression of FL-Tau and Tau35 disrupts cellular mechanotransduction in dSH-SY5Y cells. 75
4.3 Inhibition of JNK is associated with reduced actin over-stabilization and nuclear lamina damage in dSH-ST5Y cell. 77
4.4 Inhibition of GSK-3β correlates with reduced actin over-stabilization in FL-Tau overexpressing cells. 78
4.5 Conclusion 79

4.6 Limitation and future direction 80
5 References 82

List of figures

Figure 1-1: Human-specific tau isoforms 4

Figure 1-2: Tauopathies are classified according the presence of 3R and 4R isoforms in tau inclusions[12]. 9

Figure 1-4: Proportion of PTMs on tau protein according to the number of targeted residues in tau 2N4R isoform[12]. 11

Figure 1-5: Pathogenic tau, upstream and downstream events 17

Figure 1-6: Tau-related therapeutic interventions 20

Figure 2-1: Plasmids 33

Figure 2-2: Quantification of tau expression levels in transfected cells and the control group. 40

Figure 2-3: Quantification of tau phosphorylation levels in transfected cells. 41

Figure 2-4: Quantification of f-actin distribution. 42

Figure 3-1: Retinoic Acid treatment induces neuronal-like phenotypes in SH-SY5Y cells. 44

Figure 3-2: Differentiation of SH-SY5Y cells with retinoic acid (RA). 46

Figure 3-3: Higher Tau expression has been detected in the transfected groups compared to the controls. 48

Figure 3-4: The effect of FL-Tau and Tau35 overexpression on tau phosphorylation 50

Figure 3-5: The effect of FL-Tau and Tau35 overexpression on tau phosphorylation in CHO cells. 51

Figure 3-6: Autophagosome clearance was not affected in this cellular model of tauopathy model. 52

Figure 3-7: Tau35 overexpression enhances lysosomal activity in comparison with Tau-FL and control proliferative SH-SY5Y cells. 53

Figure 3-8: No evidence of increased lysosomal synthesis was observed in FL and Tau35 overexpressing pSH-SY5Y cells. 54

Figure 3-9: Tau overexpression is associated with increased nuclear lamina invagination in dSH-SY5Y cells 56

Figure 3-10: Nuclear lamina invagination in FL-Tau / Tau35 overexpression does not induce Lamin-B1 proteolytic degradation in SH-SY5Y cells. 57
Figure 3-11: Tau overexpression is associated with alterations in f-actin distribution in dSH-SY5Y cells. 58
Figure 3-12: Tau overexpression is associated with f-actin over-stabilization in dSH-SY5Y cells. 59
Figure 3-13: Overexpressing FL-Tau or Tau35 in dSH-SY5Y cells do not show evidence of enhanced DNA damage. 61
Figure 3-14: No epigenetic alteration has been detected in the experimental models. Overexpression of tau or its pathologic fragment did not result in any detectable DNA methylation in proliferating (a) or differentiated (b) SH-SY5Y cells. 62
Figure 3-15: Global DNA methylation is not significantly changed in FL-Tau and Tau35 overexpression. 63
Figure 3-16: JNK inhibitor (SP600125) and GSK3-β inhibitor (AR-A014418) cell toxicity assessment.. 64
Figure 3-17 JNK inhibition had no significant effect on tau phosphorylation levels in the experimental groups. 65
Figure 3-18 GSK3-β inhibition had no significant effect on tau phosphorylation levels in the experimental groups. 66
Figure 3-19 JNK and GSK3-β inhibition did not reduce PHF-1 phosphorylation levels in dSH-SY5Y cells..... 67
Figure 3-20: JNK inhibition can attenuate nuclear envelope invagination in dSH-SY5Y cells. 70
Figure 3-21: JNK and GSK-3β inhibition significantly attenuated f-actin distribution in FL-dSH-SY5Y cells..... 72

List of tables

Table 1-1: Recent preclinical and clinical therapeutic interventions for tauopathies. 23

Table 2-1: Reagents, buffers and kits used in this project..... 29

Table 2-2: Primary and secondary antibodies used in this project..... 32

Table 2-3: PCR-specific primers for human LINE-1 39

List of abbreviations

Alzheimer's disease (AD)
Ammonium persulphate (APS)
Amyloid β (Aβ)
Analyses of variance (ANOVA)
Antisense oligonucleotides (ASOs)
Argyrophilic grain disease (AGD)
Blood brain barrier (BBB)
Bovine serum albumin (BSA)
c- JNK interacting protein 1(JIP-1)
c-JUN N-terminal kinase (JNK)
Caspase-6 (CASP6)
Cathepsin L (CTSL)
Central nervous system (CNS)
Cerebrospinal fluid (CSF)
Chinese hamster ovary (CHO)
Chronic traumatic encephalopathy (CTE)
Corticobasal degeneration (CBD)
Cyclin-dependent-like kinase 5 (CDK5)
Digital PCR (dPCR)
Dihydroartemisinin (DHA)
Dityrosine (DiY)
Dulbecco's modified Eagle's medium (DMEM)
Dysfunction of autophagy-lysosomal pathway (ALP)
Epigallocatechin-3-gallate (EGCG)
Ethylenediaminetetraacetic acid (EDTA)
Fetal bovine serum (FBS)
Frontotemporal lobar degeneration (FTLD)
Glycogen synthase kinase-3β (GSK3β)
Lamin B1 (LB1)
Leucine-rich repeat kinase 2 (LRRK2)
Liquid-liquid phase separation (LLPS)
Locked-nucleic-acid (LNA)
Long interspersed repeat-1 (LINE-1)
Long-term potentiation (LTP)
Lysosomal membrane associated protein 2 (LAMP2)
Lysosomal membrane permeabilization (LMP)
Lysosomal two-pore channel 2 (TPC2)
Microtubule-associated protein 1-light chain 3 (LC3-II/LC3-I)
Microtubule-binding (MTB)
Middle frontal gyrus (MFG)
Middle temporal gyrus (MTG)
N-methyl-D-aspartate (NMDA)Neurofilament Light chain (NfL)
Neurofibrilary Ttangles (NFT)
Neurofibrillary tangle dementia (NTD-dementia)
Nitric Oxide (NO)

Nuclear Lamina (NL)
Pick's disease (PiD)
Primary age-related tauopathy (PART)
Progressive supranuclear palsy (PSP)
Reactive oxygen species (ROS)
Retinoic acid (RA)
Small interfering RNA (siRNA)
Sodium dodecyl sulfate polyacrylamide gel electrophoresis (SDS-PAGE)
TAE buffer (Tris-acetate-EDTA)
Tau oligomer monoclonal antibodies (TOMAs)
Tetramethylethylendiamine (TEMED)
Tris-buffered saline (TBS)
5-methylcytosine (5mC)
5-hydroxymethylcytosine (5hmC)

Contribution

1. The contents of introduction chapter were written for this dissertation, independently. This chapter has been also published in a peer-reviewed journal.

Tabeshmehr, Parisa, and Eftekhar Eftekharpour. 2023. "**Tau; One Protein, So Many Diseases**" *Biology*: 12 (2) 244. https://doi.org/10.3390/biology12020244 [1]

My contribution to this work included performing the literature review, drafting the manuscript and generating the figures. My supervisor, Dr. Eftekharpour edited the final manuscript.

2. Nagakannan, Pandian, **Parisa Tabeshmehr**, and Eftekhar Eftekharpour. 2020 "**Oxidative damage of lysosomes in regulated cell death systems: Pathophysiology and pharmacologic interventions**." *Free Radical Biology and Medicine*: 157, 94-127 [2]

My contribution to this work included performing the literature review and generating all tables.

1 Chapter I: Introduction

1.1 Tauopathies, Types and Importance

Tauopathies are a group of progressive neurodegenerative diseases characterized by tau protein inclusions in the human brain. Clinically, there are twenty-six different types of tauopathies that are recognized by complicated neurodegenerative symptoms, including dementia. A series of cognitive/behavioral and memory deficits manifest in individuals affected by tauopathies[3]. From a clinical pathology perspective, those neurodegenerative diseases in which tau protein plays the main pathophysiological role are classified as "primary tauopathies". Pick's disease (PiD), progressive supranuclear palsy (PSP), argyrophilic grain disease (AGD), primary age-related tauopathy (PART), neurofibrillary tangle dementia (NTD-dementia) and corticobasal degeneration (CBD) are several examples of primary tauopathies. On the other hand, for the "secondary tauopathies" tau protein aggregation is not the major neurodegenerative mechanism. For instance, Alzheimer's disease (AD), the most common form of dementia, is known as a secondary tauopathy in which tau aggregation co-exists with accumulation of β-amyloid peptide (Aβ) [4]. Chronic traumatic encephalopathy (CTE) is another form of secondary tauopathy in which tau depositions are present in neurons, astrocytes and neurites around the blood vessels but are associated with other pathophysiological features[5]. According to the World Health Organization, nearly 50 million people are currently suffering from dementia, and each year, around 10 million new cases are diagnosed with dementia. It is predicted that by 2050, the number of patients will approximately reach 140 million worldwide. Due to the debilitating nature of dementia, these patients require constant care, which significantly impacts their careers, their families and society. In 2017, WHO proposed a "Global action plan on the public health response

to dementia 2017– 2025" in which dementia has been identified as a public health priority[6]. This rationalizes the need for better understanding all aspects of dementia's pathophysiology, including tauopathies.

1.2 Tau

Tau protein, a member of the microtubule-associated protein family, is encoded by the microtubule-associated protein tau gene (MAPT) (Gene ID: 4137), located on human chromosome 17q21.31. Tau is primarily responsible for maintaining microtubules' stability and promoting their assembly in axons. In the central nervous system (CNS), tau is mostly found in cortical and hippocampal neurons and, to a lesser degree, in astrocytes and oligodendrocytes[7]. Tau is not specific to the CNS, but it is also found in the peripheral nervous system (PNS), both intracellularly and extracellularly. The presence of tau protein has been reported in the interstitial fluid and cerebrospinal fluid (CSF)[8]. Structurally, there are four tau protein domains, including the N- and C-terminal domains, the proline-rich domain and the microtubule-binding domain. The proline-rich domain participates in the cell signaling process, as it is particularly the target of protein kinases. Phosphorylation of serin and threonine residues, which are mainly located in this domain can affect tau binding affinity in the microtubule-binding domain. The N-terminal domain may regulate the distance between microtubules. In contrast, the C-terminal domain is involved in microtubule polymerization[9].

The MAPT gene contains 16 exons [10] but its complex and highly regulated splicing results in a variety of developmental stage-specific messenger RNA (mRNA) species, which are mostly present in the brain tissue. In the adult human brain, this alternative splicing generates six isoforms, ranging from 352 to 441 amino acids[11]. Alternative splicing in exons 2 and 3 leads to three different isoforms, including 0N, 1N and 2N. Two additional isoforms, 3R and 4R, are also

generated when splicing occurs in exon 10, resulting in production of two proteins with three and four microtubule-binding domains, respectively. The impact of MAPT alternative splicing on human brain development and pathology has not been adequately investigated and may prove to be important.

Expression levels of various tau isoforms reflect neuronal maturation state and axonal growth capability. Lower levels of tau expression have been reported in immature regions of the human brain such as ganglionic eminence and rhombic lip, while tau expression pattern and splicing could be slightly different in more mature brain regions[12]. Additionally, in human prenatal brain, an abrupt shift happens in MAPT exons 2 and 10 expressions. This shift is evolutionary conserved and may be a crucial step in transition to the mature neurons. Exon 3 undergoes small temporal variations compared to the exons 2 and 10[12]. Specifically, during early embryonic stages, the predominant tau isoform is 0N3R. Healthy adult human brain contains a balanced level of 4R and 3R isoforms. The other expressing human tau isoforms include 1N3R, 2N3R, 0N4R, 1N4R and 2N4R, which is the full-length form of tau protein. 2N4R isoform contains both inserts of exons 2 and 3 in the N terminal region and all four microtubule-binding domains in the C terminal domain. Collectively, this longest tau isoform includes all 441 amino acids [13], (Figure 1-1).

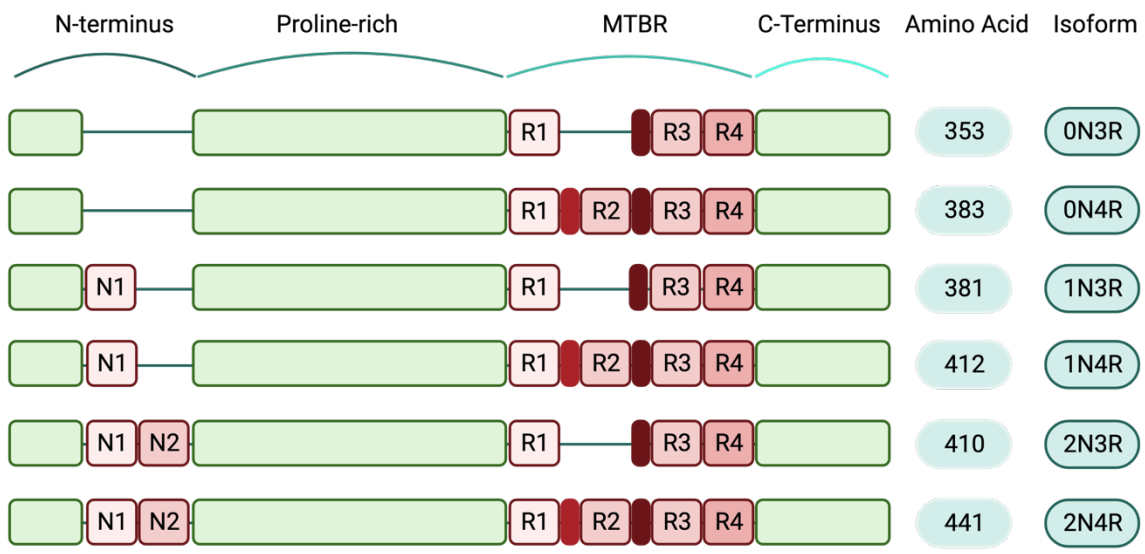

Figure 1-1: Human-specific tau isoforms (Created with BioRender.com)[1]. Schematic diagram depicting the composition of different Tau isoforms. The shortest tau variant which is mainly expressed during the human embryonic stage consists of 352 amino acids (0N3R) and the full-length isoform (2N4R) includes all structural domains of tau protein and 441 amino acids. Structurally, tau isoforms are comprised of N-terminus regions which contain two inserts, N1 and N2. Tau N-terminals are followed by the proline-rich domains, the microtubule-binding regions (MTBR) and the C-terminals. In the full-length tau isoform, all four repeat domains (R1-4) are present in the MTBRs.

1.3 Physiologic Tau

Tau is an important component of the neuronal cytoskeletal compartment. The cellular skeleton is mainly composed of microtubules and is vital for the regulation of critical cell processes, including maintaining the cell shape, proper cell division, and healthy intracellular transport of organelles. In neurons, microtubular organization is critical for axonal stability and the trafficking of materials and organelles to and from the cell body. The dynamic of the cytoskeleton is highly dependent on microtubule-associated proteins (MAPs)[14], and amongst these, tau protein plays a critical role. Weingarten et al., in their milestone discovery, were able to identify tau protein as an essential factor for microtubule polymerization and microtubule assembly and dynamics[15]. As the microtubule dynamic network is essential for neurite formation and axonal pathfinding, the

importance of tau protein has also been reported during neuronal development and CNS maintenance [16] [17]. While tau protein expression is sharply increased during embryonic stages, this seems to reach a plateau in the mature rodent brain[18]. Authors showed that post-translational modification (PTM) of tau and its site-specific phosphorylation were differentially regulated between developing and mature brains. While some residues were more phosphorylated in mature brain, overall, there was a decrease in tau phosphorylation in mature brain that might be due to an increase in tau-specific phosphatases[18].

The microtubule-binding inserts in the C-terminal region of tau protein are the critical domains not only for binding to the microtubules, but also for interacting with the actin filaments in the cytoskeleton structure [19][20]. Actin bundling is regulated by short fragments of microtubule-binding domain in the C-terminal region of tau protein. In cell free experiments, a synthetic version of C-terminal region was able to bind to both monomeric and filamentous actin but this interaction did not result in actin bundling. Authors showed that MAP2 and tau are capable of bundling actin [21]. The tau/f-actin interaction is an important player in dendritic morphology and post-synaptic structure, therefore directly affects synaptic stability [22]. Tau PTMs such as acetylation can modulate actin polymerization and cause synaptic dysfunction [23]. Formation of f-actin bundles is mainly produced by high-affinity interaction between proline-rich and microtubule-binding domains on tau protein and f-actin. This is mediated by hydrophobic interactions between the tau microtubule-binding domain and actin filaments. On the other hand, an electrostatic bond also exists between tau proline-rich domain and f-actin. These offer a highly flexible interaction between tau and f-actin complex, as the tau residues serve as “flexible linkers”. Structurally, one tau molecule contains seven actin-binding regions and these “flexible linkers” are located between these actin-binding sites. Conformational changes in the actin-binding segments have the

regulatory role for cross-linking between the three components of the cytoskeleton: tau, actin filaments and microtubules. Many aspects of tau/f-actin complex, such as the exact binding sites, the bundling mechanism and the cross-linking between actin, tau and microtubules are yet to be understood [24].

Neurons are structurally, morphologically and functionally distinct from any other cells. They have developed long processes and maintain an intricate functional connection through synapses with other proximal and distal target cells. This has evolutionally forced them to have a sophisticated trafficking system for transport of nutrients, energy and synaptic vesicles. “Fast axonal transport” is a complex intracellular trafficking process by which neurons transport the synthesized proteins in somatodendritic compartment to the synapses or haul away the recycled materials and organelles. Axonal microtubules through their molecular motors, kinesins and dyneins, play a crucial role in this bidirectional transport. While kinesin is used for transporting the cargo towards the cell periphery, dyneins are responsible for moving the cargo centrally towards the cell body, allowing for bidirectional traffic and navigating the crowded cytoplasmic environment to correctly conduct the transport tasks[25]. The connection between tau protein and microtubules can directly regulate this special ability of kinesins and dyneins motors. This has been recently proposed to be mediated by differential interaction of tau with different isoforms of dynein and kinesins. While kinesin-1 is more sensitive to inhibition by tau, kinesisn-2 and dynein are only inhibited at very high concentration of tau. The overall sum of connection between tau protein and microtubules regulates the forward movement or processivity of kinesin and dynein and therefore can affect directional bias of axonal trafficking [26]. Of note, this kinesin-driven transport is tau phosphorylation-dependent and inhibition of glycogen synthase kinase-3β (GSK3β) and reduction of tau phosphorylation is detrimental for axonal transport [27]. Increased GSK3β activity has been

documented in AD which can explain the hyperphosphorylation of tau and its detrimental effect on intracellular traffic in neurodegenerative diseases. In this active transport mode that is mediated by tau-bound microtubule/actin network, tau is assumed to be stationary, although in a dynamic equilibrium with free tau molecules in the cytoplasm that are believed to be able to freely diffuse in the cytosol and axoplasm. This form of diffusion is one-directional and is dependent upon the existing microtubule network. There is no need for external energy sources and for short distances up to 1 μm, this form of tau diffusion is faster than the motor-driven active transport. In this model, diffusing tau molecules occurs using the microtubules lattice and ensure proper distribution of tau molecules at different sites, i.e., somatic or axonal ends. This ensures that tau is always available for anterograde or retrograde transport systems [28].

Tau protein plays a critical role in post-synaptic scaffolding in dendrites. It interacts with the kinase Fyn through its phosphatase activating domain (PAD) which is located on tau extreme N-terminal domain. The tyrosine kinase Fyn is responsible for phosphorylation of N-methyl-D-aspartate (NMDA) receptors, implying the impact of tau protein in synaptic signaling [29]. Moreover, in oligodendrocytes, tau-Fyn interaction affects the process outgrowth and is important in the initiation of axon myelination by oligodendrocytes[30].

Tau protein is not restricted to dendrites and axons, as it is also found in neuronal nuclei. In this compartment, tau serves as a DNA protection element against peroxidation through co-localizing with AT-rich heterochromatin regions of DNA and nucleoli; therefore, it contributes to the genomic stability and preservation of genomic organization [31][32][33].

1.4 Pathologic tau

In 1906, Dr. Alois Alzheimer, a German psychiatrist and neuropathologist, described a five-year study on a clinical case with peculiar neuroanatomic features. His 50-year-old female patient

suffered from paranoia, memory disturbance, sleep disorders and progressive confusion. After her death, Dr. Alzheimer investigated her brain autopsy and discovered intracellular neurofibrillary tangles (NFTs) and consequently, described AD as an "unusual illness of the cerebral cortex"[34]. In 1963, these NFTs were characterized in the cerebral cortex neurons in AD cases. These studies showed that NFTs are predominantly composed of insoluble fibers called paired helical filaments (PHFs) [35]. Two decades later, immunological assessments showed that "hyperphosphorylated tau aggregates" are the major components of PHFs [36]. Recent discoveries related to the tau protein and its pathological forms confirmed its key role in modulation of neuronal physiology. To gain a better understanding of tau pathology, various aspects of this protein should be considered, including tau structure and distribution, its exact subcellular locations, possible posttranslational modifications and disease-specific isoforms.

1.4.1 One protein and various conformers

Examination of tau aggregates obtained from different types of tauopathies revealed that tau filaments and inclusions are widely different in various types of tauopathies. This observation resulted in this hypothesis that variations in tauopathy-related symptoms and also disease progression may be related to its pattern of tau aggregation. Tau filaments show astonishing variation in aggregation patterns, both in *in vitro* cell-free conditions and different tauopathy cases [37][38]. The predominant isoform of tau filaments in tau inclusions is used as a classification method for different tauopathies (Figure 1-2)[39][40]. The complexity of different disease-specific tau structures may be a contributing factor in complexity of tauopathies and finding treatments.

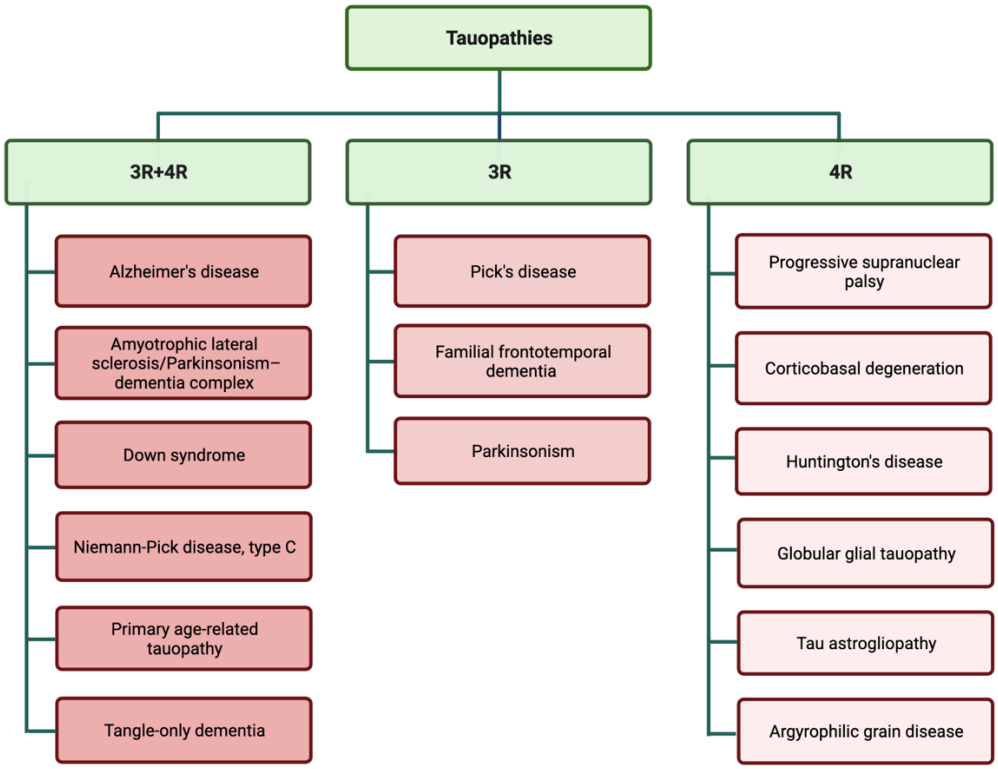

Figure 1-2: Tauopathies are classified according the presence of 3R and 4R isoforms in tau inclusions[1].

1.4.2 Abnormal post-translational modifications of tau

Tau protein is the target of many physiologic and pathologic post-translational modifications (PTMs). The real complex pattern of tau PTMs is not fully elucidated due to the fact that observing intermediate alterations in soluble human tau in the process of PHF formation and NFT aggregation is not possible. Pathophysiologically, the formation of NFTs requires the release of tau in a soluble (monomeric) form with lower affinity for the microtubules than the physiologic tau. Hyperphosphorylation of specific tau residues strongly induces tau-microtubule dissociation which leads to conformational changes. These alterations promote stable structures of anti-parallel tau dimers, oligomers, protomers and ultimately turn into the PHFs and NFTs [41]. Structurally, there are 85 phosphorylation sites on tau which are mainly serin, threonine and tyrosine

residues[13]. Hyperphosphorylation of tau residues (244-368) located in the microtubule-binding domain can affect microtubule stability. In adjacent regions, phosphorylation of serin residues (Ser262 and Ser356) correlates with tau-microtubule dissociation [42]. In contrast, hyperphosphorylation of other residues, Ser214 and Thr231, can adversely affect tau affinity to the microtubules. Collectively, in full-length tau, there are 45 serins, 35 threonine and 5 tyrosine residues that are prone to the hyperphosphorylation [43](Figure 1-3). This adds another layer of complexity to the heterogeneity of tauopathies.

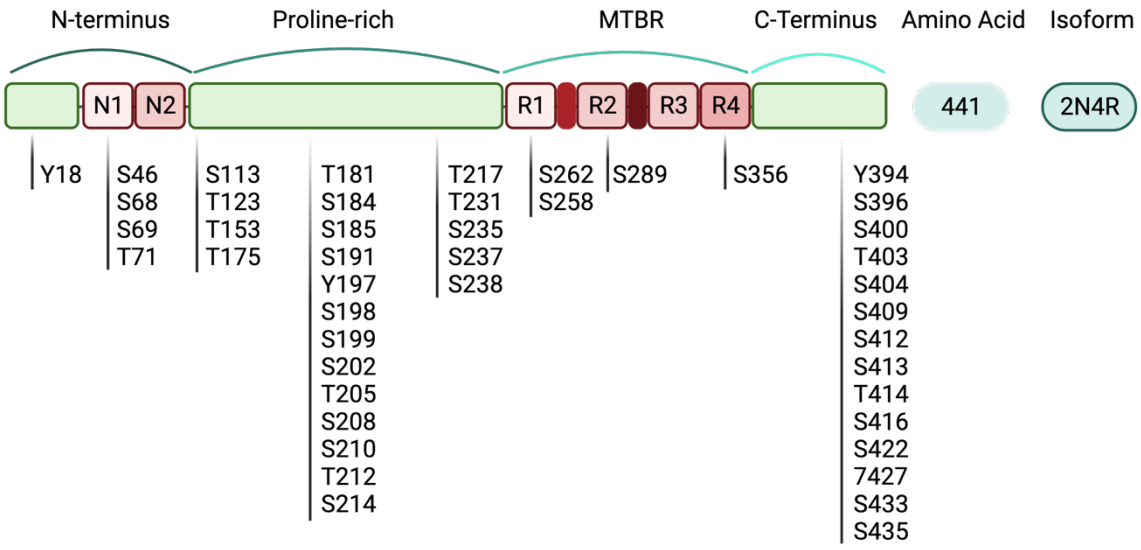

Figure 1-3: Tau phosphorylation sites which are predominantly located in the proline-rich domain and C-terminal region of 2N4R isoform. In full-length tau, there are 45 serins (S), 35 threonine (T) and 5 tyrosine (Y) residues that are prone to the hyperphosphorylation[1]

Hyperphosphorylation of tau in neurons reflects abnormal activity of protein phosphatases and dysregulation of kinases. According to the published literature, alterations in the levels of active kinases are associated with tau hyperphosphorylation in tauopathies. For instance, aberrant activation of cyclin-dependent-like kinase 5 (CDK5), glycogen synthase kinase-3β (GSK3β), and its regulator c-JUN N-terminal kinase (JNK) are associated with NFT formation[44][45][46].

Dysfunction of protein phosphatase 2A (PP2A) has also been identified as another activator of tau hyperphosphorylation. Reduced PP2A expression levels and upregulation of PP2A inhibitors closely correlate with PP2A deregulation mechanisms in tauopathies. PP2A directly enhances tau phosphorylation by preventing tau dephosphorylation and indirectly, by upregulation of tau kinases [47].

In addition to the phosphorylation, tau can undergo other PTMs, including glycosylation, glycation, nitration, truncation, ubiquitination, acetylation and methylation. The pie chart below represents the proportion of PTM-related residues on tau protein (Figure 1-4) [48,49]. Additionally, abnormal acetylation and ubiquitination of tau can also contribute to neurodegeneration [50].

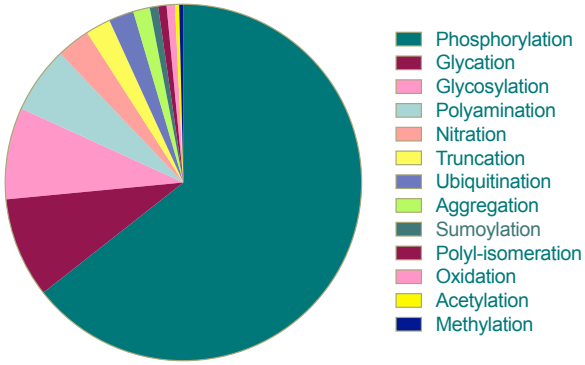

Figure 1-4: Proportion of PTMs on tau protein according to the number of targeted residues in tau 2N4R isoform[1]**.**

Oxidation is another form of tau PTMs that has been identified as the inducer of tau fibrilization under oxidative stress conditions. This can affect five tyrosine residues in the 2N4R tau isoform, at positions 18, 29, 197, 310 and 394 [51]. Under oxidative stress, these tyrosine residues are prone to the formation of dityrosine (DiY) cross-links, which prevent tau elongation and form trapped, stable and insoluble tau species, by which NFT formation can be promoted[52].

Post-translational modification of tau, particularly tau phosphorylation and acetylation, can trigger a tau condensation mechanism known as liquid-liquid phase separation (LLPS) in neurons. This mechanism is reported in both physiological and pathological conditions and is regulated by electrostatic interactions between oppositely charged regions of tau isoforms or between tau proteins and RNA. LLPS leads to the formation of liquid droplets containing high levels of concentrated tau, which can electrostatically interact with other tau isoforms or RNA molecules. Although the mechanistic details of LLPS are poorly understood in neurons, it has been shown to accelerate neuronal tau fibrilization and facilitate neurotoxicity in tauopathies[53][54].

1.4.3 Inducers of pathologic tau, upstream mechanisms of tau dysfunction

There are approximately 57 neurodegenerative-related mutations on MAPT gene, which were mainly discovered in pedigrees with familial frontotemporal lobar degeneration (FTLD). Predominantly, inherited mutations in MAPT gene (FTDP-17) are associated with neuronal and glial tau inclusions in FTLD individuals[55]. The mutation site has been shown to affect the outcome. For instance, mutations in exon 10 can affect microtubule-binding affinity of the protein and consequently, changes the ratio of 3R:4R in adults. Even intronic mutations (e.g., intron 10) may affect tau protein structure and the isoform ratio, demonstrating MAPT mutations are sufficient to stimulate pathogenic tau formation [56][57]. To date, no association between MAPT mutations and PTMs in tau protein has been discovered [58].

The second identified cause of pathogenic tau is chronic traumatic encephalopathy which is also listed as a type of progressive neurodegenerative tauopathy. Mechanistically, brain injury can induce tau cleavage, its aberrant phosphorylation and aggregate formation. These processes can adversely affect axonal microtubule organization, resulting in tau-microtubule dissociation and

subsequent tau accumulation in axons. The key link between brain injury and tau hyperphosphorylation is attributed to the reduction in alkaline phosphatase levels which is mainly responsible for tau dephosphorylation. All these pathophysiological conditions can ultimately trigger chronic inflammation and apoptosis and neuronal degeneration in the brain tissue[25]. Accumulation of pathologic tau also occurs as part of normal aging as it has been detected in temporal neocortex of people over the age of 65. This condition, known as “primary age-related tauopathy” is a normal senescence feature in primates [59].

In addition to the aforementioned stimulators, pathogenic tau can also be induced in people with metabolic syndrome. Examination of *in vitro*, in vivo and post-mortem reports depict a strong relationship between tauopathy and the neurons with increased levels of phosphorylated insulin receptor substrate-1. This results in impaired insulin signaling which can drive pathogenic tau aggregation through reducing phosphoinositide 3-kinase–Akt activity and activating GSK3β. GSK3β activation induces tau hyperphosphorylation and its dissociation from microtubules [60], (Figure 1-5).

Additionally, pathogenic tau formation is shown to be triggered through neuron-to-neuron transmission, in a prion-like manner. Various mechanisms are identified as the stimulator of this type of pathogenic tau aggregation. For instance, the pathogenic tau spreads trans-synaptically from one cell to another or through “exosomes” which are present in CSF and plasma [61][62]. These secretory extracellular micro-vesicles that contain hyperphosphorylated tau aggregates might be released from affected neurons or microglia [63]. The other factor in this type of pathogenic tau propagation are ectosomes: larger vesicles than micro-vesicles which are packaged in the affected cells via plasma membrane budding. These vesicles participate in the pathological spreading of tau protein [64].

The mechanistic target of rapamycin (mTOR) has been identified as another potential driver of pathogenic tau formation. This Serin/Threonine protein kinase plays a crucial role in neuronal growth and maintenance. In neurons, mTOR regulates prominent cellular functions including autophagy, signal transduction, metabolism and cytoskeletal dynamics[65]. Hyperactivation of mTOR can induce tau expression and abnormal tau phosphorylation. It has been also revealed that mTOR activation can adversely affect autophagy rate that subsequently reduces pathogenic tau clearance in neurons [66].

1.4.4 Pathologic tau and cell toxicity, downstream events of tau dysfunction

The association of pathogenic tau with neuronal toxicity and disruption of neuronal networks, as well as glial damage, has been well documented in the literature. However, the exact mechanisms and physiological events that link pathogenic tau formation to neurotoxicity and cell death remain unknown. As AD is well-characterized microscopically by the combined presence of intracellular NFT aggregates and extracellular Aβ plaques, inevitably, the tauopathy-related studies are vastly focused on AD models. The impact of tau pathology on the cellular cytoskeleton and its negative effect on intracellular traffic of synapse machinery were discussed previously. We know that hyperphosphorylated tau can stabilize dendritic microtubules and induce synaptic dysfunction [67]. These peri-synaptic alterations induce synaptic malfunction by adversely affecting synaptic anchoring and glutamate receptor trafficking[68]. In addition to the peri-synaptic alterations, pathogenic tau might disrupt dendritic spines. Recent proteomic data obtained from an *in vivo* study on Tau-P301S transgenic mice demonstrated that several proteins and pathways may change in post-synaptic densities (PSDs). For instance, the levels of GTPase-regulatory proteins which participate in cytoskeletal actin dynamics and dendritic spine stability may decline significantly.

Although synapse loss is identified as an early event and direct consequence of tau pathology, how exactly the pathogenic tau induces synapse loss is yet to be understood [69].

Impaired axonal transport is another identified pathologic event that is attributed to tau toxicity. "Long-range transport" in neurons is mediated by kinesin motors which can be inhibited by tau protein. Mechanistically, tau can limit the cargo travel distance by reducing kinesin velocity [70]. Under pathologic condition in soma, tau traps kinesin adaptor-molecule c- JNK interacting protein 1(JIP-1) and prevents long-range transport. On the other hand, kinesin deficiency can trigger tau hyperphosphorylation which further exacerbates the transport efficiency[71].

The impact of oxidative stress in neurodegenerative diseases, including AD, has been well recognized; however, it is not clear whether tau-aggregation results in excessive production of reactive oxygen species (ROS) or whether tau hyperphosphorylation is mediated by ROS levels. It has been shown that neurons containing tau aggregates produce high levels of ROS and externalize a considerable amount of phosphatidylserine. Microglial cells can detect the aberrant levels of phosphatidylserine and phagocytose both the affected neurons and tau aggregates. Additionally, microglia can release opsonin milk fat globule EGF-factor-8 (MFGE8) and nitric oxide (NO), which helps facilitate the engulfment process[72]. In another study the leading role of ROS is suggested by induction of tauopathy in *Drosophila* model in which downregulation of thioredoxin-1 or superoxide dismutase was associated with increased tau hyperphosphorylation. Activation of JNKs has been reported after decreased thioredoxin activity[73]. Activation of JNKs has been reported after decreased thioredoxin activity[74][75].

Tau-mediated neurotoxicity can also be mediated by overstabilization of actin filaments which ultimately disrupts the cytoskeleton and synaptic plasticity. Recent findings demonstrate that pathologic tau formation triggers f-actin stabilization, weakens the nuclear pore

localization/function and disrupts nucleocytoplasmic trafficking [76][77]. Consequently, f-actin bundling can also affect mitochondrial dynamics and induce elevated levels of ROS [78]. Some evidence suggests the involvement of epigenetic changes with tau-hyperphosphorylation. Overstabilization of f-actin has been shown to exert pressure on the nuclear envelope, resulting in invagination of nuclear envelope and proteolytic degradation of nuclear lamina. Structurally, nuclear lamina serves as a strong scaffold for DNA and is important for DNA heterochromatin/euchromatin ratio. Damage to nuclear lamina will result in changes in heterochromatin relaxation and transcription of the normally dormant/silenced regions of DNA. An elegant example of these changes is the re-expression of cell cycle entry-related proteins in postmitotic and fully-differentiated neurons which is a strong signal for apoptotic cell death[79]. In parallel with chromatin changes, the expression patterns of RNA is also affected that may promote RNA instability and activate transposable elements[79]. Overexpression of tau in *Drosophila* and mice models of tauopathy was shown to activate the normally silenced retrotransposons. These results were also confirmed in the post-mortem brains obtained from AD and progressive supranuclear palsy (PSP) patients[80][81][82] (Figure 1-5)

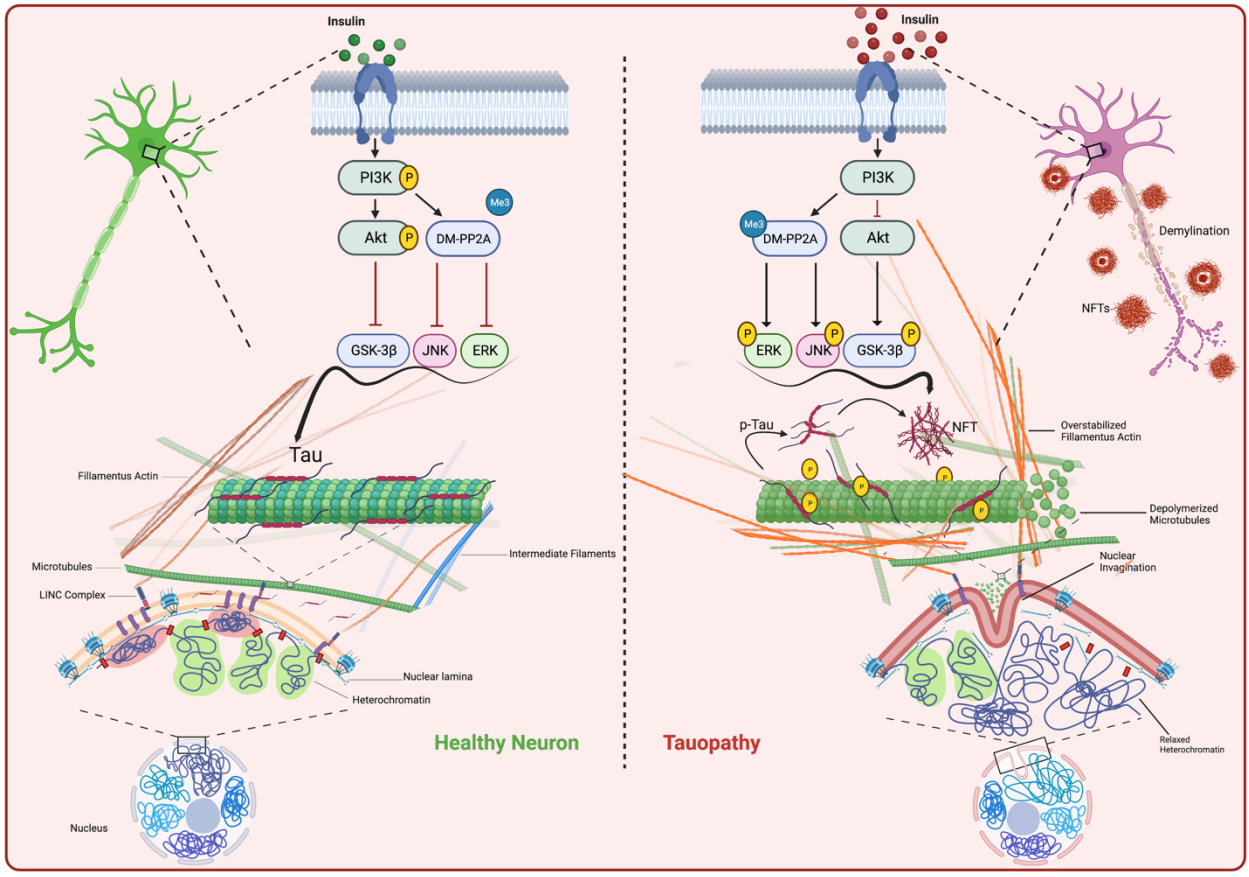

Figure 1-5: Pathogenic tau, upstream and downstream events (Created with BioRender.com)[1]. In healthy neurons (**left**), physiologic tau is responsible for microtubule assembly and maintenance of critical cellular components such as cytoskeleton, nucleoskeleton and DNA integrity. Under pathologic conditions (**right**), PTMs can alter tau functions. For instance, activated ERK, JNK or GSK3β induces tau hyperphosphorylation which is the main trigger of tau aggregation and NFT formation in the neurons. Consequently, this may lead to the microtubule disassembly, actin overstabilization and nuclear lamina invagination. These circumstances can dysregulate genomic DNA integrity. Moreover, extracellular release of NFTs facilitates their neuron-to-neuron transmission. These pathophysiological events ultimately result in progressive neurodegeneration.

1.5 Diagnosis and therapeutic strategies for tauopathies

Accurate diagnosis of tauopathies has been made possible by tau positron emission tomography (PET) scans. Tau-PET scan allows for detection of tau deposition in the patient's brain. Using this technique allows detection of tauopathy severity and progression and can also be used for monitoring the efficacy of therapeutic interventions. The growing list of tau-PET tracers is a

promising tool for tauopathy discrimination, among which THK5317, THK5351 and PBB3s are available for clinical assessments [83]. Additionally, [^{18}F]GTP1, [^{18}F]flortaucipir, [^{18}F]MK-6240, and [^{18}F]RO948 tau-PET have been studied as other tau tracers [84]. [^{18}F]-flortaucipir (AV1451) is a first-generation FDA-approved tau tracer that strongly correlates with identifying NFT distribution in AD[3].

The complexity and multifactorial nature of tauopathies is the major obstacle in better understanding the pathology and designing new therapeutic interventions for slowing the disease's progress. The current clinical tools cannot be used for the detection of early-stage diseases, and the diagnosis can only occur in the late stages, when the currently prescribed drugs can only treat the symptoms. There is an urgent need for developing early diagnosis tools and developing disease-modifying drugs and, accordingly, many preclinical and clinical trials are currently in progress. Since AD is the most common form of tauopathy, the efforts to discover novel therapeutic interventions have also been mostly focused on this disease. However, considering the complexity of tau isoforms and inclusion bodies, it is not clear whether an effective drug for AD-associated tauopathies can also cure other forms of tauopathies. Whether treatments targeted for tauopathies may need to be personalized remains to be investigated. The timing of the application of any potential treatments represents the next challenge in human diseases. Notably, the pathologic events in tauopathies, including tau hyperphosphorylation and protein aggregation, occur a long time before the possibility of a clinical diagnosis, when experimental treatments are proven to be ineffective. These limitations urge the need for the discovery of novel biomarkers to allow diagnosis at earlier stages of the diseases. Two categories of tau biomarkers have been identified in CSF and blood. In CSF, increased levels of phosphorylated tau at residue 217 (p-tau217) and p-tau235 as well as p-tau231 are shown to be correlated with the early stages of AD

[85], while p-tau181 can be used as a prognostic tool for the advanced phases of AD[86]. The presence of axonal protein Neurofilament Light chain (NfL) in CSF has also been identified as a promising diagnostic tool for AD and FTLD[87]. Targeting CSF biomarkers has various limitations as obtaining CSF is relatively invasive, and can be performed in more advanced clinical centers. This makes it not very cost-effective that can be widely used for all patients[88]. Identification of Plasma biomarkers such as p-tau181 [89] and p-tau217 [90] in plasma can be alternative and reliable biomarkers for AD. Interestingly, plasma p-tau217 is not associated with non-AD tauopathies and helps to discriminate AD from the other forms of tauopathies [91]. Critiques for plasma biomarkers argue that they may not properly reflect the CNS pathophysiological changes, since these proteins are degraded in kidney and liver which may affect their reliability [88].

Numerous studies have demonstrated evidence of considerable achievement in designing therapeutic interventions for tauopathies. Proper identification of druggable pathophysiological mechanisms in tauopathies is fundamental to this achievement. Some of the potential mechanisms that can be targeted for this purpose include: (1) tau PTMs, particularly tau hyperphosphorylation, by phosphatase modifiers and kinase inhibitors, (2) targeting cytoskeleton/nuclear disruption and genomic architecture dysfunction and (3) reducing tau expression levels with small interfering RNA (siRNA) and antisense oligonucleotides (ASOs). Additional approaches include reducing the levels of plasma tau, inhibiting the aggregation of different forms of pathogenic tau such as PHFs, NFTs and small oligomeric tau aggregates, as well as enhancing tau clearance by active and passive tau immunization[92] (Figure 1-6).

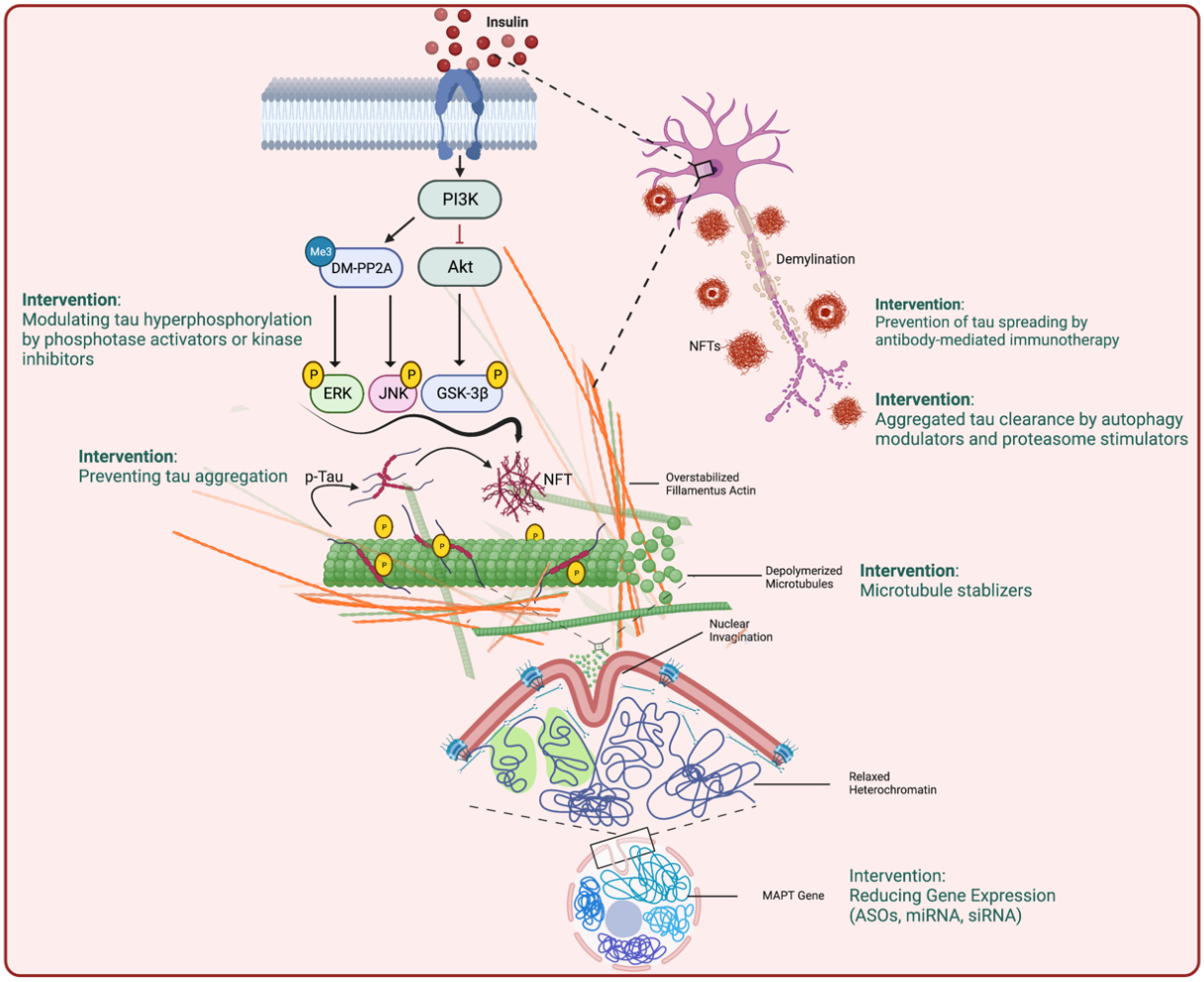

Figure 1-6: Tau-related therapeutic interventions (Created with BioRender.com)[1]. Clinical trials and preclinical studies on tauopathies mainly focus on various aspects of pathogenic tau and its consequences, including modulating tau hyperphosphorylation and inhibiting other PTMs such as O-deglycosylation, preventing tau aggregation or stimulating tau clearance by autophagy modulators or proteasomal degradation, active or passive immunotherapies, applying microtubule stabilizers and reducing MAPT gene expression levels.

Passive immunotherapy has been the focus of tau clinical trials, with the aim of slowing neurodegeneration process through preventing the spread of pathogenic tau and removing its extracellular aggregates. The main barrier to finding an effective treatment for clinical purposes is finding a suitable epitope on tau protein that is commonly present in all patients despite their genetic background or the specific type of tauopathy disease. Active tau immunotherapy has also been explored. AADvac1 is a therapeutic tau vaccine candidate that has shown successful

reduction of neurofilament light chain (NfL) in plasma and CSF in AD patients by recognizing a 12-amino acid sequence (KDNIKHVPGGGS) in tau MTBR. Reported results from its phase I clinical trial have raised hope for tauopathy treatment. According to these results, AADvac1 leads to reduced cognitive decline and lower brain atrophy in AD patients in mild to moderate stages[93][94][95]. Obtained results from its phase II trials confirmed its safety and well-tolerance; however, it was not completely successful in cognition improvement[96]. The other candidate tau-targeted vaccine for patients with early AD is ACI-35. This immunotherapy vaccine can target the pathological tau phosphorylation at S396 and S404. This phase I/II clinical trial is expected to be completed before October 2023[96][97]. Among the wide range of tau therapeutic approaches, clinical trials for developing effective tau ASO therapeutics are also ongoing, now. Tau antisense oligonucleotides (ASOs) are short single-stranded DNA-like molecules synthesized to target tau mRNA in a highly selective mode which consequently can reduce both intercellular and extracellular tau levels. Although they are highly selective and safe, ASOs cannot cross the blood brain barrier (BBB) and they need to be administrated intrathecally[98]. IONIS-MAPTRx (BIIB080) is the first clinical trial of tau ASOs which aims to reduce MAPT mRNA in the patients with mild AD[99]. A list of most recent therapeutic interventions for tauopathies is presented in Table-1.

Model/ Cell Line	Therapeutic Intervention	Intended Mechanism	Potential Target	Reference
Human patients with probable AD or MCI-AD	Hydromethylthionine mesylate	Inhibiting tau aggregation by targeting pathological tau oligomers and filaments -In Phase 3 clinical trial.	Tau aggregation	[100]
Human patients with mild to advanced AD	Cerebrolysin® & Donepezil	Unknown	Tau expression and tau phosphorylation	[101]
Prodromal to mild AD patients	Semorinemab	Not slowing tau accumulation pathology (not effective), No change in clinical AD progression.	Oligomeric tau	[102]
Cyno monkeys, C57Bl/6J mice model, PAC transgenic mice, hESC line SA001 cell line	ASO-001933	Selective and long-lasting reduction in tau levels by locked-nucleic-acid (LNA)- modified ASOs	Tau aggregation	[103]
3xTg mice model	Norvaline	Diminishing tau phosphorylation levels	Phosphorylated tau	[104]
Murine polytrauma mouse model	Propranolol	Decreasing hippocampal p-tau accumulation	Accumulation of phosphorylated tau	[105]
Ty1-hTau.P301S mice & SH-SY5Y cell line	Tetrandrine	Promoting tau clearance and degradation via autophagy, rescuing lysosomal Ca^{2+} homeostasis, diminishing NFT development	Lysosomal two-pore channel 2 (TPC2)	[106]
Htau and JNPL3 mouse models	Tau oligomer monoclonal antibodies (TOMAs)	Reducing tau oligomers levels by tau passive immunotherapy	Tau oligomeric strains	[107]
P301S mice model	Glimepiride	Decreasing GSK3β, increasing phosphorylated-AKT/total-AKT, increasing PP2A, normalizing of CDK5 levels Decreasing neuroinflammation and apoptosis by reducing NF-kB, TNF-α and caspase 3 levels	Phosphorylated tau	[108]
Human AD patients	Donanemab	Slowing tau accumulation	Tau accumulation	[109], [110]
PS19 mice model	Etanercept & TfRMAb-TNFR	Reducing phosphorylated tau and microgliosis, increasing PSD95 expression and attenuating hippocampal neuron loss	TNF-α (Inhibitors)	[111]
AAVhTau mice model	Dihydroartemisinin (DHA)	Inducing tau O-Glc-N-Acylation modification, reducing tau phosphorylation, improving learning and memory, increasing hippocampal CA1 long-term potentiation (LTP)	PTMs on tau protein	[112]

Tau-P301S mouse model	Rutin	inhibiting tau aggregation and its oligomer-induced cytotoxicity, reducing production of proinflammatory cytokines and preserving neurons	Tau aggregation	[113]
rTg4510 mouse model	BSc3094	Reducing tau phosphorylation, improving cognition and reducing anxiety-like behavior	Tau aggregation	[114]
Neuroblastoma cell model (with methyl glyoxal (MG)-induced Tau glycation)	Epigallocatechin-3-gallate (EGCG)	Inhibiting glycation, modulating tau phosphorylation, enhancing actin-rich neuritic extensions and preserving actin and tubulin cytoskeleton	Cytoskeleton stabilizer	[115]
SH-SY5Y & HEK293 cell lines hTau-transgenic, tauP301L and 3xTg-AD mice models	C004019	Promoting tau ubiquitination-proteasome-dependent proteolysis Improving synaptic and cognitive functions in animal models	Tau clearance	[116]
3xTg-AD mouse model	Intravenous administration of mesenchymal stem cells	Decreasing pathological tau phosphorylation at T205, S214, T231 and S396 but not levels of Aβ-42	Phosphorylated tau	[117]
Human PSP patients	Gosuranemab	Decreasing unbound N-terminal tau in CSF -In spite of this effect, gosuranemab did not showed clinical efficacy in PSP patients. -Phase 2 clinical trial is completed.	N-terminal tau	[118]

Table 1-1: Recent preclinical and clinical therapeutic interventions for tauopathies[1].

1.6 Summary and Conclusion

Dementia is an umbrella term for many neurodegenerative diseases. As we age longer, the rate of dementia is exponentially increasing, imposing a significant emotional cost for the family and financial burden for the human societies. Tauopathies are a major contributor to dementia and despite extensive research, the underlying neurodegenerative mechanism remain to be elucidated. Tauopathy diseases present extensive neuropathological and phenotypical differences which impose considerable challenges in developing diagnostic and therapeutic strategies. Despite significant transformative achievements in the field of tauopathy, several fundamental questions

remain to be addressed. Novel drugs are in clinical trial phases with some promising outcome, however, proving their safety and efficacy will require large human studies that may take several years to complete. Preclinical studies in *Drosophila* and mice models of tauopathy has revealed a new aspect of tauopathy which is characterized with nuclear envelope invagination and changes in gene expression. Interestingly, nuclear envelope invagination has also been confirmed in human post-mortem brain tissue which results in re-emergence of endogenous ancient retroviruses. Calorie restriction in *Drosophila* effectively attenuated the endogenous retroviral expression[73]. The protective effect of calorie restriction has been related to decrease in tau hyperphosphorylation in *Drosophila* [73] and in ApoE-deficient mouse model of neurodegeneration[119] as well as in Tg4510 mouse model of tau deposition[120]. While there is no information on similar impact in human, these data indicate that changes in life style may be an effective preventive way to decrease the impact of age-associated diseases. With the application of new imaging tools such as Tau-PET tracers, it will be possible to diagnose the patients in earlier stages of the disease that may respond better to the available treatments. Alongside these changes, the need for identification of new biomarkers is a high priority that will ultimately improve patient's response to drugs and their quality of life.

1.7 Study rational, hypothesis and research objectives

1.7.1 Study Rational

Despite numerous research, tauopathies remain incurable and their etiology is largely unknown. Accumulating evidence suggests that deposition of abnormally phosphorylated tau protein in neurons is the histopathological signature of tauopathies[121]. Pathophysiologically, NFT aggregation causes impaired axonal transport, loss of synaptic connections and f-actin overstabilization which ultimately triggers neurodegeneration and apoptosis [122]. Multiple

studies have reported that NFTs can induce nuclear lamina invagination, that is linked with epigenetic alterations, heterochromatin relaxation and aberrant gene expression in neurons, including those associated with cell cycle re-entry [79]. In AD, which is one of the most common forms of tauopathies, aggregated NFT and Aβ plaques have been identified as the pathological hallmarks [123]. Recent discoveries from our laboratory and other groups revealed that nuclear lamina invagination is a new feature of AD-affected neurons [124][125]. Using mouse models of AD (3xTg and APP/PS1) and an *in vitro* model of Aβ42 toxicity in primary neuronal cultures and SH-SY5Y neuroblastoma cells, our laboratory has shown that nuclear lamina invagination is mediated by two enzymes: Caspase-6 [126] and cathepsin L [125]. Whether nuclear lamina invagination and f-actin overstabilization can be alleviated by application of pharmaceutical approaches remains to be examined.

1.7.2 Hypothesis

I hypothesized that overexpression of FL-Tau and the pathogenic fragment of tau protein (Tau35) is sufficient to induce downstream events of tauopathy, including tau hyperphosphorylation, cytoskeletal alteration, nuclear lamina disruption and heterochromatin relaxation.

1.7.3 Research Objectives

Aim 1: To generate a model of tauopathy in differentiated SH-SY5Y (dSH-SY5Y) cells.

I will characterize the effect of full-length tau (FL-Tau) and pathologic Tau35 overexpression in human neuroblastoma cells from different aspects upstream and downstream of tau overexpression. These features, upstream-to-downstream, include changes in tau phosphorylation levels, autophagy-lysosomal pathway, f-actin stability status, nuclear lamina integrity, nuclear envelope morphology and DNA methylation levels.

Aim 2: To examine whether tau phosphorylation, nuclear lamina damage and f-actin overstabilization can be inhibited/reversed. After characterizing this cellular model of tauopathy, two small molecules which are recognized as kinase inhibitors will be used to examine whether tauopathy-related properties can be attenuated or not.

2 Chapter II: Materials & Methods

2.1 Materials

Cell Culture	
SH-SY5Y Proliferation Medium (100ml)	86.5 mL Dulbecco's modified Eagle's medium (DMEM) (Gibco #11960-051) 2 mL Glutamine (Gibco #35050-061) 500 µL Sodium Pyruvate 10 ml Fetal Bovine Serum (FBS) (Gibco #12483-020) 1 mL Penicillin/Streptomycin (Gibco #15640–055)
SH-SY5Y Differentiation Medium	95.5 mL DMEM-F-12 (Gibco #11320-033) 2 mL glutamine 500 µL Sodium Pyruvate 1 mL Bovine Serum (FBS) 1 mL Penicillin/Streptomycin 10 µM Retinoic Acid (Sigma #R2625)
TrypLe	Gibco (#12604-021)
Trypan blue	0.4% (w/v) Trypan blue solution
Dimethyl sulfoxide	Sigma (#SHBH5547V)
TurboFect Transfection reagent	TurboFect (#R0531)
G418 Sulfate (Neomycin)	Goldbio (#108321-42-2)
SP600125	Sigma (#SLCF3483)
AR-A014418	Sigma (#164384)
DQ Red BSA	Molecular Probes
Cell Counting Kit	Dojindo Molecular Technologies (#CK04)
Protein Extraction	
Protein Lysis Buffer (NP-40)	50 mM Tris HCl pH 8 (Sigma) 150 mM NaCl (Sigma) 5 mM EDTA (Inhibitor cocktail) 1% NP-40 with protease and phosphatase inhibitors (Thermo scientific)

Phosphate-buffered saline (PBS)	137mM NaCl 2.7mM KCl 10mM disodium phosphate (Na2HPO4) 2mM monopotassium phosphate (KH2PO4) pH: 7.4
Pierce BCA Protein Assay Kit	(Thermo scientific)
Immunoblotting	
Resolving gel	10% (w/v) acrylamide (BIO-RAD) 25% (v/v) resolving buffer 0.01% (w/v) ammonium persulphate (APS) 0.1%(v/v) N,N,N',N', Tetramethylethylendiamine (TEMED) (Fisher Bioreagents) pH 8.8
Stacking gel	4% (w/v) acrylamide 25% (v/v) stacking buffer 0.075% (w/v) APS 0.15% (v/v) TEMED pH 6.8
Electrophoresis molecular weight markers (Protein Ladder)	Bio-Helix
Tris-buffered saline (TBS)	50mM Tris-HCl 150mM NaCl pH: 7.6
Protein Running buffer	25mM Tris base 192mM glycine 0.1% (w/v) SDS (Fisher Bioreagents) pH 6.8
Transfer buffer	20% (v/v) Transfer buffer (5X) (BIO-RAD) 20% (V/V) Ethanol 100%
Blocking solution (milk)	5% (w/v) skimmed milk powder in TBS + 0.1% (v/v) Tween 20 (Thermo scientific)
Blocking solution (BSA)	5% (w/v) bovine serum albumin (BSA) (Sigma) in TBS
Wash solution	TBS + 0.1% (v/v) Tween 20
Clarity Max Western ECL substrate	BIO-RAD (#1705061) and (#1705062)
Immunocytochemistry	

Fixation solution (PFA)	4% paraformaldehyde (PFA) in PBS pH 7.4
Blocking solution (BSA)	1% (w/v) bovine serum albumin (BSA) in PBS
Permeabilizing solution	0.5% (v/v) Triton-X100 (Fisher scientific) in PBS
DNA Extraction	
DNA Extraction Kit	Pure link genomic DNA kit (Invitrogen)
Agarose gel electrophoresis	
50x TAE buffer (Tris-acetate-EDTA)	40 mM Tris, pH 7.6 20 mM Acetic acid 1 mM EDTA pH 8.0
Agarose	Fisher bioreagents
Nuclear acid molecular weight marker	1 kb DNA ladder (New England Biolabs) Molecular weight sizes: 0.5, 1, 2, 3, 4, 5, 6, 8 and 10kb
LINE-1 Bisulfite Pyrosequencing	EZ DNA Methylation-Gold™ Kit (D5005, D5006)

Table 2-1: Reagents, buffers and kits used in this project.

Primary Antibodies					
Antibody	**Antigen/Epitope**	**WB**	**ICC**	**Source**	**Identifier**
Tau	Total Tau	1:10,000	1:1000	DAKO	A0024
PHF-1	Tau phosphorylated at S396/S404	1:5000	-	Professor P. Davies[127]	
AT180	Phosphorylated Tau at Thr231	1:500	1:200	Invitrogen	MN1040
AT8	Phosphorylated Tau at Ser202/Thr205	1:500	1:200	Invitrogen	MN1020B
Lamin B1	Lamin B1	-	1:250	Abcam	ab16048
Actin Phalloidin	Filamentous actin	-	1:400	Invitrogen	A30107
β-Tubulin III	β-Tubulin III	-	1:600	Sigma	T8660
GAP43	Growth associated protein 43	-	1:500	Sigma	G9264
MAP2A	microtubule-associated protein 2A	-	1:500	Millipore	MAB3418
NF-200	Neurofilament 200	-	1:500	Sigma	N4142
Ki67	Human Ki67	-	1:50	BD Pharmingen™	550609
p-Histone H2A.X	Phosphorylated Histone at Ser139	-	1:1000	Cell Signaling Technology	9718T
DAPI	Nucleic Acid	-	1:10000	Millipore Sigma	D9542

p62	Sequestosome1 (SQSTM1, p62)	1:1000	-	Cell Signaling Technology	5114S
LC3B	LC3 B	1:4000	-	Millipore Sigma	L7543
Histone H3	Histone H3	1:2500	-	Abcam	ab32521
β-Actin	Actin	1:4000	-	Santa Cruz Biotechnology	sc-47778
Lamin B1	Lmin B1	1:1000	-	Santa Cruz Biotechnology	sc-377000
LAMP-2	LAMP-2	1:1000	-	Santa Cruz Biotechnology	sc-19991
5mC	5-methylcytosine	1:1000	-	Cell Signaling Technology	D3S2Z
5hmC	5-hydroxymethylcytosine	1:1000	-	Cell Signaling Technology	AMC31
Secondary Antibodies					
Antibody	**Species Reactivity**	**WB**	**ICC**	**Source**	**Identifier**
HRP - conjugated secondary	Anti-Mouse IgG	1:2500	-	Bio-Rad	170-6516
HRP - conjugated secondary	Anti-Rabbit IgG	1:2500	-	Cell Signaling Tecjnology	7074S
Alexa Flour 488	Anti-Mouse IgG	-	1:500	Invitrogen	A11029

Alexa Flour 568	Anti-Mouse IgG	-	1:500	Invitrogen	A11031
Alexa Flour 647	Anti-Mouse IgG	-	1:500	Invitrogen	A21236
Alexa Flour 488	Anti-Rabbit IgG	-	1:500	Invitrogen	A11034
Alexa Flour 568	Anti-Rabbit IgG	-	1:500	Invitrogen	A11036
Alexa Flour 647	Anti-Rabbit IgG	-	1:500	Invitrogen	A21245

Table 2-2: Primary and secondary antibodies used in this project.

2.2 Methods

2.2.1 Plasmids

Plasmids for this study were kind gifts from Prof. Diane P. Hanger (King's College, London, UK)[128]. These plasmids encode full-length human tau isoform (FL-Tau) and the 35 kDa C-terminus region of this isoform (Tau35) regulated by CMV promoters. They were generated in pcDNA 3.1D/V5-His-TOPO vector (Invitrogen) carrying the Neomycin resistance gene (Figure 2-1).

a)

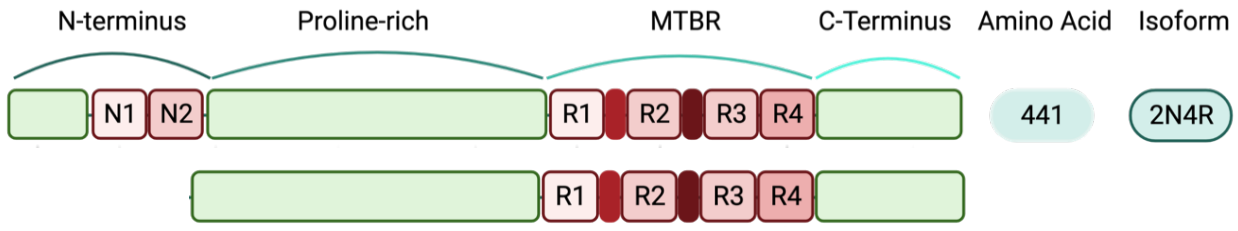

b)

MAEPRQEFEVMEDHAGTYGL[20] GDRKDQGGYTMHQDQEGDTD[40]

AGLKESPLQTPTEDGSEEPG[60] SETSDAKSTPTAEDVTAPLV[80]

DEGAPGKQAAAQPHTEIPEG[100] TTAEEAGIGDTPSLEDEAAG[120]

HVTQARMVSKSKDGTGSDDK[140] KAKGADGKTKIATPRGAAPP[160]

GQKGQANATRIPAKTPPAPK[180] TPPSSGEPPKSGDRSGYSSP[200]

GSPGTPGSRSRTPSLPTPPT[220] REPKKVAVVRTPPKSPSSAK[240]

SRLQTAPVPMPDLKNVKSKI[260] GSTENLKHQPGGGKVQIINK[280]

KLDLSNVQSKCGSKDNIKHV[300] PGGGSVQIVYKPVDLSKVTS[320]

KCGSLGNIHHKPGGGQVEVK[340] SEKLDFKDRVQSKIGSLDNI[360]

THVPGGGNKKIETHKLTFRE[380] NAKAKTDHGAEIVYKSPVVS[400]

GDTSPRHLSNVSSTGSIDMV[420] DSPQLATLADEVSASLAKQG[440] L

c)

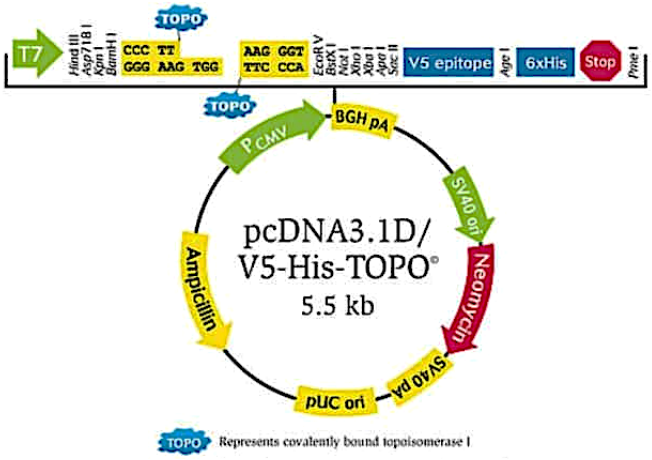

Figure 2-1: Plasmids a: Protein sequence of full-length isoform of human tau and its 35 kDa fragment containing majority of proline-rich domain, MTB and the C-terminal regions (residues 187–441 of FL-tau). **b:** Amino acid sequence of FL-Tau, Tau35 sequence is presented in red[129]. **c:** pcDNA 3.1D/V5-His-TOPO vector (Invitrogen), FL-Tau and Tau35 sequences were inserted into this plasmid which carries Neomycin resistance gene.

2.2.2 Generation of stable tau-expressing SH-SY5Y cell line

The human neuroblastoma cell line SH-SY5Y (purchased from ATCC® - Cedarlane, Canada) were grown in supplemented SH-SY5Y proliferative medium in a humidified incubator containing 5% CO_2 at 37°C. Pre-confluent cells (70-80% confluence) between passages 5-10 were used for these experiments. 24 hours before stable transfection, cells were seeded at the density of 4×10^4 cells/cm^2 in 6-well plates. SH-SY5Y cells were transiently transfected with plasmids (2mg/well) using TurboFect Transfection reagent according to the manufacturer's instruction. Non-transfected cells were included as control group. To generate stable SH-SY5Y cell lines expressing FL-Tau and Tau35, 48 hours after transfection, the medium was switched to the Neomycin-containing media. 600 µg/mL G418 was added to media for selecting stable colonies. From the second week, G418-resistant cells were transferred to the T-75 flasks containing media with 300 µg/mL G418 antibiotic for the future experiments. The isolated stable colonies expressing full-length tau, the c-terminal tau domain and non-transfected cells were named pSH-SY5Y-FL, pSH-SY5Y-Tau35 and pSH-SY5Y-CTL, respectively.

2.2.3 Cell culture

Obtained stable lines, pSH-SY5Y-FL, pSH-SY5Y-Tau35 and pSH-SY5Y-CTL were maintained in supplemented SH-SY5Y proliferative medium at the confluency of 70-80%. To passage the confluent flasks, prior to splitting the cells into the new flasks, they were treated with pre-warmed TrypLE and incubated at 37°C, for 5 min. To obtain the exact density, 10 µl of cell suspension was diluted in 90 µl of Trypan Blue solution. 10 µl of this mixture was loaded on a hemocytometer. To calculate cell density, the following formula was used:

$$Cell\ density\ in\ 1\ ml = \frac{Total\ number\ of\ cells}{\text{Number of squares } counted} \times 10^5$$

For long-term storage, 10% (v/v) cell suspension containing 1 million cells was resuspended in DMSO and aliquoted in cryogenic tubes. Tubes were transferred to -20°C and kept for 5 hours. Before transferring to liquid nitrogen, they were maintained at -80°C, overnight.

2.2.4 Neuronal differentiation of stable SH-SY5Y cells (dSH-SY5Y)

To induce differentiation process in SH-SY5Y cells, pSH-SY5Y-FL, pSH-SY5Y-Tau35 and pSH-SY5Y-CTL were plated at the density of 4×10^4 cells/cm^2 in 100mm dishes for cell harvesting and on glass coverslips for immunocytochemistry. After 24 hours, the medium was replaced with pre-warmed differentiation medium containing retinoic acid (RA) at the concentration of 10 μM for 7 days in low-serum supplemented media (FBS, 1%). 50% of medium was refreshed every three days. The differentiated cells were named dSH-SY5Y-FL, dSH-SY5Y-Tau35 and dSH-SY5Y-CTL.

2.2.5 Cell treatments and determination of cell viability

Proliferative non-transfected and transfected SH-SY5Y cells, including pSH-SY5Y-CTL, pSH-SY5Y-FL and pSH-SY5Y-Tau35, were seeded in 96-well plates at the density of 8000 cells/well. After 24 hours, cells were treated with kinase inhibitors, SP600125 (10 and 20 μM), AR-A014418 (10 and 20 μM), and 0.2% DMSO as vehicles, for 4 h. Following the treatment, 10μl of Cell Counting Kit-8 reagent was added to each well and incubated for 4 h at 37◦C to determine cell survival. Absorbance at 450 nm was measured using Synergy H1 Hybrid Reader (BioTeK Instruments, USA) and the absorbance at 650 nm was used for background correction. The relative cell viability as percentage of control is presented.

2.2.6 Inhibition of protein kinases

Both non-differentiated and differentiated cells were treated with 10 μM c-Jun N-terminal kinase (JNK) inhibitor, SP600125, and 10 μM glycogen synthase kinase-3β (GSK-3β) inhibitor, AR-A014418, and 0.2% DMSO as vehicles, for 4 h.

2.2.7 Immunoblotting

For western blot analysis, cells were scraped and collected by centrifugation at 7000 g for 2 min at 4°C. The collected cell pellets were washed once with ice-cold PBS and lysed in NP-40 lysis buffer. Protein extraction process was followed by sonicating the cell pellets in the lysis buffer, three times and for 5 sec, on ice. Then, sonicated mixture centrifuged at 12,500 g for 15 min at 4°C. The obtained supernatants were transferred to the clean tubes and the protein concentration in the cell extracts were measured using Pierce BCA Protein Assay Kit.

Western blotting was performed using the routine protocols. Briefly, extracted proteins were separated on sodium dodecyl sulfate polyacrylamide gel electrophoresis (SDS-PAGE). Electrophoresed proteins were transferred onto polyvinylidene fluoride (PVDF) membrane. Membranes were blocked with 5% (w/v) bovine serum albumin (BSA) in Tris-buffered saline containing 0.2% Tween 20 (TBS-T) for one hour at ambient temperature. Then, membranes were incubated overnight in the primary antibodies in 1% BSA in TBST, overnight at 4◦C. After washing, membranes were incubated in the appropriate HRP-conjugated secondary antibodies for two hours, at ambient temperature. Actin and Histon.H3 were used for loading controls. The antigens were visualized using Clarity™ and Clarity Max™ ECL Western blotting Substrates. Images were analyzed using ImageJ software (version 1.0) and were normalized to appropriate loading controls.

2.2.8 Immunocytochemistry

2.2.8.1 Neuronal, Nuclear and Tau Immunostaining

Cells were seeded at the density of 50,000 cells/well on glass coverslips. After differentiation according to the abovementioned protocol, cells were washed with pre-warmed PBS and fixed with cold Methanol for 10 min at -20°C. Proliferative cells were fixed after 48h of seeding. Then, they were washed twice with ice-cold PBS. Fixed cells were permeabilized using 0.25% (v/v) Triton X-100 in PBS for 10 min at ambient temperature and washed with PBS. Next, they were incubated with blocking buffer (10% (v/v) FBS in PBS, pH 7.4), for 30 min at ambient temperature. Cells were incubated with the primary antibodies overnight at 4°C. After three washes with PBS, this process was followed by incubation in respective Alexa flour conjugated secondary antibodies for one hour at ambient temperature. Nuclei were stained using DAPI for 8 min at ambient temperature. Finally, all coverslips were mounted onto glass slides with Mowiol.

2.2.8.2 DQ-BSA Immunostaining

Cells were incubated with 10 µg/ml DQ-BSA Red reagent, for 4 h at 37 °C followed by 3 PBS washes. Then, they were fixed with 4%(w/v) paraformaldehyde in PBS and stained with DAPI. Confocal imaging was carried out for all samples and red fluorescence intensity was measured by ImageJ software.

2.2.8.3 Actin Phalloidin Immunostaining

For actin phalloidin immunostaining, cells were fixed with 4%(w/v) paraformaldehyde in PBS after washing twice with PBS and incubated at ambient temperature for 15 min. Then, they were permeabilized with 0.1% (v/v) Triton X-100 in PBS and incubated for 15 min. Next, they were blocked with 1% (w/v) BSA in PBS for 30-40 min. 0.5 µl 400x actin phalloidin antibody was added in 200 µl blocking solution for each coverslip and incubated for one hour at ambient

temperature. After washing twice, next primary/secondary antibodies and DAPI were added. Stained coverslips were mounted with Mowiol.

2.2.9 DNA Methylation Assessment

2.2.9.1 DNA dot blot assay for 5mC and 5hmC

To assess general DNA methylation levels in the experimental groups, genomic DNA was extracted from cell lysates of pSH-SY5Y and dSH-SY5Y cells using Pure link genomic DNA kit (Invitrogen) according to the manufacturer's instructions. For DNA dot blot assessment, 250 ng of DNA was added to sodium hydroxide (NaOH, 0.4 M), ethylenediaminetetraacetic acid (EDTA, 10 mM) and neutralized with ice-cold ammonium acetate (2 M, pH 7.0). Prepared mixture was heat-denatured at 100°C for 10 min. Using dot blot apparatus (Bio Rad), denatured DNA was loaded on Zeta-Probe GT blotting membrane (Bio Rad). Then, the membranes were subjected to UV cross-linking. To block the membranes, they were kept at 3% BSA in TBST for 3 h, at ambient temperature. They were also overnight-incubated in primary antibodies, 5mC or 5hmC in TBST. After three washes, they were incubated in secondary HRP-conjugated antibodies for 2 h, at room temperature. Signals were visualized by enhanced chemiluminescence. To quantify total DNA, the membranes were stained with methylene blue (MB, 0.02%) in sodium acetate (0.3 M, pH 5.2). Fiji-ImageJ was used for blot quantifications.

2.2.9.2 LINE-1 Bisulfate Pyrosequencing

500 ng of isolated DNA of all experimental groups, including pSH-SY5Y and dSH-SY5Y cells were bisulfite-converted. Using PCR, amplification of a 92-base pair long region of the LINE-1 promoter was carried out. PCR amplification condition was the following: PCR activation at 95°C for 15 min, 45 cycles including denaturation at 95°C for 30 s, annealing at 58°C for 30 s and 30 s extension at 72°C, final extension lasting for 5 min at 72°C. To examine PCR product specificity,

gel electrophoresis on 2% agarose gel was carried out. To assess CpG levels of the LINE-1 retro-transposonic sequence, PCR-pyrosequencing was caried out using EZ DNA Methylation-Gold™ Kit, according to the manufacturer's protocols. To ensure the success of pyrosequencing and completion of bisulfite modification, 5 groups of high/low standard methylated controls were included. In addition to the methylated controls, negative controls were also included to ensure purity of samples. In these control groups, DNA was replaced by water. This experiment was performed on both proliferative and differentiated SH-SY5Y cells, and on two independent experimental points.

	Sequence
LINE-1 Forward Primers	ATTTTGGTGTTATGAATTTGATTTGAA
LINE-1 Reverse Primers	CTAATCCACTAAACTACTTACCAAATCTC
Sequencing Primers	GAGTAGATTAGAGTTTTGTT

Table 1-3: PCR-specific primers for human LINE-1

2.2.10 Data Analysis

2.2.10.1 Western blot analysis

Western blots were quantified using Fiji-ImageJ. To quantify the expression levels of total tau in pSH-SY5Y and dSH-SY5Y cells, measured signal from the whole lane was normalized to its Histone.H3 or β-actin signal (Figure 2-2). This analysis on the entire lane has been carried out as a basic step only to validate the expression levels of total tau protein in the experimental groups, including the controls.

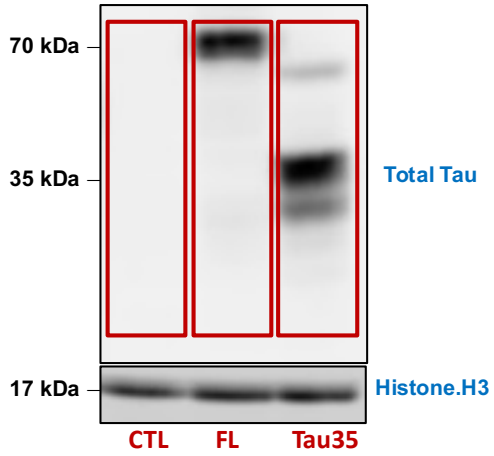

Figure 2-2: Quantification of tau expression levels in transfected cells and the control group. Measured signal from the whole lane was normalized to its housekeeping protein, Histone.H3 or Actin signal as the internal loading controls.

To quantify phosphorylation levels of PHF-1, AT180 and AT8 epitopes in the experimental groups, signals in FL- and Tau35- corresponding regions were measured around 70 kDa for FL and the region around 35 kDa for Tau35-expressing cells. The obtained quantity was divided by the same regions on the second step of staining with total tau. To obtain relative quantitation, housekeeping proteins, Histone.H3 or Actin, have been used as the internal loading controls (Figure 2-3).

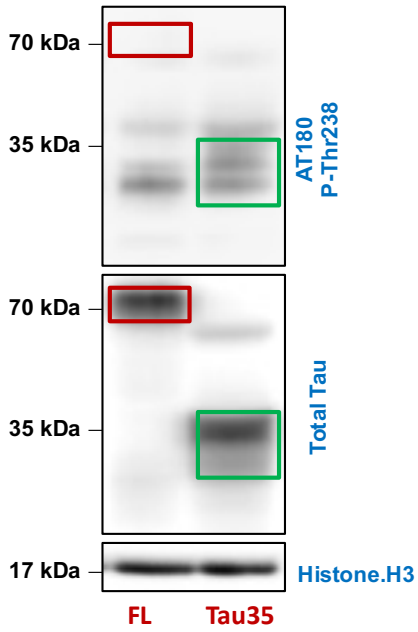

Figure 2-3: Quantification of tau phosphorylation levels in transfected cells. Measured signals around 70 kDa for FL-Tau and the region around 35 kDa for Tau35-expressing cells were divided by the same regions on total tau-stained blots. Housekeeping protein was included as the internal loading control.

2.2.10.2 Image Analysis

Confocal microscopy of the stained cells was performed using LSM710 Zeiss confocal microscope (Zeiss, Germany). ImageJ software (version 1.0) was used for analyzing images. Changes in f-actin distribution and structure have been analyzed using a Fiji Macro[130]. To assess f-actin distribution, phalloidin actin intensity was measured through the cell by 2-D confocal microscopy. To normalize the effect of differences in the cell size, cell shape and nuclear position, a line was automatically drawn perpendicular to the major (long) axis of the cell and over the nucleus (Figure 2-4a). This line divided the cytoplasm area into ten equal bins (Figure 2-4b). This specific feature provided equal and unbiased quantification of actin intensity over the cell[130]. Image analysis has been caried out on approximately 100 cells in 50 fields, and all experiments have been repeated three times and reported as three independent replicates.

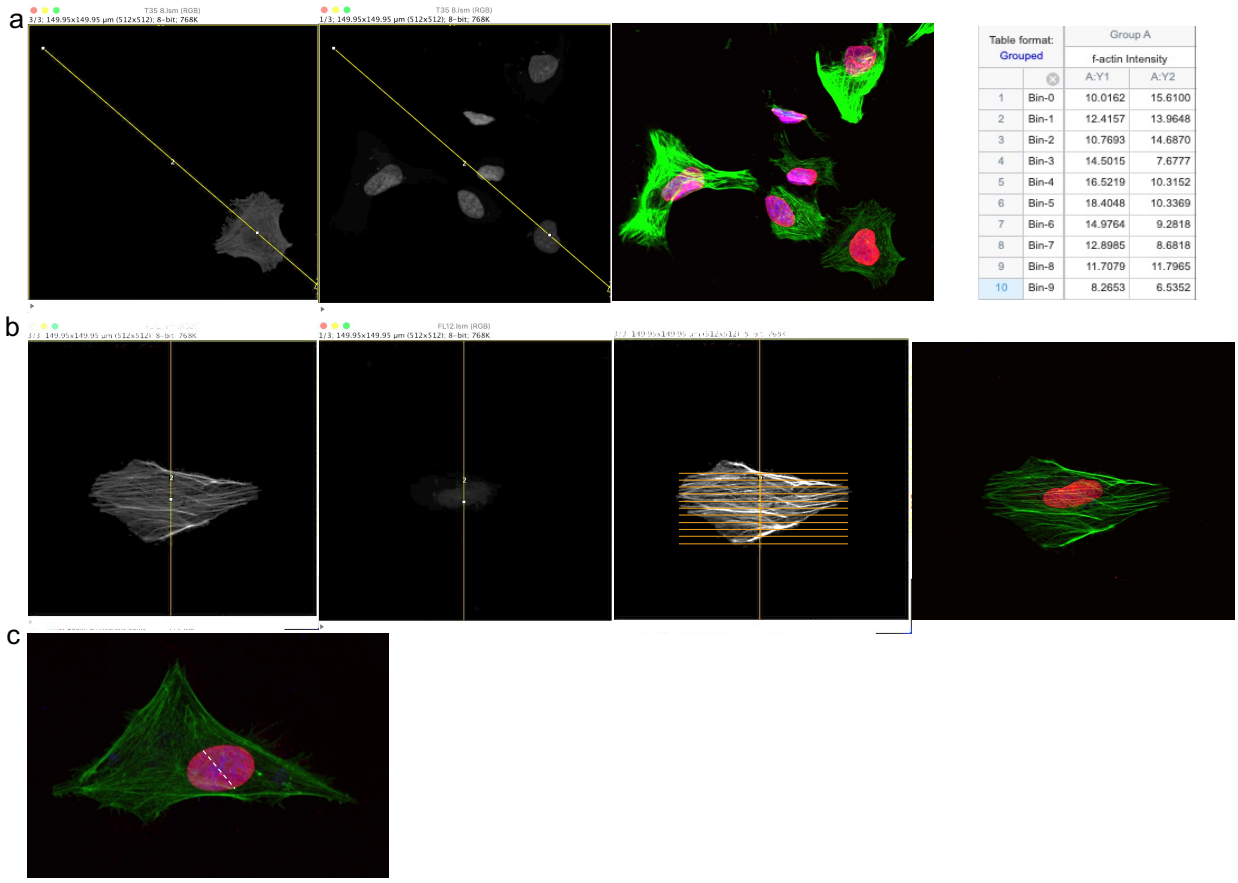

Figure 2-4: Quantification of f-actin distribution. a: The Fiji Macro by drawing a line perpendicular through the cell and over the nucleus could quantify the actin intensity in the cell. **b:** As the cells are not equal in size and morphology, macro automatically splited the pixel intensity data obtained from the line into 10 equal bins, meaning that the first bin is the first outer 10% of the cell. **c:** According to the defined channels for the macro, by passing over the nucleus, it could also measure the actin intensity over the nucleus.

2.2.10.3 Statistical Analysis

Quantitative analyses were performed using GraphPad Prism (Version 8.4.3). All obtained results were expressed as mean ±SEM. Two-tailed unpaired Student's t test was used to compare two means and one-way or two-way analyses of variance (ANOVA) with Tukey's post-hoc test was used to compare multiple means, as appropriate. Differences were considered statistically significant at p values less than 0.05.

3 Chapter III: Results

3.1 Retinoic Acid treatment induces neuronal-like phenotypes in SH-SY5Y cells.

Aiming to develop this cellular model of tauopathy, I selected SH-SY5Y human neuroblastoma cells. Human neuroblastoma cell line is an *in vitro* model widely used in the neuroscience research. Differentiated SH-SY5Y cells possess fundamental biochemical and functional features of neurons [131][132]. Retinoic acid (RA) is one of the best-characterized methods to induce differentiation process in SH-SY5Y cells. This vitamin A-derivative is an effective growth inhibitor and differentiation inducer[133][134]. In my experimental model, RA treatment could successfully induce neurite outgrowth after 7 days (Figure 3-1a). To understand how the differentiation processes affected these cells, I performed immunostaining. Labeling differentiated SH-SY5Y cells with neuron-specific markers confirmed expressions of β-Tubulin III, GAP43, MAP2A and NF-200 in dSH-SY5Y cells (Figure 3-1b). Further investigations and labeling with proliferation-related marker, Ki67, reveled reduced expression of this protein in differentiated cells compared to the proliferative SH-SY5Y cells (Figure 3-1c).

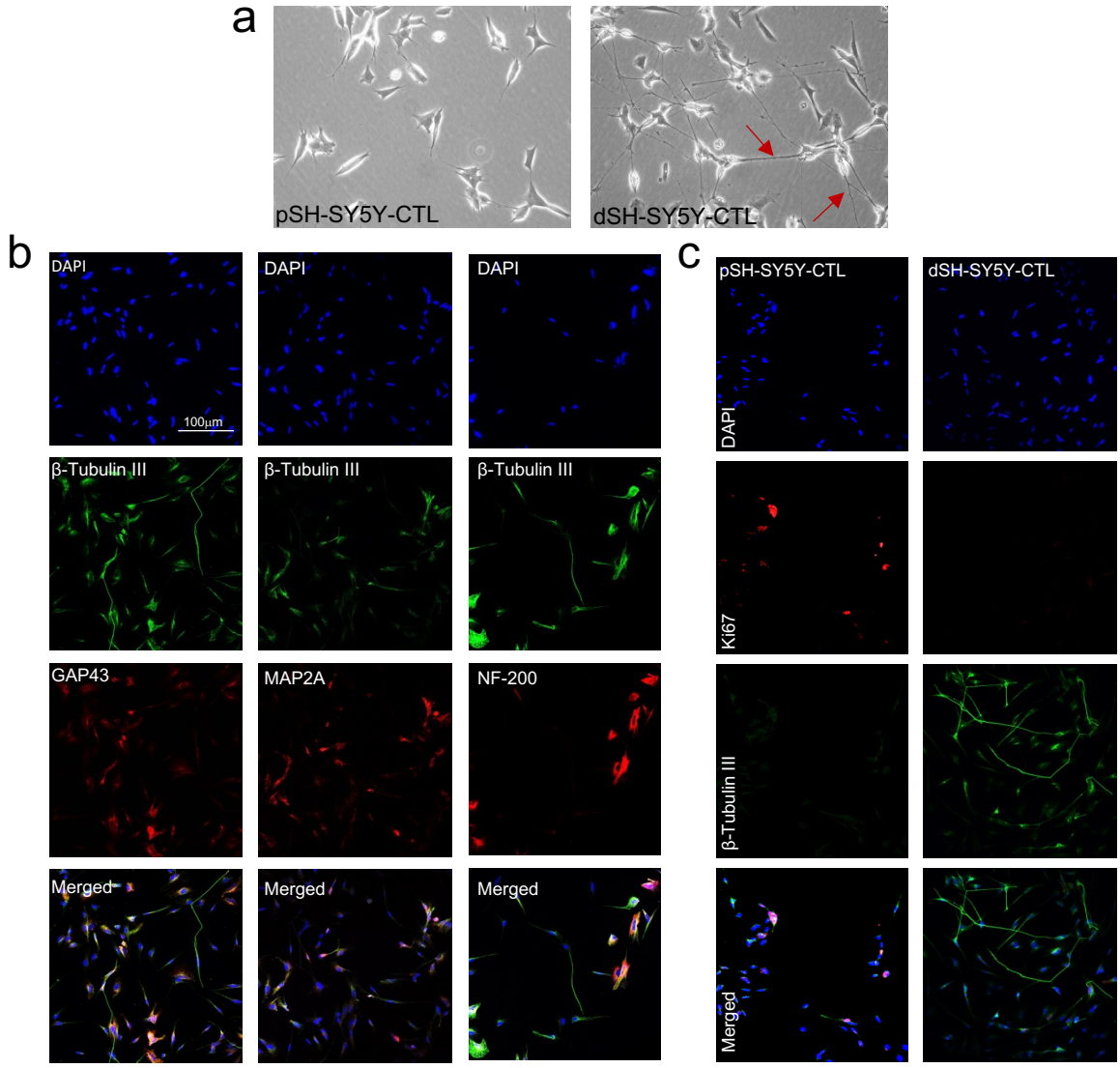

Figure 3-1: Retinoic Acid treatment induces neuronal-like phenotypes in SH-SY5Y cells. a: Phase contrast microscopy of SH-SY5Y cells representing a 7-day RA treatment (10uM) can lead to developing outgrowth dendritic/axonal processes in these cells (shown by red arrows). **b:** Confocal microscopic micrographs depicting expression of neuronal markers in differentiated SH-SY5Y cells: DAPI (blue), β-Tubulin III (green), GAP43, MAP2A, NF-200 (red). **c:** Confocal microscopy demonstrating effects of RA treatment on cellular morphology and proliferation levels. In the growth media, SH-SY5Y cells expressing Ki67 marker (red) but not high levels of β-Tubulin III (green) (left). After RA treatment, SH-SY5Y cells expressing β-Tubulin III but not Ki67 marker (right). Scale bar 100 µm.

3.2 SH-SY5Y cells can express high levels of FL-Tau and Tau35 by transient transfection

Guo et al. previously demonstrated inducing stable expression of human FL-Tau and Tau35 in Chinese hamster ovary (CHO) cells can provide a tool for evaluating the functional effects and signaling outcomes following pathogenic cleavage of tau protein. According to their results, CHO cells expressing Tau35 showed aberrant tau phosphorylation and less microtubule binding affinity which in turn led to defective microtubule organization. Moreover, Tau35 fragment affected upstream signaling pathways. Through gaining toxic functions and perturbation of Akt signaling pathway, Tau35 overexpression led to activation of GSK-3β, which is the stimulator of tau hyperphosphorylation [128]. To generate the cellular model of tauopathy, I transiently transfected human neuroblastoma cells (SH-SY5Y) with the same constructs, human FL-Tau and the 35 kDa C-terminal fragment of FL-Tau protein (Tau35). Administration of RA (10 μM) in growth medium containing 1% FBS for 7 days has been previously shown to induce post-mitotic neuronal-like phenotypes in SH-SY5Y cells[135]. Following the same protocol, I induced transfected cells. Morphologically, RA treatment developed longer neurites in dSH-SY5Y-CTL cells compared to the two groups of transfected cells. However, during RA treatment, SH-SY5Y-FL and -Tau35 appeared to maintain their proliferation abilities in comparison with SH-SY5Y-CTLs (Figure 3-2).

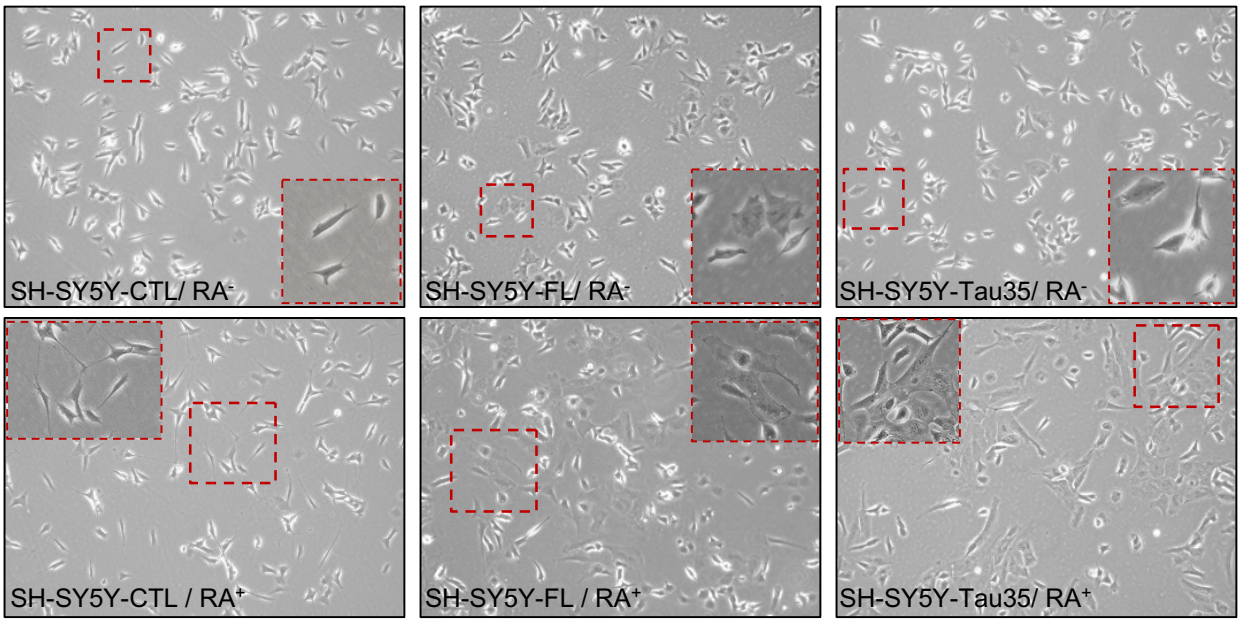

Figure 3-2: Differentiation of SH-SY5Y cells with retinoic acid (RA). Bright field images representing SH-SY5Y cells morphology before (/RA^-) and after (/RA^+) treating with 10 µM retinoic acid for 7 days. Three groups of proliferative cells (pSH-SY5Y) were plated on desired dishes at the same density. After 24h, growth media have been switched with differentiation media. After 7 days, these cells have been named as dSH-SY5Y cells and used for future experiments.

To confirm the successful transfection and evaluate the expression levels of FL-Tau and Tau35, after antibiotic-selection of colonies, western blotting has been carried out on the cell lysates obtained from generated cell lines. Blots were labeled with the human-specific anti-tau antibody. According to the blot analysis, FL-Tau stable transfection was confirmed by the presence of a band near 70 kDa in FL-expressing cells, and Tau35-transfected cells showed a prominent band at 35 kDa but multiple bands ranging from 25 kDa to 37 kDa were also detected with an antibody against total Tau. Quantitative immunoblotting carried out to validate FL-Tau and Tau35 levels in transfected cells (pSH-Y5Y-FL, pSH-SY5Y-Tau35) compared with the non-transfected cells (pSH-SY5Y-CTL). These western blot analyses showed stronger human tau expression levels in transfected cells compared to the control group (p=0.2699 for pSH-FL and p=0.0090 for pSH-Tau35)(Figure 3-3a).

After seven days of RA treatment and differentiation, tau expression levels were assessed using western blotting and immunocytochemistry. According to these results, human tau expression levels in dSH-SY5Y-FL and dSH-SY5Y-Tau35 were higher than control group (p=0.0028 for dSH-FL and p=0.2538 for dSH-Tau35 in western blot analysis and p<0.0001 for dSH-FL and p=0.0010 for dSH-Tau35 obtained from ICC) (Figure 3-3b/d). As the positive controls, I tested two antibodies on normal and AD human brain samples. Representative blots exhibited a band for human total tau below 70 kDa and for PHF-1 at the same region only for human AD samples (Figure 3-3c).

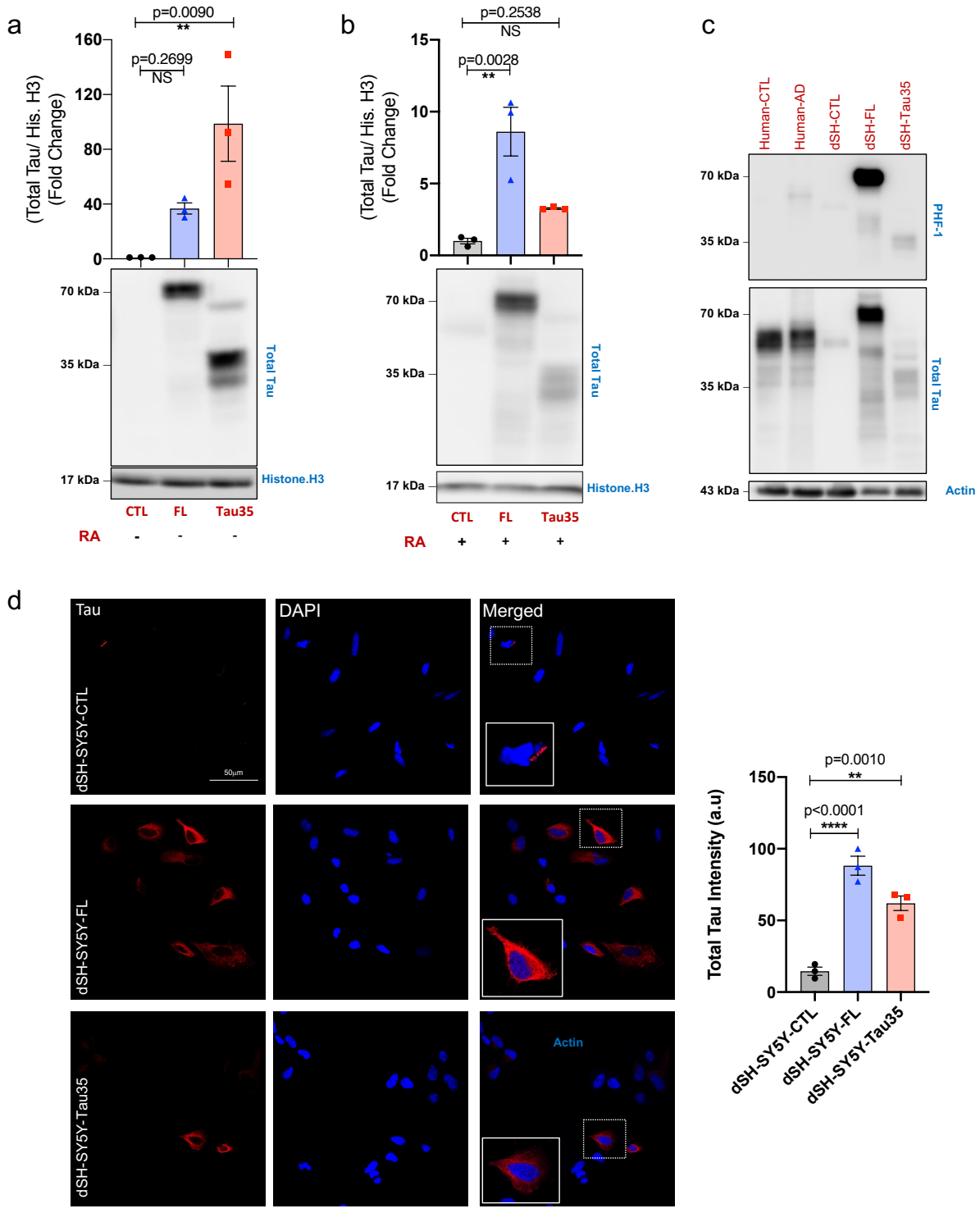

Figure 3-3: Higher Tau expression has been detected in the transfected groups compared to the controls. a: Western blot of pSH-SY5Y cell lysates probed with anti-total tau antibody depicted total tau expression is higher in both transfected groups (pSH-SY5Y-FL, pSH-SY5Y-Tau35) compared with the control group (pSH-SY5Y-CTL). **b:** Same analysis on dSH-SY5Y cells confirmed that transfected cells retain their higher tau expression after

differentiation. **c:** Representative western blots to compare normal and AD human brain samples with my experimental groups (dSH-SY5Y cells). **d:** Immunofluorescence of dSH-SY5Y cells labeled with total tau (red) and DAPI (blue, nuclei) showing differences in tau intensity between experimental groups. Scale bar 50 μm. Values represent mean ± SEM., N=3, one-way ANOVA, *$p < 0.05$ is considered as significant difference.

3.3 Tau phosphorylation levels did not increase significantly in this cellular model of tauopathy.

Tau hyperphosphorylation has often been considered as one of the main causes of pathology associated with tauopathy, and it was recently shown that overexpression of Tau-35 fragment is sufficient to induce more severe molecular changes in CHO-cells[128]. I first examined the status of tau hyperphosphorylation after overexpression of these two constructs in SH-SY5Y cells. I focused on three specific residues located at the C-terminal domain of full-length isoform of tau, Thr231, Ser202/Thr205 and S396/S404. Aberrant phosphorylation of these three residues is associated with development of human tauopathy phenotypes[136]. Both proliferative and differentiated cells were labeled with three phospho-dependent tau antibodies, AT180, AT8 and PHF-1 that recognize p-Thr231, p-Ser202/Thr205 and p-S396/S404 residues, respectively.

Guo et al. previously demonstrated that overexpression of Tau35 fragment in CHO cells correlates with elevated phosphorylation at Thr231, Ser202/Thr205 and S396/S404 epitopes compared to the FL-expressing cells. According to their western blot analysis, CHO-FL cells showed modest or negligible immunoreactivity of these three epitopes while CHO-Tau35 cells showed multiple bands in 35 kDa region, indicating exacerbated tau phosphorylation after pathologic tau overexpression. Gel densitometry revealed that Tau35 phosphorylation was approximately 2-3-fold higher than FL-tau. In my experimental model, although I observed some increased phosphorylation of Thr231, Ser202/Thr205 residues in proliferative and differentiated SH-SY5Y cells, these increases were not statistically significant, (p>0.05 for p-Thr231 epitope and p-

Ser202/Thr205 residue) (Figure 3-4 a/b). Additionally, immunoblotting against p-S396/S404 and labeling with PHF-1 antibody demonstrated phosphorylation levels of this residue is higher in differentiated FL-tau expressing cells compared to dSH-SY5Y-Tau35 cells. This difference was not significant (p=0.6737) (Figure 3-4c).

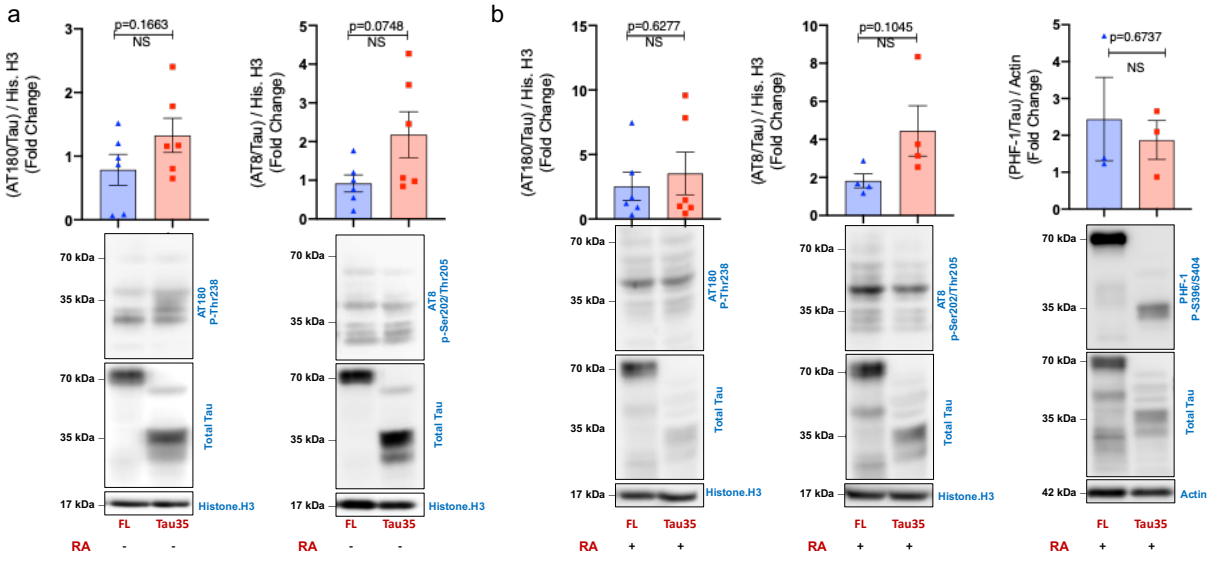

Figure 3-4: The effect of FL-Tau and Tau35 overexpression on tau phosphorylation a: Representative western blots showing phosphorylation levels of human tau at three residues, AT180 and AT8 in proliferative cells, pSH-SY5Y-FL and pSH-SY5Y-Tau35. Quantification of p-Tau/Total Tau is shown in transfected cells, (70 kDa in SH-SY5Y-FL and 35 kDa in SH-SY5Y-Tau35). (n=6 independent experiments) data shown as mean ± SEM, unpaired Student's t test, *p< 0.05 is considered as significant difference. **b:** Same assessments on dSH-SY5Y-FL and dSH-SY5Y-Tau35 were carried out. PHF-1 antibody has been also used in differentiated cells.

To test whether the discrepancies between my results and those reported by Guo et al. in CHO cells [128] is indicative or the cell type, I also performed these experiments in CHO cells but did not observe any significant difference between the two different cell types (p=0.5353) (Figure 3-5).

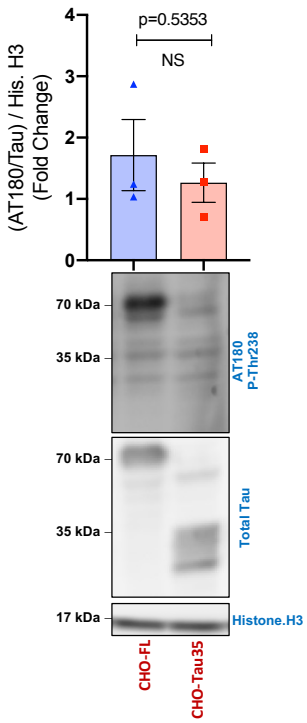

Figure 3-5: The effect of FL-Tau and Tau35 overexpression on tau phosphorylation in CHO cells. Representative western blots showing phosphorylation levels of human tau AT180 CHO cells. Quantification of p-Tau/Total Tau is shown in transfected cells, (70 kDa in CHO-FL and 35 kDa in CHO-Tau35). (n=3 independent experiments) data shown as mean ± SEM, unpaired Student's t test, *$p < 0.05$ is considered as significant difference.

Moreover, I applied the same commercial antibodies used in the abovementioned research. It is possible that the differences are indicative lot differences between these antibodies.

3.4 Autophagy-lysosomal pathway was unaffected in pSH-SY5Y and dSH-SY5Y tauopathy model

Dysfunction of autophagy-lysosomal pathway (ALP), known as macrophagy, is another hallmark of human tauopathies[137]. In healthy neurons, dysfunctional tau is primarily cleared by autophagy[138] and tau toxicity could be the contributor or a consequence of impaired autophagy[139][140]. Therefore, in my experimental model, I assessed various major ALP

indicators, including the substrate selection and autophagosome biogenesis marker, microtubule-associated protein 1-light chain 3 (LC3-II/LC3-I), ubiquitin-binding autophagy receptor protein p62, lysosome-associated membrane glycoproteins-2 (LAMP2), and lysosomal activity.

In autophagy, cargo targeted for lysosomal degradation is packed with phagophore, a membranous vesicle that is coated by LC3-II. LC3-II is generated by conjugation of cytosolic form of LC3-I to phosphatidylethanolamine [141][142]. Additional tag for identification of macro autophagy targets is p62 which transports cargo into the autophagosomes by interacting with LC3-II [143]. The ratio of LC3-II/LC3-I and p62 levels in the cells are indicators of autophagy progression. Using western blotting, I found a significant accumulation of LC3-II/LC3-I in pSH-SY5Y-FL (p=0.0209) and dSH-SY5Y-Tau35 cells (p=0.0147) compared to their controls; however, there were no significant changes in the expression levels of p62 in all experimental groups. This can indicate an increase in cargo turnover without significant changes in autophagosome clearance (Figure 3-6).

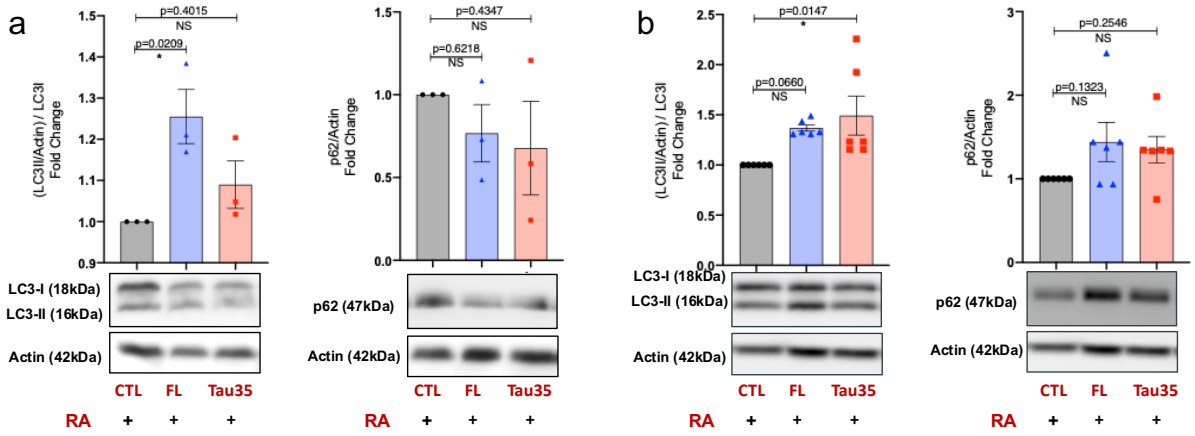

Figure 3-6: Autophagosome clearance was not affected in this cellular model of tauopathy model. Western blot analysis depicting the cellular levels of LC3-II/LC3-I ratio and p62 in pSH-SY5Y **(a)** and dSH-SY5Y **(b)** cells. The data represent mean ± SEM., (n=3 proliferative cells, n=6 dSH-SY5Y cells), one-way ANOVA, *p< 0.05 is considered as significant difference.

To further examine lysosomal activity involved in this process, I opted to measure the protein degradation capacity of lysosomes in pSH-SY5Y cells. DQ-BSA is a fluorescent reagent that is activated in the acidic environment of lysosomes and therefore is used as an indicator of lysosomal activity [137]. While control and Tau-FL overexpressing cells did not show significant differential DQ-BSA fluorescence activities, the Tau35 overexpression in pSH-SY5Y cells induced a significant increase in fluorescence indicating enhanced lysosomal activity (p=0.0088 vs. pSH-SY5Y-CTLs and p=0.0190 vs. pSH-SY5Y-FLs) (Figure 3-7).

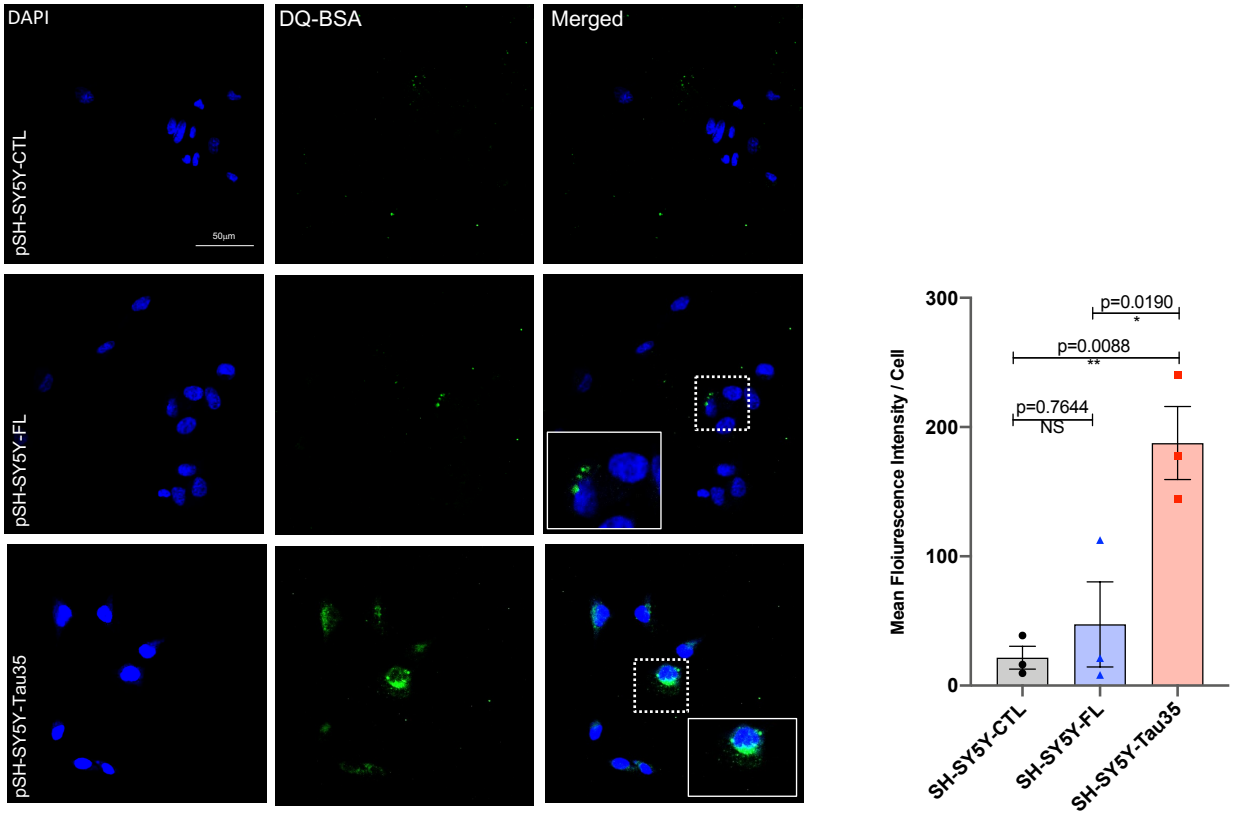

Figure 3-7: Tau35 overexpression enhances lysosomal activity in comparison with Tau-FL and control proliferative SH-SY5Y cells. All three proliferative experimental groups were loaded with DQ-BSA (10µg/ml). Representative confocal microscopic micrographs depicting degradation of DQ-BSA (green signal) in pSH-SY5Y-CTL, -FL and-Tau35 cells. Scale bar 50 µm. DQ-BSA fluorescence normalized to per cell are shown. Values represent mean ± SEM., n=3, ~90 cells/group, one-way ANOVA, *$p < 0.05$ is considered as significant difference.

To examine the increased lysosomal activity observed in Tau-35 cells, I opted to compare the levels of lysosomal membrane associated protein 2 (LAMP2) which is a prominent component of lysosomal membrane and its role in autophagy and lysosomal membrane permeabilization (LMP) has been confirmed [144]. However, using western blot analysis on pSH-SY5Ycells did not show any significant changes in LAMP2 protein levels for pSH-SY5Y-FL (p=0.2595) and in pSH-SY5Y-Tau35 (p=0.2131) groups when compared to the controls (Figure 3-8). As I did not detect evidence of damage in this pathway, differentiated cells were not targeted for these assessments.

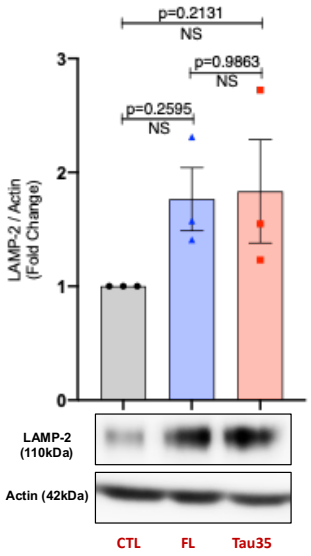

Figure 3-8: No evidence of increased lysosomal synthesis was observed in FL and Tau35 overexpressing pSH-SY5Y cells. Representative bands from transfected and non-transfected pSH-SY5Y cell lysates were evaluated by western blotting. Values represent mean ± SEM., n=3, one-way ANOVA, *p< 0.05 is considered as significant difference.

3.5 Tau35 overexpression is associated with exacerbated cytoskeletal and nucleoskeletal alterations.

3.5.1 Overexpression of Tau35 in dSH-SY5Y neurons exacerbates nuclear lamina invagination.

Nuclear lamina invagination has been described in *Drosophila* model of tauopathy [71] and was also confirmed by our group in human AD hippocampal tissue [123]. I therefore asked whether my model of tauopathy is also associated with nuclear lamina invagination and whether there is any difference between the two tau constructs. As differentiated cells are recognized as neuronal-like human neuroblastoma cells, I examined the status of cyto-nucleoskeleton in my experimental model by performing immunocytochemistry on differentiated SH-SY5Y-FL, -Tau35 and -CTL cells. Nuclear invagination was assessed using an arbitrary grading system. The severity of nuclear lamina invagination was scored between 0 (no NL invagination) to 3 (most severe invagination). Between this range of damage, nuclei detected with one or two lines of invagination have been categorized as Grade 1. Grade 2 damage has been allocated to the ones with damages one level milder than the severest and fully-shrunken nuclei. I observed that while overexpression of tau was sufficient for a significant raise in nuclear invagination in comparison with the control cells (p=0.0436), Tau35-overexpressing dSH-SY5Y cells displayed the highest rate of nuclear lamina invagination when compared to the control group (p=0.0149) (Figure 3-9 a/b). My grading scale confirmed that tau overexpression is inversely related with the percentage of normal nuclei, as in dSH-SY5Y-CTLs there were significantly higher numbers of normal nuclei compared to the -FLs (p=0.0002) and -Tau35s (p<0.0001). In contrast, Tau35-overexpressing dSH-SY5Y cells displayed the highest number of severely-damaged nuclei (Grade-3) compared to the controls (p=0.0012) (Figure 3-9c).

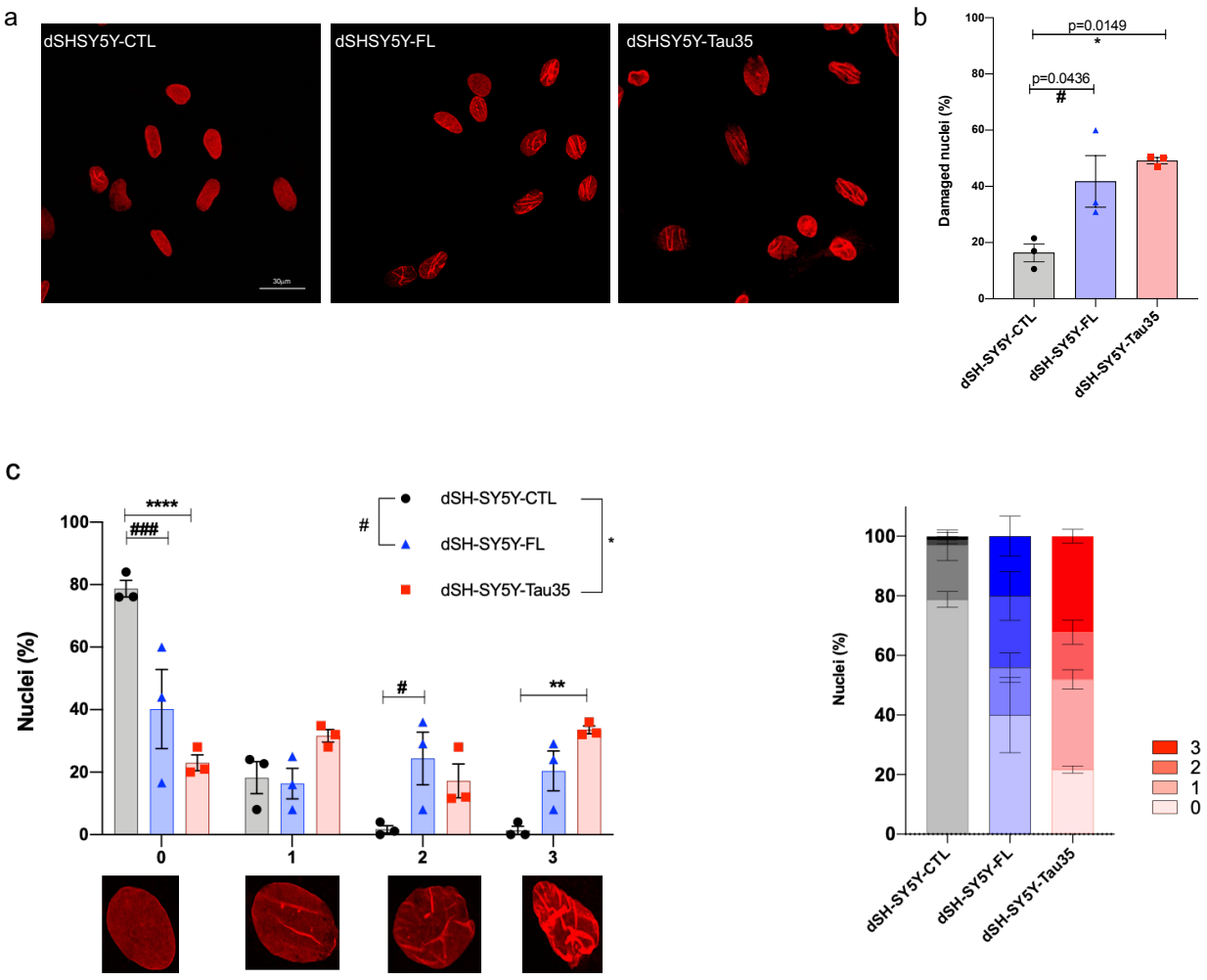

Figure 3-9: Tau overexpression is associated with increased nuclear lamina invagination in dSH-SY5Y cells. a,b: Confocal microscopic micrographs depicting nuclear lamina status in dSH-SY5Y cells, LB1 (red), DAPI (blue) and image analysis. Scale bar 30 µm. **c:** An arbitrary scaling system was used to show differential invagination severity: grade 0 (normal nuclear lamina) to grade 3 (the most severe invagination). The numbers of invaginated nuclei were expressed as % of total cells and analyzed by one-way ANOVA (nuclear lamina damage). Two-way ANOVA analysis was used to assess graded nuclear lamina damages in different conditions. Values represent mean ± SEM., n=3, 300 cells/group and $p < 0.05$ was considered as significant difference.

3.5.2 Nuclear lamina invagination after FL-Tau and Tau35 overexpression is not associated with nuclear Lamin-B protein degradation.

Nuclear lamina invagination has been originally reported in tauopathies. Therefore, I tested the molecular integrity of nuclear lamina in my experimental groups. Lamin B1 (LB1) protein

degradation was originally reported in *Drosophila* model of tauopathy shown by Frost et al. [73] [145]. Our lab also previously discovered two C-terminal fragments of LB1in hippocampal tissue lysate obtained from our 3xTg mouse model: a 46 kDa and a 21 kDa[125]. Further investigation revealed that the 46 kDa fragment is a product of caspase-6 (CASP6) activation and the 21 kDa fragment is cleaved by cathepsin L (CTSL)[126]. To identify whether nuclear lamina degradation is generated by FL-Tau or Tau35 overexpression in SH-SY5Y cells, western blotting was used for assessment of LB1 protein in both proliferative and differentiated experimental groups. The results indicated the nuclear lamina invagination in these conditions was not associated with lamin-B1 proteolytic degradation as no lamin-B1 positive band was observed (Figure 3-10).

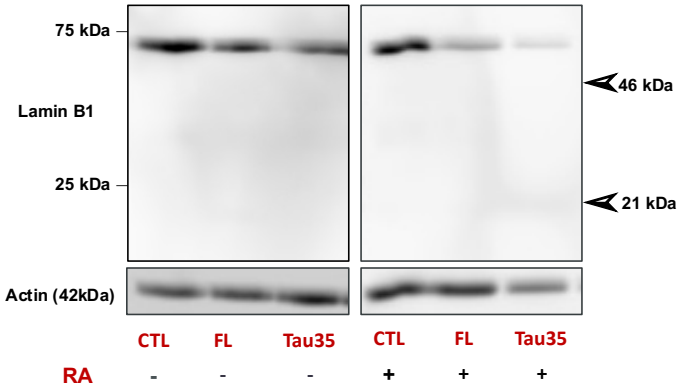

Figure 3-10: Nuclear lamina invagination in FL-Tau / Tau35 overexpression does not induce Lamin-B1 proteolytic degradation in SH-SY5Y cells. Western blots examining Lamin-B1 integrity in transfected cells (proliferative and differentiated groups). No evidence of Caspase-6 or cathepsin L was detected in these conditions (n=3).

3.5.3 FL-Tau and Tau35 overexpression adversely affects f-actin distribution in dSH-SY5Y cells

The importance of tau and its interaction with actin and microtubules in cytoskeleton structure and function has been well-documented. Recent reports linked tau hyperphosphorylation with actin

fibrilization and induction of nuclear damage, including nuclear lamina invagination and disruption of nucleocytoplasmic trafficking by weakening nuclear pore localization/function [142][74][75]. To further investigation of the tau involvement and developing therapeutic strategies, I first examined whether pathogenic tau fragment and FL-Tau overexpression can induce f-actin overstabilization in dSH-SY5Y cells. I used immunocytochemistry to assess the status of actin filaments in my experimental groups. Several aspects of actin filament were tested including average total cellular actin intensity, perinuclear actin density where the tau/f-actin/nuclear lamina interact, and also f-actin distribution through the cells.

Analyzing f-actin distribution in the dSH-SY5Y cells revealed the distribution of f-actin changes upon FL-Tau and Tau35 overexpression (Figure 3-11). In control cells, and in FL-Tau overexpressing cells, actin was distributed evenly in the cell, while in Tau35-overexpressing dSH-SY5Y cells f-actin intensity was more prominent in the center than the peripheral regions, when compared to both FL-overexpressing cells and the control group (Figure 3-11b).

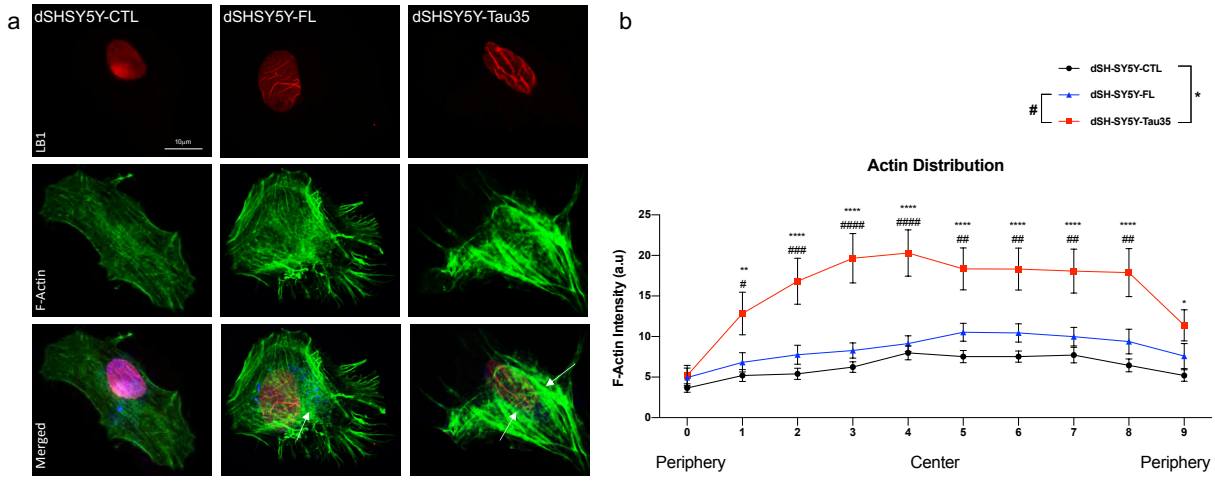

Figure 3-11: Tau overexpression is associated with alterations in f-actin distribution in dSH-SY5Y cells. a: Micrographs obtained from confocal microscopy representing distribution of actin filaments through the experimental groups. F-actin was stained with actin-phalloidin (green), nuclear lamina with LB1 (red). Nuclei were counter stained with DAPI (blue) and included in the merged panel. Scale bar 10 µm. Note the clear remodeling of f-actin cytoskeleton in close association with nuclear envelope invagination in dSH-SY5Y cells

(white arrows). **b:** Graphs representing actin distribution through the cells by comparing average actin intensity through the bins splitted by Fiji Macro in each experimental group. Mean fluorescent intensity for f-actin was quantified and shown as mean ± SEM., n=3, 300 cells/group, and $p < 0.05$ was considered as significant difference. Two-way ANOVA with Sidak's multiple comparisons for each bin was performed.

Examination of perinuclear actin intensity showed that overexpression of both isoforms of tau leads to increased arrangement of actin filaments when compared to the control cells. Additionally, higher f-actin intensity was found over the nucleus in FL- and Tau35- overexpressing dSH-SY5Y cells compared to the controls (p=0.0001 and p=0.0395, respectively) (Figure 3-12). Average actin intensity was also significantly higher in dSH-SY5Y-Tau35 cells compared to two other groups (p<0.001) (Figure 3-12b).

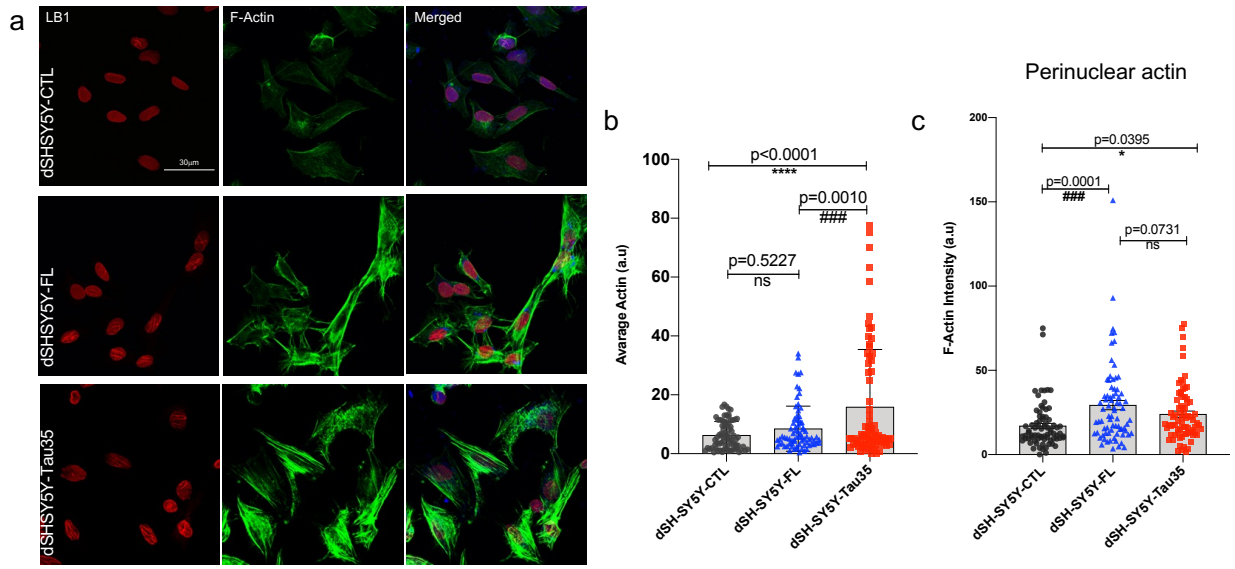

Figure 3-12: Tau overexpression is associated with f-actin over-stabilization in dSH-SY5Y cells. a: In all panels, f-actin cytoskeleton was stained with actin-phalloidin (green), nuclear lamina with LB1 (red). Nuclei were counter stained with DAPI (blue). Scale bar 30 µm. Graphs representing average actin intensity through the cell **(b)**, perinuclear **(c)**. Mean fluorescent intensity for f-actin was quantified and shown as mean ± SEM., n=3, 300 cells/group, and $p< 0.05$ was considered as significant difference. One-way ANOVA analysis for graphs b and c.

3.6 Nuclear lamina invagination in tau constructs overexpressing cells is not associated with chromatin changes.

3.6.1 FL-Tau and Tau35 overexpression did not correlate with double-strand breakage in DNA

Previous reports have linked nuclear lamina damage in tauopathy and AD to chromatin rearrangement and changes in gene expression. Using a cellular model of Aβ toxicity in SH-SY5Y cells, our lab has also shown a connection between NL invagination and changes in nuclear architecture including histone modification in SH-SY5Ycells [125]. Additionally, in *Drosophila* and mice models of tauopathy and human AD brains have been also shown that tau-induced f-actin over-stabilization leads to nuclear lamina damage which ultimately promotes heterochromatin relaxation, reduces DNA methylation levels and activates normally silenced transposable elements[79][145]. Since my cells showed evidence of nuclear and cytoskeletal changes in this model, I aimed to further investigate whether these nuclear events are observed in this cellular model. Therefore, I evaluated one of the early cellular responses to the induction of double-strand DNA breakage, γH2AX formation, using immunocytochemistry[146][147]. Quantifying number of γH2AX foci in dSH-SY5Y experimental groups, I did not detect any robust changes in γH2AX foci per nucleus in FL- and Tau35- overexpressing dSH-SY5Y cells compared to the controls (p=0.2514, p=0.9990, respectively) (Figure 3-13).

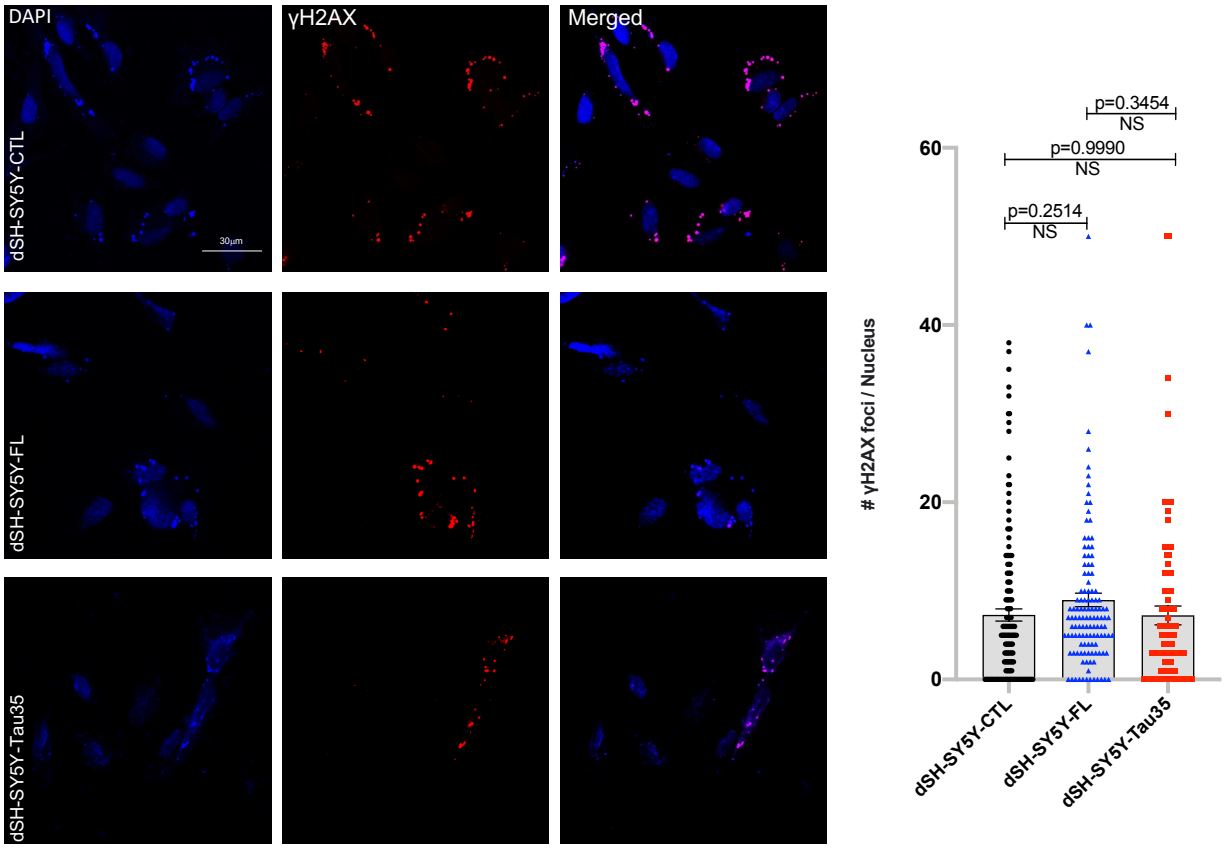

Figure 3-13: Overexpressing FL-Tau or Tau35 in dSH-SY5Y cells do not show evidence of enhanced DNA damage. Representative images of immunocytochemistry for anti-γH2AX (red) and DAPI (blue) in dSH-SY5Y cells. Scale bar 30 μm. The p-value was obtained by one-way ANOVA analysis. Graphs are shown as mean ± SEM., n=3, and $p < 0.05$ was considered as significant difference.

3.6.2 FL-Tau and Tau35 overexpression did not epigenetically affect SH-SY5Y cells

3.6.2.1 Global DNA Methylation Assessment

In tauopathies, epigenetic alteration through DNA methylation is identified as a major hallmark of neurodegeneration[148]. 5-methylcytosine (5mC) and its oxidized form, 5-hydroxymethylcytosine (5hmC) are prominent markers of DNA methylation and DNA hydroxy methylation in tauopathies and neurodegeneration. Increase in 5mc levels represents inhibition of gene expression, while rise in 5hmC is associated with increased gene expression. For instance, immunohistochemistry and double-fluorescent immunolabeling on the human middle frontal gyrus (MFG) and middle temporal gyrus (MTG) obtained from AD patients and age-matched

controls demonstrated global levels of DNA methylation positively correlates with the presence and loads of AD pathogenic markers, such as tau, Aβ, and ubiquitin[149]. To investigate whether DNA methylation level is globally changed in pSH-SY5Y and dSH-SY5Y experimental groups, I evaluated changes in 5hmC and 5mC levels. Quantitative DNA methylation analysis by DNA dot blot assay showed that FL and Tau35 overexpression did not cause any significant alteration in the 5mC and 5hmC levels in pSH-SY5Y and dSH-SY5Y cells ($p \geq 0.5$) (Figure 3-14).

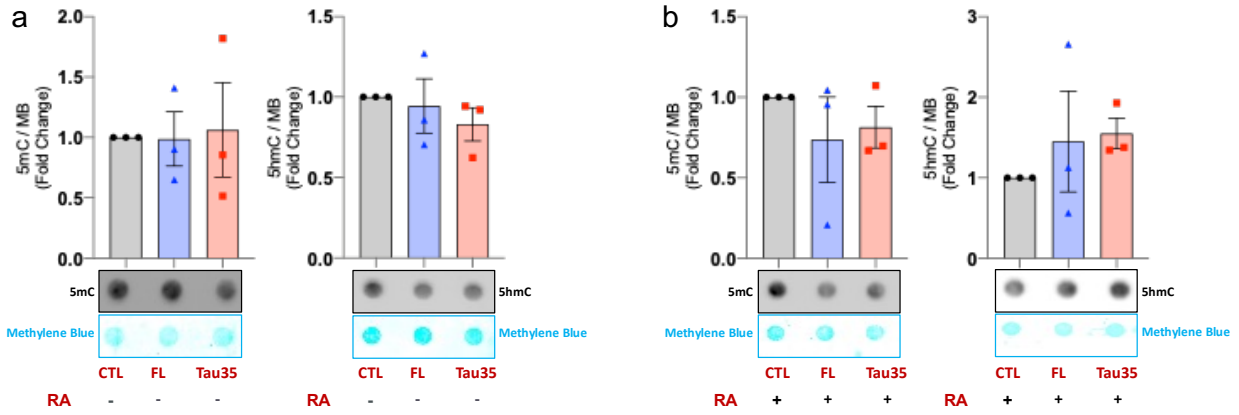

Figure 3-14: No epigenetic alteration has been detected in the experimental models. Overexpression of tau or its pathologic fragment did not result in any detectable DNA methylation in proliferating **(a)** or differentiated **(b)** SH-SY5Y cells. DNA dot blot experiments have been performed to detect global DNA methylation alterations at 5mC and 5hmC. Quantification of global 5mC and 5hmC levels was normalized to the total DNA levels stained with methylene blue. Fold changes were calculated for each group. Graphs are shown as mean ± SEM., n=3, and $p < 0.05$ was considered as significant difference.

3.6.2.2 LINE-1 CpG Methylation Assessment

Increased expression of transposable elements or repetitive families is reported in tauopathies. Long interspersed repeat-1 (LINE-1) has often been used as an indicator of global DNA methylation as it is abundantly present the human retroelements in the genome in animal models of tauopathy [78]. To examine the effect of tau-mediated nuclear lamina invagination on LINE-1 methylation, three probes were designed for LINE-1 pyrosequencing in both experimental groups, proliferative and differentiated SH-SY5Y cells. As shown in Figure 3-15, FL-Tau and Tau35 over expression did not trigger any considerable changes in the percentage of LINE-1 CpG methylation compared to the controls.

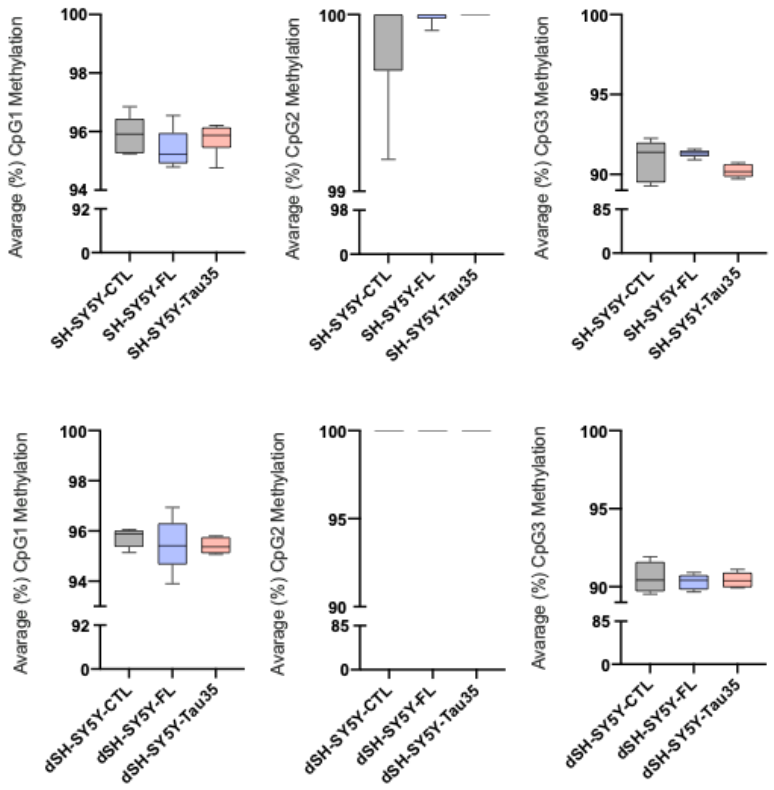

Figure 3-15: Global DNA methylation is not significantly changed in FL-Tau and Tau35 overexpression. Validation of CpG methylation using methylation pyrosequencing in proliferative and differentiated SH-SY5Y cells. Analysis was performed on two independent replicates (n=2).

3.7 Pharmacological interventions to inhibit tauopathy-related characteristics in SH-SY5Y-derived model of tauopathy

As the second aim of the current study, I decided to examine whether the nuclear lamina invagination can be decreased in this model of tauopathy. Therefore, I targeted upstream compartments of nuclear lamina and the key factor of tauopathy pathology, aberrant tau phosphorylation. Activation of two critical kinases, JNK and GSK-3β, is associated with aberrant tau phosphorylation and their inhibition could be effective in reducing tau pathology consequences[45][46]. I tested the effect of my candidate kinase inhibitors, JNK inhibitor (SP600125) and GSK3-β inhibitor (AR-A014418) on viability of proliferating SH-SY5Y cells as the basic cellular model of this study. Cells were treated for four hours with 10 and 20 µM of these small molecule inhibitors[150]. Cell viability assessment showed that both concentrations do not

cause excessive cell death and therefore I used 10uM which is well-tolerated by these cells (Figure 3-16).

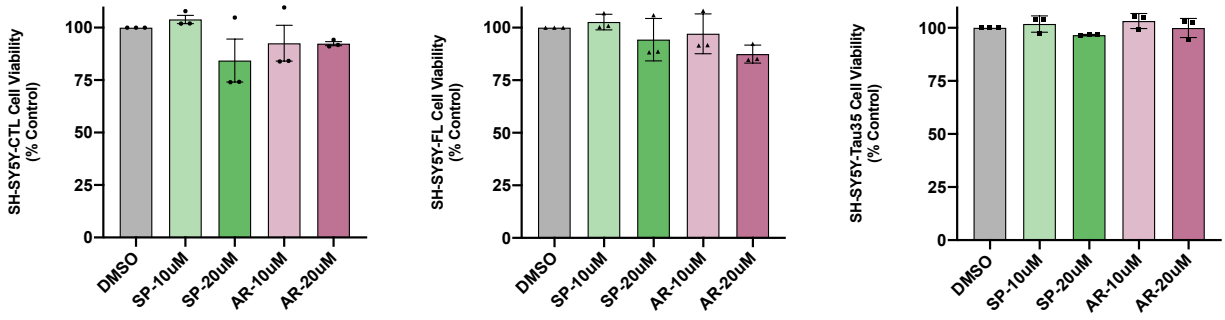

Figure 3-16: JNK inhibitor (SP600125) and GSK3-β inhibitor (AR-A014418) cell toxicity assessment. Proliferative SH-SY5Y cells were cultured and 24 hours after seeding were treated with 10 and 20 μM of kinase inhibitors. Cell viability was assessed after the four-hour treatment by CCK8 assay. The bars in graphs indicate mean ± SEM of average from n=3 independent experiments. One-way ANOVA analysis was performed for data analysis and $p< 0.05$ was considered as significant difference.

3.8 Administration of inhibitors did not alter tau phosphorylation significantly.

Based on toxicity assay, I treated the main experimental groups, proliferative and differentiated SH-SY5Y cells with 10 μM of JNK inhibitor (SP600125) and GSK3-β inhibitor (AR-A014418) for four hours. To examine whether these small molecules affect tau phosphorylation at three residues, Thr231, Ser202/Thr205 and S396/S404, I performed western blot assessment on the cell lysates. According to the immunoblotting results, treating with JNK inhibitor (SP-600125) lowers phosphorylation of Thr231 in pSH-SY5Y-FL and dSH-SY5Y-FL cells (Figure 3-17a/b). GSK3-β inhibition reduces p-Ser202/Thr205 levels in both proliferative and differentiated SH-SY5Y-Tau35 cells (Figure 3-18c/d). Regarding Thr231 residue, AR-A014418 lowers its phosphorylation levels in dSH-SY5Y-FL cells (Figure 3-18a). None of these alterations were statistically significant ($p>0.05$). Obtained blots from other residues revealed that antibodies recognizing Thr231, Ser202/Thr205 and S396/S404 did not exhibit detectable bands prior or post treatments. These blots were not quantified and only representative figures are available in Figures 3-17-19.

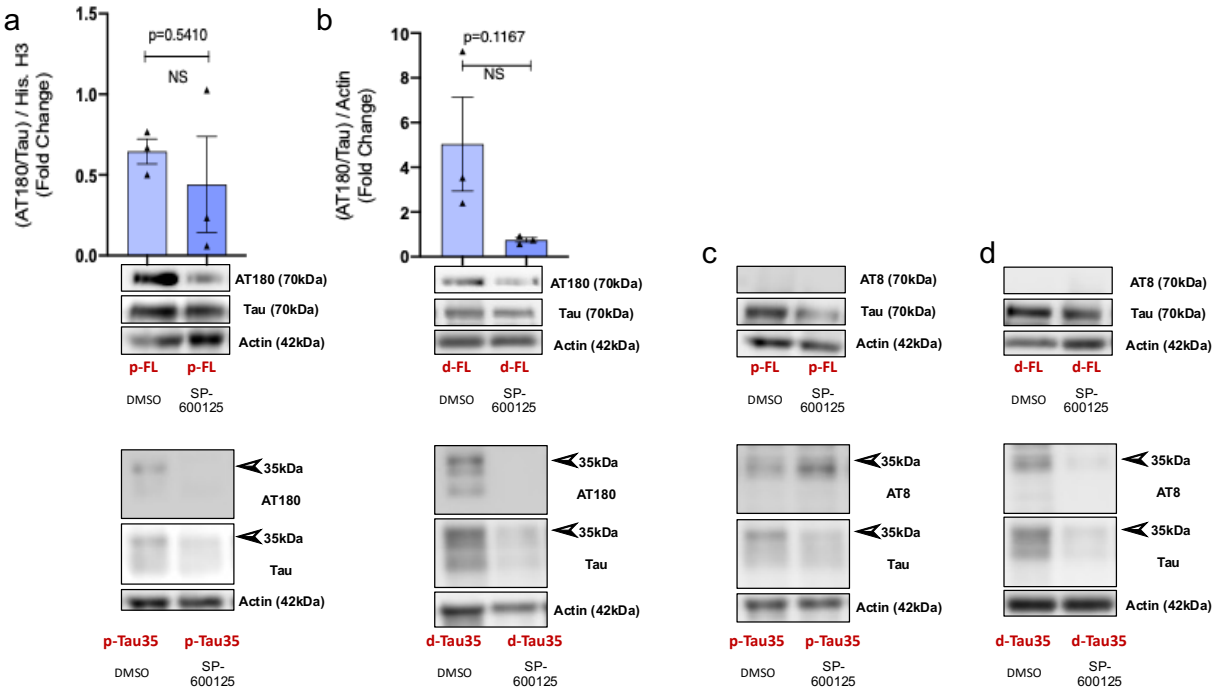

Figure 3-17 JNK inhibition had no significant effect on tau phosphorylation levels in the experimental groups. Representative western blots showing phosphorylation levels of human tau at two residues, AT180 **(a/b)** and AT8 **(c/d)** in proliferative **(a/c)**, and differentiated cells **(b/d)**, post-SP-600125 treatment. Quantification of p-Tau/ Total Tau is shown in transfected cells, (70 kDa in SH-SY5Y-FL and 35 kDa in SH-SY5Y-Tau35). (n=6 independent experiments) data shown as mean ± SEM, unpaired Student's t test, *$p < 0.05$ is considered as significant difference.

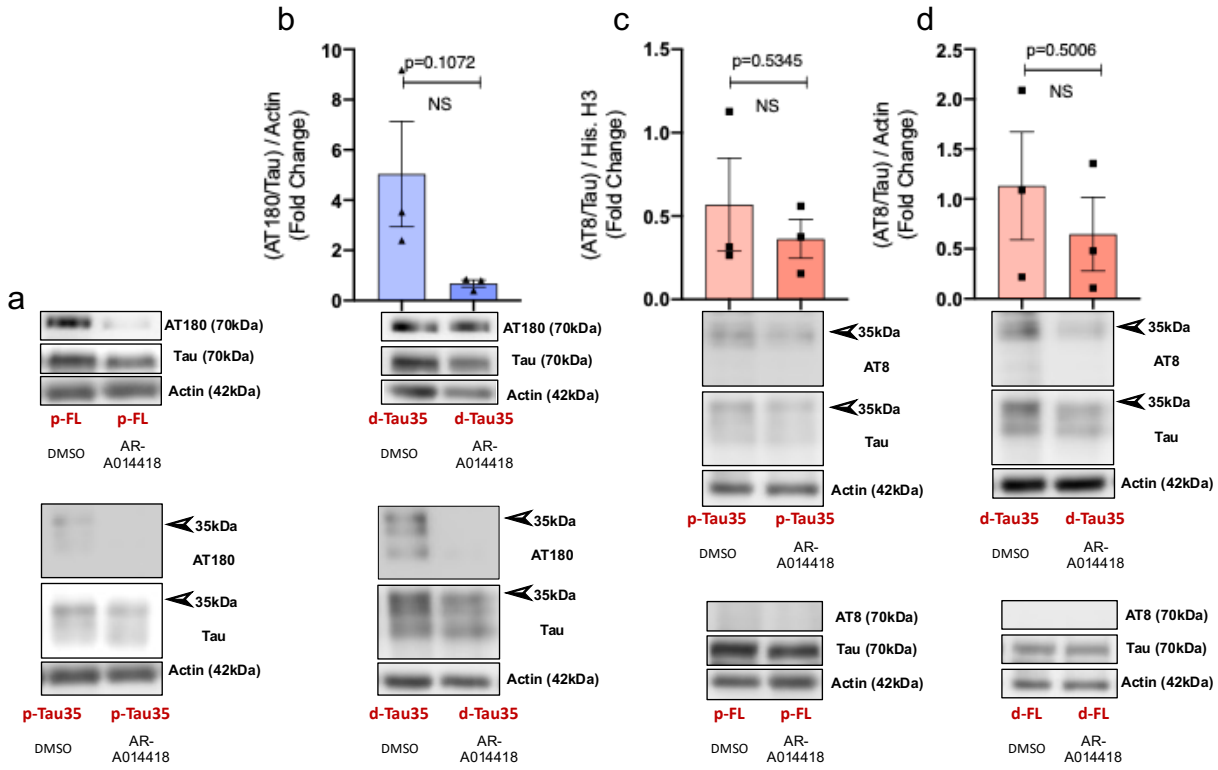

Figure 3-18 GSK3-β inhibition had no significant effect on tau phosphorylation levels in the experimental groups. Representative western blots showing phosphorylation levels of human tau at two residues, AT180 **(a/b)** and AT8 **(c/d)** in proliferative **(a/c)**, and differentiated cells **(b/d)**, post-AR-A014418 treatment. Quantification of p-Tau/ Total Tau is shown in transfected cells, (70 kDa in SH-SY5Y-FL and 35 kDa in SH-SY5Y-Tau35). (n=6 independent experiments) data shown as mean ± SEM, unpaired Student's t test, *p < 0.05 is considered as significant difference.

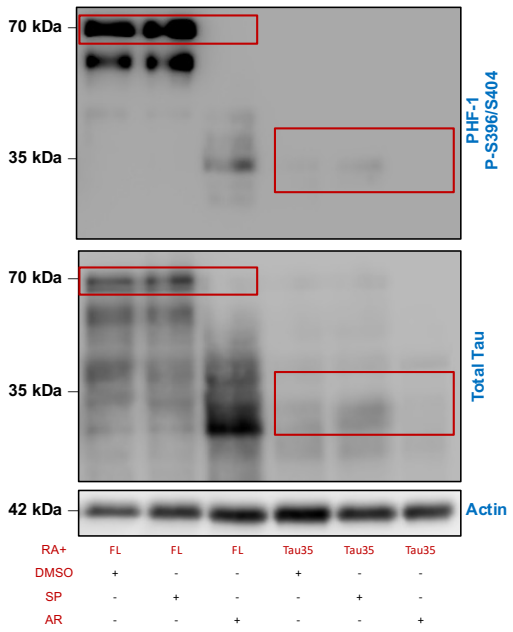

Figure 3-19 JNK and GSK3-β inhibition did not reduce PHF-1 phosphorylation levels in dSH-SY5Y cells. Representative western blots showing phosphorylation levels of human tau at p-S396/S404 in differentiated cells, after treating with the small molecules. n=3 independent experiments have been performed.

3.9 JNK inhibition can reduce nuclear envelope invagination in dSH-SY5Y cells.

To determine the effects of JNK and GSK-3β inhibition on nuclear envelope integrity, CTL-, FL- and Tau35-dSH-SY5Y were treated with the small molecules for four hours. The time was selected based on the previous reports[150]. Cells were fixed and labeled with anti-LaminB1 antibody. Quantitative immunostaining indicated that inhibition of JNK significantly reduces the proportion of invaginated nuclear envelopes after treatment, as 10uM concentration successfully and significantly attenuated the number of invaginated nuclei in dSH-SY5Y-CTL cells (p=0.0081), in FL-dSH-SY5Y cells (p=0.0031) and in Tau35-dSHSY5Y cells (p=0.0260). Administration of 10 μM SP600125 was enough to attenuate nuclear lamina invagination. Interestingly, nuclear invagination grading also confirmed decreased severity of invagination after treatment with

SP600125. Contrary to inhibition of JNK, administration of GSK-3β inhibitor, AR-A014418 treatment, did not reduce the nuclear invagination in these experimental groups (Figure 3-20).

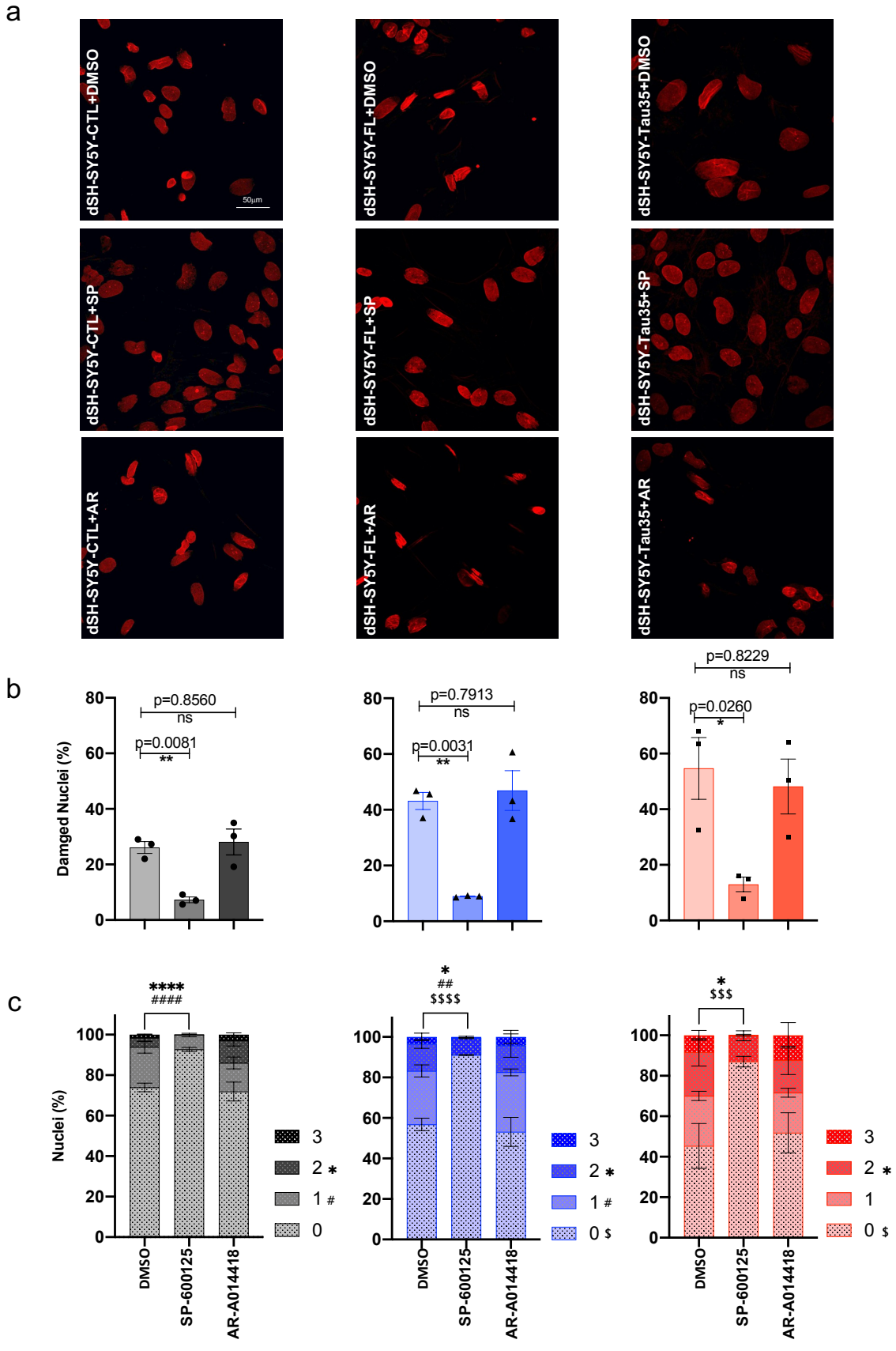
a
dSH-SY5Y-CTL+DMSO
dSH-SY5Y-FL+DMSO
dSH-SY5Y-Tau35+DMSO
dSH-SY5Y-CTL+SP
dSH-SY5Y-FL+SP
dSH-SY5Y-Tau35+SP
dSH-SY5Y-CTL+AR
dSH-SY5Y-FL+AR
dSH-SY5Y-Tau35+AR
50μm
b
Damged Nuclei (%)
p=0.8560
ns
p=0.0081
**
p=0.7913
ns
p=0.0031
**
p=0.8229
ns
p=0.0260
*
c
Nuclei (%)
****
####
*
##
$$$$
*
$$$
3
2 *
1 #
0
1
0 $
DMSO
SP-600125
AR-A014418

Figure 3-20: JNK inhibition can attenuate nuclear envelope invagination in dSH-SY5Y cells. a: Confocal micrographs depicting nuclear lamina status in the experimental groups after treating with DMSO (vehicle), SP600125 and AR-A014418. LB1 is represented in red. Scale bar 50 μm. **b:** Graphs representing the percentage of nuclei exhibiting nuclear envelope invagination in the presence of DMSO, SP-600125 and AR-A014418. **c:** Distribution graphs indicating damage severity in the nuclear envelop after treatment with SP-600125 and AR-A014418. Grade=0 represents normal nuclei and grade=3 was allocated to the severest damage in nuclei. The bars in graphs indicate mean ± SEM of average from n=3 independent experiments, approximately 100 cells/replicate. One-way ANOVA analysis was performed for data analysis and $p < 0.05$ was considered as significant difference.

3.10 JNK and GSK-3β inhibition significantly attenuated f-actin distribution in FL-dSH-SY5Y cells.

To investigate whether the cytoskeletal damages detected in FL- and Tau35- overexpressing cells can be alleviated, I assessed f-actin distribution and stability in dSH-SY5Y experimental groups after treating with the small molecules. F-actin data analysis in the aim-1 has been repeated for the second aim. According to the obtained results, only dSH-SY5Y-FL cells were responsive to the treatments. Particularly, average actin intensity adversely affected in dSH-SY5Y-CTLs and -Tau35 cells, while dSH-SY5Y-FL cells demonstrated reduced average actin intensity after SP600125 administration (p=0.0026) and post AR-A014418 treatment (p<0.0001). The same pattern has been detected related to the perinuclear f-actin intensity (Figure 3-21 a-c). Interestingly, analysis of f-actin distribution through the cells confirmed that both inhibitors, SP600125 and AR-A014418, can significantly lower the average intensity of f-actin over the bins compared to the DMSO-treated cells. This analysis did not show positive effect of JNK and GSK-3β inhibition on dSH-SY5Y-CTLs and -Tau35 cells (Figure 3-21-d).

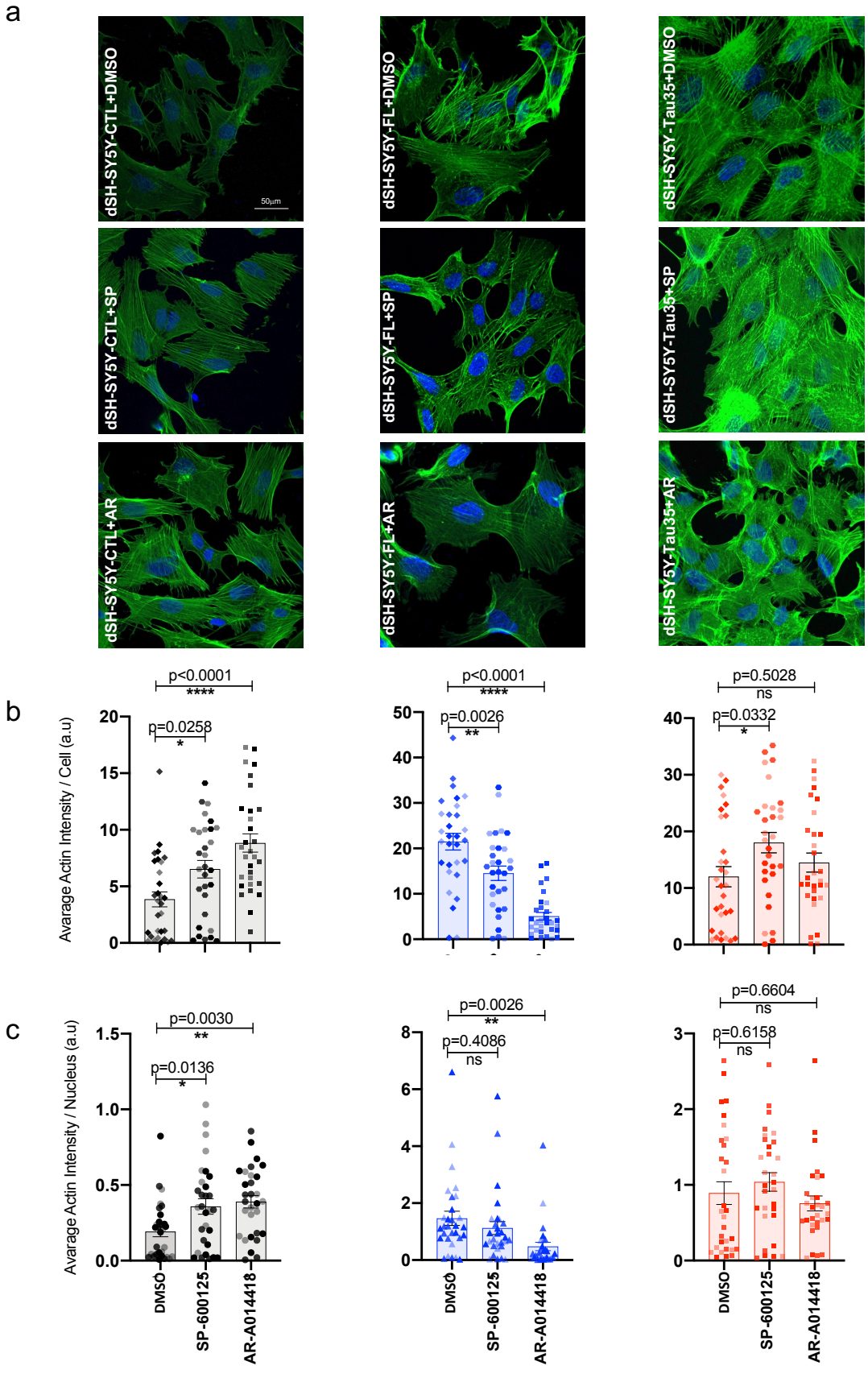
a
dSH-SY5Y-CTL+DMSO
50µm
dSH-SY5Y-FL+DMSO
dSH-SY5Y-Tau35+DMSO
dSH-SY5Y-CTL+SP
dSH-SY5Y-FL+SP
dSH-SY5Y-Tau35+SP
dSH-SY5Y-CTL+AR
dSH-SY5Y-FL+AR
dSH-SY5Y-Tau35+AR
b
Avarage Actin Intensity / Cell (a.u)
p<0.0001
****
p=0.0258
*
p<0.0001
****
p=0.0026
**
p=0.5028
ns
p=0.0332
*
c
Avarage Actin Intensity / Nucleus (a.u)
p=0.0030
**
p=0.0136
*
p=0.0026
**
p=0.4086
ns
p=0.6604
ns
p=0.6158
ns
DMSO
SP-600125
AR-A014418

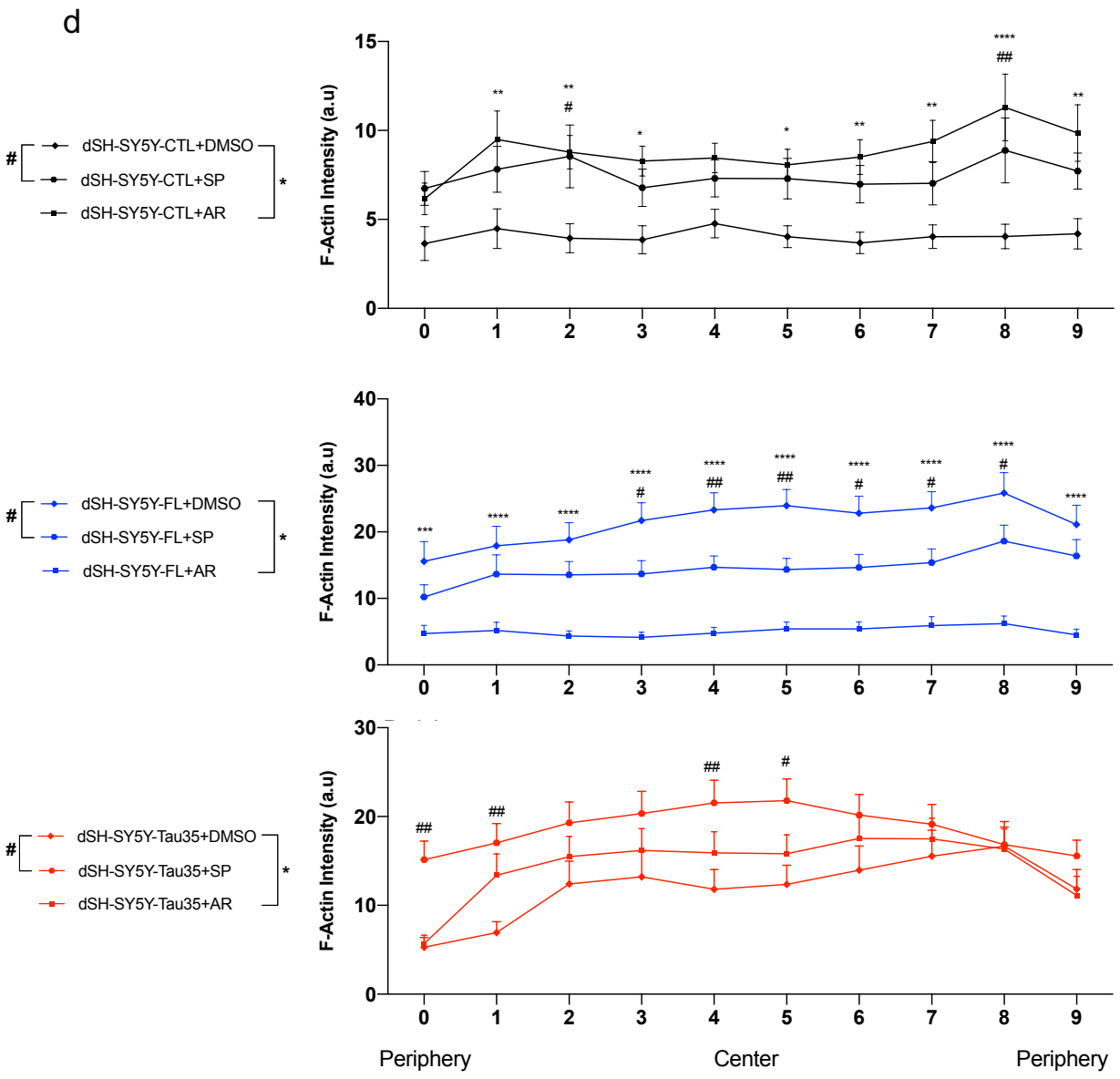

Figure 3-21: JNK and GSK-3β inhibition significantly attenuated f-actin distribution in FL-dSH-SY5Y cells. a: Confocal micrographs counter stained against f-actin (green) and nuclei (blue). Scale bar 50 µm. **b:** Graphs indicating average actin intensity in the cells. Replicates of each group are shown in shades of black, blue and red colors **c:** Representative graphs demonstrating average actin intensity over the nuclei. Replicates of each group are shown in shades of black, blue and red colors **d**: Graphs representing distribution of f-actin intensity through the cells obtained from the bins, from periphery to the central regions of the cells. The bars in graphs indicate mean ± SEM of average from n=3 independent experiments, approximately 90 cells/condition. Two- and one-way ANOVA analyses were performed for data analysis and $p < 0.05$ was considered as significant difference.

4 Chapter IV: Discussion

In the present study, I aimed to generate an *in vitro* model of tauopathy. Next, I aimed to assess whether inhibiting upstream compartments of pathologic tau can inhibit/alleviate the downstream effects. Overexpression of Full-length tau protein (FL-Tau) and its pathologic C-terminal fragment (Tau35) caused similar cytoskeletal and nuclear pathology to those reported in models of tauopathy diseases including AD[145]. In my study, these abnormalities were alleviated after pharmacological inhibition of involving kinases in pathogenic tau. In particular, JNK inhibition reduced actin over-stabilization in dSH-ST5Y cells overexpressing Tau-FL and attenuated nuclear lamina damage in both FL-Tau- and Tau35-overexpressing dSH-SY5Y cell. Additionally, GSK3β inhibition alleviated f-actin overstabilization in dSH-SY5Y-FL cells.

4.1 Inducing overexpression of FL-Tau and Tau35 in neuroblastoma cells may mimic some characteristics of tau pathology.

Tauopathies are neurodegenerative diseases identified by dysfunction and accumulation of abnormal tau proteins in neurons [144]. The molecular mechanisms leading to pathophysiological tau effects are still unclear. Thus, potential therapeutic targets remain to be identified. The aim of the current study was to generate an *in vitro* model of tauopathy demonstrating pathologic features of this disease. To mimic intracellular tau accumulation, I established this model in human neuroblastoma cell line. SH-SY5Y cell has been widely used as an *in vitro* model for neurodegenerative diseases research. Originally, SH-SY5Y cells were subcloned from cells obtained from the bone marrow biopsy taken from a four-year-old female neuroblastoma patient[151]. This is a very powerful system which overcomes limitations of using primary mammalian neurons derived from CNS tissue. For instance, they aggressively proliferate and

overcome no propagation post differentiation which is in the primary neurons[152]. Differentiated SH-SY5Y cells possess fundamental neuronal properties, including biochemical and functional features. For instance, the ability of cell migration and neurite outgrowth, cell adhesion and expression of various human-specific neuronal markers and proteins might be activated by differentiation[131][132]. Differentiation of neuroblastoma cells also increases membrane electrical excitability and synaptic function and activates neurotransmitters and their receptors[153][154][155][156]. Moreover, they were identified as robust tools for genetic manipulation, particularly stable expression of human tau[157]. For inducing tau-toxicity, I genetically manipulated cells using two constructs, human FL-Tau isoform and its 35 kDa C-terminal fragment. According to the results obtained from several studies, human FL-Tau expression induces tau pathology in both mice models and *in vitro* [158][159][160]. For instance, N2a[161], HEK293[162], CHO[163], QBI-293[164], SH-SY5Y[165], NIH and 3T3[166] cell lines have been used for transient and stable expression of full-length tau. Recent evidence indicated that minimal expression of Tau35, the FL-Tau N-terminally-cleaved fragment, exacerbated phenotypes of tauopathies in both *in vitro* (CHO cells) and an *in vivo* mouse models[128][167]. This mouse model displayed progressive and profound tauopathy-related key features and cognitive deficits. Additionally, tau aggregation, aberrant tau phosphorylation, autophagic/lysosomal dysfunction, synaptic loss, progressive cognitive/motor deficit and reduced life-span have been identified in this tauopathy model[168]. Pathophysiologically, Tau35 was first identified in 4R human tauopathy brain samples[169]. This fragment includes all four microtubule-binding (MTB) and the C-terminal domains of tau and lacks its proline-rich domain [168][128]. Although Tau35 contains all MTB domains, its ability to bind to microtubules is lower than FL-Tau and disrupts microtubule bundling[128]. Tau35 aggregation tendency is significantly higher

than longer isoforms of human tau, 2N3R and 2N4R[170][171]. Using immunoblotting and immunocytochemistry, I first verified overexpression of FL-Tau and Tau35 in pSH-SY5Y and dSH-SY5Y cells.

The confirmation of increased tau phosphorylation is one of the first critical evaluations of the tau isoforms impact on spontaneous hyperphosphorylation of tau. I targeted three verified disease-associated tau phosphoepitopes, pThr231, pSer202/pThr205 and pS396/S404 [13]. These residues were previously shown to be affected in CHO tau-overexpressing cells[128]. However, using the same antibodies as the previous report, my cells did not show consistent results.

4.2 Overexpression of FL-Tau and Tau35 disrupts cellular mechanotransduction in dSH-SY5Y cells.

I next tested the impact of tau isoforms overexpression on subcellular structural changes. Nuclear lamina dysfunction is one of the major downstream events of pathogenic tau[76][172][173][145]. Nuclear lamina substantially forms a filamentous meshwork which covers the entire inner surface of inner nuclear membrane and acts as a scaffold for anchoring of heterochromatic DNA to the nuclear envelope[174]. Nuclear lamina invagination has been considered as a downstream event after tau hyperphosphorylation in a *Drosophila* model of tauopathy, which was mediated by over stabilization of actin filaments. These invaginations mainly consist of nuclear lamina and ultimately lead to relaxation of heterochromatic DNA[175]. Studies in human iPSC-derived cortical neurons with missense and splicing MAPT mutations further confirmed the involvement of pathogenic tau in induction of nuclear invagination and demonstrated a physical apposition of tau and microtubules within the invaginated nuclear envelope[76]. Developing an optogenetic-based oligomeric tau system in primary cortical neurons depicted tau oligomerization disrupts nuclear membrane and induces nuclear deformity. Studies in PS19 mice and human AD brain

tissue uncovered lamin B and its receptor were recruited and co-localized with oligomeric tau. Interestingly, in an aged PS19 mice model, oligomeric tau directly binds to lamin proteins and the lamin B receptor and induces disruption of the nucleocytoplasmic interface[172].

Cellular mechanotransduction is primarily a cellular response which is triggered by intracellular or extracellular mechanical signal. Cells can transform these mechanical signals into biochemical responses[176]. Several cellular compartments have been identified as the key players of nuclear mechanotransduction, including actin cytoskeleton, LINC complex, nuclear lamina and nuclear pore complexes[177]. Mechanistically, actin cytoskeleton is the main cytoskeletal compartment implicated in nuclear mechanotransduction[178]. In cytoplasm, tau protein not only regulates microtubule assembly and stability but also binds to actin, and protects DNA integrity. Therefore, when tau is aggregated or oligomerized, these functions can be impaired which leads to neurodegeneration[179]. This fact also should be considered that regulation of physiologic and pathogenic tau is complicated and discovering involved factors is not completed yet. Cytoplasmic actin is identified as one of these prominent tau binding partners. Tau regulates cytoskeleton integrity through its proline-rich domain where interacts with microtubules and actin filaments[180]. In terms of f-actin/tau binding, there is another short repeat in MTB domain of tau where provides a key link between tau/microtubule and f-actin. Investigation of crosstalk between the actin microfilament network and the microtubule cytoskeleton in *Drosophila* and mouse models of tauopathy confirmed that actin cytoskeletal changes occur downstream of tau phosphorylation and are specific to tau-induced neurotoxicity[181]. Pathogenic tau either phosphorylated or aggregated appears to have toxic gain of function. Hyperphosphorylated tau negatively affects formation of kinesin complex through interacting with c-Jun N-terminal kinase-interacting protein 1(JIP1)[71]. Moreover, in a transgenic *Caenorhabditis elegans* model of

tauopathy, loss of function of actin- and microtubule-binding proteins suppressed neurotoxicity[182]. More investigations in *Drosophila* and mouse models of tauopathy uncovered the interactions of leucine-rich repeat kinase 2 (LRRK2) and tau. These results revealed that either increasing or decreasing Lrrk expression induces tau neurotoxicity and this tau-induced neurotoxicity ultimately results in over-stabilization of f-actin and altered mitochondrial dynamics[183]. Consistent with previous findings related to the effects of tau toxicity on cytoskeleton and neucleoskeleton integrity, I observed that in my *in vitro* model, overexpression of both FL-Tau and the pathogenic tau fragment (Tau35) correlates with over-stabilization of f-actin in the perinuclear region in dSH-SY5Y cells. Interestingly, since the f-actin over-stabilization was more severe in the presence of Tau35, this fragment appears to be associated with exacerbated phenotype. Due to the direct interactions between f-actin and neucleoskeleton, I also observed increased number of invaginated nuclear lamina in FL-Tau- and Tau35-overexpressing dSH-SY5Y cells. This result suggests nuclear envelop invaginations and changes in shapes of nuclei are downstream events of tau aggregation and f-actin over-stabilization.

4.3 Inhibition of JNK is associated with reduced actin over-stabilization and nuclear lamina damage in dSH-ST5Y cell.

Hyperphosphorylated tau is one of the major forms of pathogenic tau in which kinases are involved, extensively. Physiologically, c-Jun N-terminal kinases (JNKs) are critical CNS enzymes controlling brain functions, while under pathological condition, their activation or phosphorylation lead to tau phosphorylation[184][185][186]. Regulatory roles of JNK pathway has been studied widely in various AD models and identified as one of the therapeutic candidates of AD[187]. Tau can be phosphorylated at multiple sites by JNKs. For instance, Ser202/Thr205 and Ser422 are two targets of JNKs[188][189]. Phosphorylation at Ser202/Thr205 tau residues is reported to be

associated with early stage of AD, while Ser422 phosphorylation correlates with tangle formation[190][191].

SP600125 (Anthra[1,9-cd]pyrazol-6-(2H)-one is a synthesized JNK inhibitor which has been used in both *in vitro* and *in vivo* models of AD[192]. According to the published results, SP600125 can effectively prevent pathological effects of p-JNK up-regulation[46]. For instance, in a neuroblastoma Neuro2a model of tauopathy, overexpression of FL-Tau increased JNK phosphorylation and inhibited insulin signaling through activation of JNK and administrating JNK inhibitor, SP600125, attenuated tau overexpression-induced disruption of insulin signaling pathway[193]. Based on these results, I hypothesized that dysregulation of cytoskeleton or nucleoskeleton can be attenuated/inhibited in dSH-SY5Y cells overexpressing FL-Tau and Tau35. Therefore, I administrated JNK inhibitor, SP600125, in my *in vitro* model of tauopathy. SP600125 reduced actin over-stabilization in dSH-ST5Y cells overexpressing Tau-FL and attenuated nuclear lamina damage in both FL-Tau- and Tau35-overexpressing dSH-ST5Y cell.

4.4 Inhibition of GSK-3β correlates with reduced actin over-stabilization in FL-Tau overexpressing cells.

In addition to JNKs, glycogen synthase-3 kinase (GSK-3β) up-regulation is also identified as one of the factors in driving pathogenic tau[194]. In a model of tauopathy, a selective activation of GSK3β has been reported in the mice expressing human-derived Tau35 fragment [168]. Inhibition of GSK-3β protein is extensively applied in preclinical studies in tauopathies[195].

AR-A014418 (N-(4-methoxybenzyl)-N'-(5-nitro-1,3-thiazol2-yl) is a selective GSK3β inhibitor suppressing tau phosphorylation and tau aggregation[196]. In a tau transgenic mice model of tauopathy, one month ingestion of AR-A014418 was associated with significant attenuation in tau pathology, including decreasing tau hyperphosphorylation/aggregation in the brain stem and

axonal deterioration[196]. Administrating AR-A014418 in differentiated SH-SY5Y-TMHT441 cells was associated with inhibition of tau phosphorylation at Ser396[150]. In a cell-based model of tauopathy, in differentiated rat primary neuronal cortical cell cultures, AR-A014418 reduced tau hyperphosphorylation at various disease-associated epitopes, including Ser202/Thr205, Thr238, Ser202, and Thr181[197]. In my experiments, tau hyperphosphorylation has not been detected in FL-Tau- and Tau35-overexpressing SH-SY5Y cells, by immunoblotting analysis of Thr231, Ser202/Thr205 and Ser396/Ser404 residues. Post-treatment western blot analysis also did not show consistent results and significant effects of the small molecules on phosphorylation levels of tau at above-mentioned epitopes. Although hyperphosphorylation of tau is yet an unresolved question in my study, I investigated the impacts of small molecules on the other pathologic downstream events of tau over expression. After AR-A014418 treatment, analyzing f-actin status and invagination levels of nuclear envelope demonstrated f-actin overstabilization were rescued only in dSH-SY5Y-FL cells, while it was not effective in alleviating nuclear lamina invagination in all experimental groups.

4.5 Conclusion

In summary, FL-Tau and Tau35 overexpression was induced in neuroblastoma cells in the current study. This cellular model has been characterized and used for screening cytoskeletal/nucleoskeletal alterations in tauopathy. I provided an upstream-to-downstream charachterization of this cellular model and examined two well-described drug candidates (SP600125 and AR-A014418) on tau-induced actin stabilization and nuclear envelope status. In dSH-SY5Y cell model of tauopathy, FL-Tau and Tau35 overexpression correlates with actin overstabilization and nuclear envelope invagination. The pathogenic tau fragment, Tau35, is associated with exacerbated cytoskeleton/nucleoskeleton damages in the cells. inhibiting JNKs can

significantly alleviate nuclear lamina invagination in both FL-Tau and Tau35 overexpressing cells and actin stabilization in FL-Tau overexpressing dSH-SY5Y cells. Although GSK3β inhibition did not affect neucleoskeleton, it reduced actin overstabilization in FL-Tau overexpressing dSH-SY5Y cells. Taken together, the current study can propose that tau-induced dysregulation of cytoskeleton and nucleoskeleton could be reversable and this cellular model can provide a tool for actin/lamin- related drug screening in tauopathies. A more detailed mechanistic characterization will be necessary to establish the causative role of these structural alterations and those pathogenic tau-related features which have not been detected in this model, including autophagy-lysosomal pathway or heterochromatin relaxation.

4.6 Limitation and future direction

The current study has several main limitations. Tau is a major protein in nerve cells and is subject of several post-translational modifications including phosphorylation. There are tens of residues that are identified as potential phosphorylation sites that adds to the complexity of the pathology. I have focused on investigating three major tau hyperphosphorylation-prone residues that are located in the C-terminal region of the protein. The study method was adopted from a previously published study in non-neuronal cells. Despite using several technical replicates, and quantification methods, I did not detect any significant increase in tau phosphorylation levels in the experimental groups, as was expected from the previous reports. The quantification method was also the same as the original report as communicated with the corresponding author. Despite several attempts to establish a few stable tau-transfection cell lines, my attempts to minimize variations in these experiments were not successful, and I could not obtain data showing significant increase in tau phosphorylation. To assess tau hyperphosphorylation, I used three different antibodies that have been successfully used in the previous report. These probes are commonly

used for tau phosphorylation. This issue inevitably affected the second aim and administration of kinase inhibitors did not show consistent results.

Another limitation of the study was limiting the assessments only to phosphorylation, as other post-translational modifications are reported that affect the cytoskeleton organizations. For instance, modeling FL-Tau overexpression in HeLa cells and transgenic mice, tauKQ and tauWT mice, Peter Dongmin Sohn et al. demonstrated that tau acetylation can destabilize the cytoskeleton in the axon initial segment. Acetylated Tau may be mislocalized to the somatodendritic compartment and cause aberrant activity[198]. Tau glycation is another post-translational modification that is reported in a neuroblastoma cell model of tauopathy[115], here, administration of EGCG, a green tea polyphenol, reduced advanced tau glycation and remodeled neuronal cytoskeletal integrity[115]. These additional tau modifications should be included in the future evaluation of these cellular models.

Future studies should also include further assessment of kinase inhibitor effects on the observed changes in cytoskeleton/nucleoskeleton damage in FL-Tau- and Tau35-overexpressing cells. For instance, examining direct effects of these two small molecules on JNK and GSK3β signaling pathways and their phosphorylation status before and after treatment would be helpful in verifying their effects.

Although, nuclear damage in this cellular model was not associated with downstream pathogenic effects such as DNA methylation of LINE-1, chromatin rearrangement and activation of transposable elements, including LINE, LTR have been reported in neurodegenerative diseases and aging[199] [200]. Therefore, future studies should further evaluate the downstream events after nuclear damage. Additional techniques such as digital PCR (dPCR) and RNA sequencing will aid it in high throughput detection/quantification of retrotransposons.

References

1. Tabeshmehr, P.; Biology, E.E.-; 2023, undefined Tau; One Protein, So Many Diseases. *mdpi.com* **2023**, doi:10.3390/biology12020244.
2. Nagakannan, P.; Tabeshmehr, P.; Eftekharpour, E. Oxidative Damage of Lysosomes in Regulated Cell Death Systems: Pathophysiology and Pharmacologic Interventions. *Free Radic. Biol. Med.* **2020**, *157*, 94–127, doi:10.1016/j.freeradbiomed.2020.04.001.
3. Sexton, C.; Snyder, H.; Beher, D.; Boxer, A.L.; Brannelly, P.; Brion, J.P.; Buée, L.; Cacace, A.M.; Chételat, G.; Citron, M.; et al. Current Directions in Tau Research: Highlights from Tau 2020. *Alzheimers Dement* **2021**, *18*, 988–1007, doi:10.1002/alz.12452.
4. Gallo, D.; Ruiz, A.; Sánchez-Juan, P. Genetic Architecture of Primary Tauopathies. *Neuroscience* **2022**, doi:10.1016/J.NEUROSCIENCE.2022.05.022.
5. McKee, A.C.; Cairns, N.J.; Dickson, D.W.; Folkerth, R.D.; Dirk Keene, C.; Litvan, I.; Perl, D.P.; Stein, T.D.; Vonsattel, J.P.; Stewart, W.; et al. The First NINDS/NIBIB Consensus Meeting to Define Neuropathological Criteria for the Diagnosis of Chronic Traumatic Encephalopathy. *Acta Neuropathol.* **2016**, *131*, 75–86, doi:10.1007/S00401-015-1515-Z.
6. WHO Dementia Available online: https://www.who.int/health-topics/dementia#tab=tab_2 (accessed on 27 August 2022).
7. Sjölin, K.; Kultima, K.; Larsson, A.; Freyhult, E.; Zjukovskaja, C.; Alkass, K.; Burman, J. Distribution of Five Clinically Important Neuroglial Proteins in the Human Brain. *Mol. Brain* **2022**, *15*, 52, doi:10.1186/S13041-022-00935-6.
8. Blennow, K.; Wallin, A.; Agren, H.; Spenger, C.; Siegfried, J.; Vanmechelen, E. Tau Protein in Cerebrospinal Fluid: A Biochemical Marker for Axonal Degeneration in Alzheimer Disease? *Mol. Chem. Neuropathol.* **1995**, *26*, 231–245, doi:10.1007/BF02815140.
9. Arendt, T.; Stieler, J.; bulletin, M.H.-B. research; 2016, undefined Tau and Tauopathies. *Elsevier* **2016**, doi:10.1016/j.brainresbull.2016.08.018.
10. Neve, R.L.; Harris, P.; Kosik, K.S.; Kurnit, D.M.; Donlon, T.A. Identification of CDNA Clones for the Human Microtubule-Associated Protein Tau and Chromosomal Localization of the Genes for Tau and Microtubule-Associated Protein 2. *Brain Res.* **1986**, *387*, 271–280, doi:10.1016/0169-328X(86)90033-1.
11. Goedert, M.; Spillantini, M.G.; Jakes, R.; Rutherford, D.; Crowther, R.A. Multiple Isoforms of Human Microtubule-Associated Protein Tau: Sequences and Localization in Neurofibrillary Tangles of Alzheimer's Disease. *Neuron* **1989**, *3*, 519–526, doi:10.1016/0896-6273(89)90210-9.
12. Hefti, M.M.; Farrell, K.; Kim, S.H.; Bowles, K.R.; Fowkes, M.E.; Raj, T.; Crary, J.F. High-Resolution Temporal and Regional Mapping of MAPT Expression and Splicing in Human Brain Development. *PLoS One* **2018**, *13*, doi:10.1371/JOURNAL.PONE.0195771.
13. Hanger, D.; Anderton, B.; Noble, W. Tau Phosphorylation: The Therapeutic Challenge for Neurodegenerative Disease. *TRENDS Mol. Med.* **2009**, *15*, 112–119, doi:10.1016/J.MOLMED.2009.01.003.
14. Hirokawa, N.; Takemura, R. Molecular Motors and Mechanisms of Directional Transport in Neurons. *Nat. Rev. Neurosci.* **2005**.
15. Weingarten, M.D.; Lockwood, A.H.; Hwo, S.Y.; Kirschner, M.W. A Protein Factor Essential for Microtubule Assembly. *Proc. Natl. Acad. Sci.* **1975**, *72*, 1858–1862,

doi:10.1073/PNAS.72.5.1858.
16. Brandt, R.; Lee, G. The Balance Between τ Protein's Microtubule Growth and Nucleation Activities: Implications for the Formation of Axonal Microtubules. *J. Neurochem.* **1993**, *61*, 997–1005, doi:10.1111/J.1471-4159.1993.TB03613.X.
17. Drubin, D.; MW Kirschner Tau Protein Function in Living Cells. *J. cell* **1986**.
18. Yu, Y.; Run, X.; Liang, Z.; Li, Y.; Liu, F.; Liu, Y.; Iqbal, K.; Grundke-Iqbal, I.; Gong, C.X. Developmental Regulation of Tau Phosphorylation, Tau Kinases, and Tau Phosphatases. *J. Neurochem.* **2009**, *108*, 1480–1494, doi:10.1111/J.1471-4159.2009.05882.X.
19. Moraga, D.M.; Nuñez, P.; Garrido, J.; Maccioni, R.B. A τ Fragment Containing a Repetitive Sequence Induces Bundling of Actin Filaments. *J. Neurochem.* **1993**, *61*, 979–986, doi:10.1111/J.1471-4159.1993.TB03611.X.
20. Elie, A.; Prezel, E.; Guérin, C.; Denarier, E.; Ramirez-Rios, S.; Serre, L.; Andrieux, A.; Fourest-Lieuvin, A.; Blanchoin, L.; Arnal, I. Tau Co-Organizes Dynamic Microtubule and Actin Networks. *Sci. Reports 2015 51* **2015**, *5*, 1–10, doi:10.1038/srep09964.
21. Correas, I.; Padilla, R.; Journal, J.A.-B.; 1990, U. The Tubulin-Binding Sequence of Brain Microtubule-Associated Proteins, Tau and MAP-2, Is Also Involved in Actin Binding. *Biochem. J.* **1990**, *269*, 61–64.
22. Frandemiche, M.L.; De Seranno, S.; Rush, T.; Borel, E.; Elie, A.; Arnal, I.; Lanté, F.; Buisson, A. Activity-Dependent Tau Protein Translocation to Excitatory Synapse Is Disrupted by Exposure to Amyloid-Beta Oligomers. *Soc Neurosci.* **2014**, doi:10.1523/JNEUROSCI.4261-13.2014.
23. Tracy, T.; Sohn, P.; Minami, S.; Wang, C.; Min, S.; Neuron, Y.L.-; 2016, U. Acetylated Tau Obstructs KIBRA-Mediated Signaling in Synaptic Plasticity and Promotes Tauopathy-Related Memory Loss. *Neuron* **2016**, *90*, 245–260.
24. Cabrales Fontela, Y.; Kadavath, H.; Biernat, J.; Riedel, D.; Mandelkow, E.; Zweckstetter, M. Multivalent Cross-Linking of Actin Filaments and Microtubules through the Microtubule-Associated Protein Tau. *Nat. Commun. 2017 81* **2017**, *8*, 1–12, doi:10.1038/s41467-017-02230-8.
25. Orr, M.E.; Sullivan, A.; D, C.; Frost, B. A Brief Overview of Tauopathy: Causes, Consequences, and Therapeutic Strategies. **2017**, *38*, 637–648, doi:10.1016/j.tips.2017.03.011.
26. Chaudhary, A.R.; Berger, F.; Berger, C.L.; Hendricks, A.G. Tau Directs Intracellular Trafficking by Regulating the Forces Exerted by Kinesin and Dynein Teams. *Traffic* **2018**, *19*, 111–121, doi:10.1111/TRA.12537.
27. Cuchillo-Ibanez, I.; Seereeram, A.; Byers, H.L.; Leung, K.-Y.; Ward, M.A.; Anderton, B.H.; Hanger, D.P. Phosphorylation of Tau Regulates Its Axonal Transport by Controlling Its Binding to Kinesin. *FASEB J.* **2008**, *22*, 3186–3195, doi:10.1096/FJ.08-109181.
28. Hinrichs, M.H.; Jalal, A.; Brenner, B.; Mandelkow, E.; Kumar, S.; Scholz, T. Tau Protein Diffuses along the Microtubule Lattice. *J. Biol. Chem.* **2012**, *287*, 38559–38568, doi:10.1074/jbc.M112.369785.
29. Ittner, L.M.; Ke, Y.D.; Delerue, F.; Bi, M.; Gladbach, A.; van Eersel, J.; Wölfing, H.; Chieng, B.C.; Christie, M.J.; Napier, I.A.; et al. Dendritic Function of Tau Mediates Amyloid-β Toxicity in Alzheimer's Disease Mouse Models. *Cell* **2010**, *142*, 387–397, doi:10.1016/j.cell.2010.06.036.

30. Klein, C.; Kramer, E.M.; Cardine, A.M.; Schraven, B.; Brandt, R.; Trotter, J. Process Outgrowth of Oligodendrocytes Is Promoted by Interaction of Fyn Kinase with the Cytoskeletal Protein Tau. *J. Neurosci.* **2002**, *22*, 698–707, doi:10.1523/JNEUROSCI.22-03-00698.2002.
31. Sjöberg, M.K.; Shestakova, E.; Mansuroglu, Z.; Maccioni, R.B.; Bonnefoy, E. Tau Protein Binds to Pericentromeric DNA: A Putative Role for Nuclear Tau in Nucleolar Organization. *J. Cell Sci.* **2006**, *119*, 2025–2034, doi:10.1242/jcs.02907.
32. Maina, M.B.; Bailey, L.J.; Wagih, S.; Biasetti, L.; Pollack, S.J.; Quinn, J.P.; Thorpe, J.R.; Doherty, A.J.; Serpell, L.C. The Involvement of Tau in Nucleolar Transcription and the Stress Response. *Acta Neuropathol. Commun.* **2018**, *6*, 70, doi:10.1186/s40478-018-0565-6.
33. Mansuroglu, Z.; Benhelli-Mokrani, H.; Marcato, V.; Sultan, A.; Violet, M.; Chauderlier, A.; Delattre, L.; Loyens, A.; Talahari, S.; Bégard, S.; et al. Loss of Tau Protein Affects the Structure, Transcription and Repair of Neuronal Pericentromeric Heterochromatin. *Sci. Rep.* **2016**, *6*, 33047, doi:10.1038/srep33047.
34. Alzheimer, A.; Stelzmann, R.A.; Schnitzlein, H.N.; Murtagh, F.R. An English Translation of Alzheimer's 1907 Paper, "Uber Eine Eigenartige Erkankung Der Hirnrinde". *Clin. Anat.* **1995**, *8*, 429–431, doi:10.1002/ca.980080612.
35. Terry, R.D. The Fine Structure of Neurofibrillary Tangles in Alzheimer's Disease. *J. Neuropathol. Exp. Neurol.* **1963**, *22*, 629–642, doi:10.1097/00005072-196310000-00005.
36. Brion, J. P., et al. Immunological Detection of Tau Protein in Neurofibrillary Tangles of Alzheimers-Disease. *Arch. Biol.* **1985**, *96*, 229–235.
37. Schweighauser, M.; Shi, Y.; Tarutani, A.; Kametani, F.; Murzin, A.G.; Ghetti, B.; Matsubara, T.; Tomita, T.; Ando, T.; Hasegawa, K.; et al. Structures of α-Synuclein Filaments from Multiple System Atrophy. *Nature* **2020**, *585*, 464–469, doi:10.1038/s41586-020-2317-6.
38. Zhang, W.; Falcon, B.; Murzin, A.G.; Fan, J.; Crowther, R.A.; Goedert, M.; Scheres, S.H. Heparin-Induced Tau Filaments Are Polymorphic and Differ from Those in Alzheimer's and Pick's Diseases. *Elife* **2019**, *8*, doi:10.7554/eLife.43584.
39. Rösler, T.W.; Tayaranian Marvian, A.; Brendel, M.; Nykänen, N.P.; Höllerhage, M.; Schwarz, S.C.; Hopfner, F.; Koeglsperger, T.; Respondek, G.; Schweyer, K.; et al. Four-Repeat Tauopathies. *Prog. Neurobiol.* **2019**, *180*, doi:10.1016/J.PNEUROBIO.2019.101644.
40. Ganguly, J.; Jog, M. Tauopathy and Movement Disorders—Unveiling the Chameleons and Mimics. *Front. Neurol.* **2020**, *11*, 1359, doi:10.3389/FNEUR.2020.599384/BIBTEX.
41. Meraz-Ríos, K.L.L. Tau Oligomers and Aggregation in Alzheimer's Disease. *Wiley Online Libr.* **2010**, *112*, 1353–1367, doi:10.1111/j.1471-4159.2009.06511.x.
42. Buée et al. Tau Protein Isoforms, Phosphorylation and Role in Neurodegenerative Disorders. *Brain Res.* **2000**, *33*, 95–130.
43. Cho JH, J.G. Glycogen Synthase Kinase 3β Phosphorylates Tau at Both Primed and Unprimed Sites: Differential Impact on Microtubule Binding. *J. Biol.* **2003**, *278*, 187–193.
44. Shukla, V.; Skuntz, S, et al. Deregulated Cdk5 Activity Is Involved in Inducing Alzheimer's Disease. *Arch. Med. Res.* **2012**, *43*, 655–662.
45. Tell, V.; Hilgeroth, A. Recent Developments of Protein Kinase Inhibitors as Potential AD

Therapeutics. *Front. Cell. Neurosci.* **2013**, *6*, doi:10.3389/FNCEL.2013.00189/FULL.
46. Yarza, R.; Vela, S.; Solas, M.; Ramirez, M.J. C-Jun N-Terminal Kinase (JNK) Signaling as a Therapeutic Target for Alzheimer's Disease. *Front. Pharmacol.* **2016**, *6*, doi:10.3389/FPHAR.2015.00321/FULL.
47. Sontag, J.M.; Sontag, E. Protein Phosphatase 2A Dysfunction in Alzheimer's Disease. *Front. Mol. Neurosci.* **2014**, *7*, doi:10.3389/FNMOL.2014.00016/FULL.
48. Wang, Y.; Mandelkow, E. Tau in Physiology and Pathology. *Nat. Rev. Neurosci.* **2016**, *17*, 5–21, doi:10.1038/nrn.2015.1.
49. Ercan-Herbst, E.; Ehrig, J.; Schöndorf, D.C.; Behrendt, A.; Klaus, B.; Gomez Ramos, B.; Prat Oriol, N.; Weber, C.; Ehrnhoefer, D.E. A Post-Translational Modification Signature Defines Changes in Soluble Tau Correlating with Oligomerization in Early Stage Alzheimer's Disease Brain. *Acta Neuropathol. Commun.* **2019**, *7*, 1–19, doi:10.1186/S40478-019-0823-2/FIGURES/9.
50. Min, S.-W.; Cho, S.-H.; Zhou, Y.; Schroeder, S.; Haroutunian, V.; Seeley, W.W.; Huang, E.J.; Shen, Y.; Masliah, E.; Mukherjee, C.; et al. Acetylation of Tau Inhibits Its Degradation and Contributes to Tauopathy. *Neuron* **2010**, *67*, 953–966, doi:10.1016/j.neuron.2010.08.044.
51. Maina, M.B.. A.-H.; Y.K.; Burra, G.; Rickard, J.E..; Harrington, C.R.; Wischik, C.M..; Serpell, L.C. Oxidative Stress Conditions Result in Trapping of PHF-Core Tau (297–391) Intermediates. *Cells* **2021**, *10*, 703.
52. Maina, M.B.; Al-Hilaly, Y.K.; Oakley, S.; Burra, G.; Khanom, T.; Biasetti, L.; Mengham, K.; Marshall, K.; Harrington, C.R.; Wischik, C.M.; et al. Dityrosine Cross-Links Are Present in Alzheimer's Disease-Derived Tau Oligomers and Paired Helical Filaments (PHF) Which Promotes the Stability of the PHF-Core Tau (297–391) In Vitro. *J. Mol. Biol.* **2022**, *434*, 167785, doi:https://doi.org/10.1016/j.jmb.2022.167785.
53. Boyko, Solomiia ; Surewicz, W.K. Tau Liquid–Liquid Phase Separation in Neurodegenerative Diseases. *Trends Cell Biol.* **2022**, *32*, 611–623.
54. Boyko, S., Qi, X. U., Chen, T. H., Surewicz, K., & Surewicz, W.K. "Liquid–Liquid Phase Separation of Tau Protein: The Crucial Role of Electrostatic Interactions." *J. Biol. Chem.* **2019**, *294*, 11054–11059.
55. Forrest, S.L.; Kril, J.J.; Stevens, C.H.; Kwok, J.B.; Hallupp, M.; Kim, W.S.; Huang, Y.; McGinley, C. V; Werka, H.; Kiernan, M.C.; et al. Retiring the Term FTDP-17 as MAPT Mutations Are Genetic Forms of Sporadic Frontotemporal Tauopathies. *Brain* **2018**, *141*, 521–534, doi:10.1093/brain/awx328.
56. McCarthy, A.; Lonergan, R.; Olszewska, D.A.; O'Dowd, S.; Cummins, G.; Magennis, B.; Fallon, E.M.; Pender, N.; Huey, E.D.; Cosentino, S.; et al. Closing the Tau Loop: The Missing Tau Mutation. *Brain* **2015**, *138*, 3100–3109, doi:10.1093/brain/awv234.
57. Wang, R.; Gao, H.; Xie, H.; Jia, Z.; Chen, Q. Molecular Imaging Biomarkers in Familial Frontotemporal Lobar Degeneration: Progress and Prospects. *Front. Neurol.* **2022**, *13*, 933217, doi:10.3389/fneur.2022.933217.
58. Goedert, M.; Falcon, B.; Zhang, W.; Ghetti, B.; Scheres, S.H.W. Distinct Conformers of Assembled Tau in Alzheimer's and Pick's Diseases. *Cold Spring Harb. Symp. Quant. Biol.* **2018**, *83*, 163–171, doi:10.1101/sqb.2018.83.037580.
59. Crary, J.F. Primary Age-Related Tauopathy and the Amyloid Cascade Hypothesis: The

Exception That Proves the Rule? *J. Neurol. neuromedicine* **2016**, *1*, 53–57, doi:10.29245/2572.942x/2016/6.1059.
60. Kim, B.; Sullivan, K.A.; Backus, C.; Feldman, E.L. Cortical Neurons Develop Insulin Resistance and Blunted Akt Signaling: A Potential Mechanism Contributing to Enhanced Ischemic Injury in Diabetes. *Antioxid. Redox Signal.* **2011**, *14*, 1829–1839, doi:10.1089/ars.2010.3816.
61. Liu, L.; Drouet, V.; Wu, J.W.; Witter, M.P.; Small, S.A.; Clelland, C.; Duff, K. Trans-Synaptic Spread of Tau Pathology in Vivo. *PLoS One* **2012**, *7*, e31302, doi:10.1371/journal.pone.0031302.
62. Colin, M.; Dujardin, S.; Schraen-Maschke, S.; Meno-Tetang, G.; Duyckaerts, C.; Courade, J.-P.; Buée, L. From the Prion-like Propagation Hypothesis to Therapeutic Strategies of Anti-Tau Immunotherapy. *Acta Neuropathol.* **2020**, *139*, 3–25, doi:10.1007/s00401-019-02087-9.
63. Asai, H.; Ikezu, S.; Tsunoda, S.; Medalla, M.; Luebke, J.; Haydar, T.; Wolozin, B.; Butovsky, O.; Kügler, S.; Ikezu, T. Depletion of Microglia and Inhibition of Exosome Synthesis Halt Tau Propagation. *Nat. Neurosci.* **2015**, *18*, 1584–1593, doi:10.1038/nn.4132.
64. Dujardin, S.; Bégard, S.; Caillierez, R.; Lachaud, C.; Delattre, L.; Carrier, S.; Loyens, A.; Galas, M.-C.; Bousset, L.; Melki, R.; et al. Ectosomes: A New Mechanism for Non-Exosomal Secretion of Tau Protein. *PLoS One* **2014**, *9*, e100760, doi:10.1371/journal.pone.0100760.
65. Switon, K.; Kotulska, K.; Janusz-Kaminska, A.; Zmorzynska, J.; Jaworski, J. Molecular Neurobiology of MTOR. *Neuroscience* **2017**, *341*, 112–153, doi:10.1016/j.neuroscience.2016.11.017.
66. Caccamo, A.; Magrì, A.; Medina, D.X.; Wisely, E. V; López-Aranda, M.F.; Silva, A.J.; Oddo, S. MTOR Regulates Tau Phosphorylation and Degradation: Implications for Alzheimer's Disease and Other Tauopathies. *Aging Cell* **2013**, *12*, 370–380, doi:10.1111/acel.12057.
67. Zempel, H.; Luedtke, J.; Kumar, Y.; Biernat, J.; Dawson, H.; Mandelkow, E.; Mandelkow, E.M. Amyloid-β Oligomers Induce Synaptic Damage via Tau-Dependent Microtubule Severing by TTLL6 and Spastin. *EMBO J.* **2013**, *32*, 2920–2937, doi:10.1038/EMBOJ.2013.207.
68. Hoover, B.R.; Reed, M.N.; Su, J.; Penrod, R.D.; Kotilinek, L.A.; Grant, M.K.; Pitstick, R.; Carlson, G.A.; Lanier, L.M.; Yuan, L.L.; et al. Tau Mislocalization to Dendritic Spines Mediates Synaptic Dysfunction Independently of Neurodegeneration. *Neuron* **2010**, *68*, 1067–1081, doi:10.1016/J.NEURON.2010.11.030.
69. Dejanovic, B.; Huntley, M.A.; De Mazière, A.; Meilandt, W.J.; Wu, T.; Srinivasan, K.; Jiang, Z.; Gandham, V.; Friedman, B.A.; Ngu, H.; et al. Changes in the Synaptic Proteome in Tauopathy and Rescue of Tau-Induced Synapse Loss by C1q Antibodies. *Neuron* **2018**, *100*, 1322-1336.e7, doi:10.1016/J.NEURON.2018.10.014.
70. Xu, J.; King, S.J.; Lapierre-Landry, M.; Nemec., B. Interplay between Velocity and Travel Distance of Kinesin-Based Transport in the Presence of Tau. *Biophys. J.* **2013**, *105*, L23–L25.
71. Ittner, L.M.; Ke, Y.D.; Götz., J. Phosphorylated Tau Interacts with C-Jun N-Terminal Kinase-Interacting Protein 1 (JIP1) in Alzheimer Disease. *J. Biol. Chem.* **2009**, *284*, 20909–20916.

72. Brelstaff, J.; Tolkovsky, A.M.; Ghetti, B.; Goedert, M.; Spillantini, M.G. Living Neurons with Tau Filaments Aberrantly Expose Phosphatidylserine and Are Phagocytosed by Microglia. *Cell Rep.* **2018**, *24*, 1939-1948.e4, doi:10.1016/j.celrep.2018.07.072.
73. Frost, B.; Hemberg, M.; Lewis, J.; Feany, M. Tau Promotes Neurodegeneration through Global Chromatin Relaxation. *Nat. Neurosci.* **2014**, *17*, 357.
74. Liu, Y.; Min, W. Thioredoxin Promotes ASK1 Ubiquitination and Degradation to Inhibit ASK1-Mediated Apoptosis in a Redox Activity-Independent Manner. *Circ. Res.* **2002**, *90*, 1259–1266, doi:10.1161/01.RES.0000022160.64355.62.
75. Bishopric, N.H.; Webster, K.A. Preventing Apoptosis with Thioredoxin: ASK Me How. *Circ. Res.* **2002**, *90*, 1237–1239, doi:10.1161/01.RES.0000025101.04065.83.
76. Paonessa, F.; Evans, L.D.; Solanki, R.; Larrieu, D.; Wray, S.; Hardy, J.; Jackson, S.P.; Livesey, F.J. Microtubules Deform the Nuclear Membrane and Disrupt Nucleocytoplasmic Transport in Tau-Mediated Frontotemporal Dementia. *Cell Rep.* **2019**, *26*, 582-593.e5, doi:10.1016/J.CELREP.2018.12.085.
77. Eftekharzadeh, B.; Daigle, J.; Kapinos, L.; Neuron, A.C.-; 2018, U. Tau Protein Disrupts Nucleocytoplasmic Transport in Alzheimer's Disease. *Elsevier* **2018**, *99*, 925–940.
78. Munnamalai, V.; Suter, D.M. Reactive Oxygen Species Regulate F-Actin Dynamics in Neuronal Growth Cones and Neurite Outgrowth. *J. Neurochem.* **2009**, *108*, 644, doi:10.1111/J.1471-4159.2008.05787.X.
79. Frost, B.; Götz, J.; Feany, M.B. Connecting the Dots between Tau Dysfunction and Neurodegeneration. *Trends Cell Biol.* **2015**, *25*, 46–53, doi:10.1016/J.TCB.2014.07.005.
80. Ramirez, Paulino, et al. Pathogenic Tau Accelerates Aging-Associated Activation of Transposable Elements in the Mouse Central Nervous System. *Prog. Neurobiol.* **2022**, *208*, 102181.
81. Guo; Jeong, H.H.; Hsieh, Y.C.; Klein, H.U.; Bennett, D.A.; De Jager, P.L.; Liu, Z.; Shulman, J.M. Tau Activates Transposable Elements in Alzheimer's Disease. *Cell Rep.* **2018**, *23*, 2874–2880, doi:10.1016/J.CELREP.2018.05.004.
82. Sun, W.; Samimi, H.; Gamez, M.; Zare, H.; Frost, B. Pathogenic Tau-Induced PiRNA Depletion Promotes Neuronal Death through Transposable Element Dysregulation in Neurodegenerative Tauopathies. *Nat. Neurosci. 2018 218* **2018**, *21*, 1038–1048, doi:10.1038/s41593-018-0194-1.
83. Saint-Aubert, L.; Lemoine, L.; Chiotis, K.; Leuzy, A.; Rodriguez-Vieitez, E.; Nordberg, A. Tau PET Imaging: Present and Future Directions. *Mol. Neurodegener.* **2017**, *12*, 19, doi:10.1186/s13024-017-0162-3.
84. Teng, E.; Manser, P.T.; Sanabria Bohorquez, S.; Wildsmith, K.R.; Pickthorn, K.; Baker, S.L.; Ward, M.; Kerchner, G.A.; Weimer, R.M. Baseline [18F]GTP1 Tau PET Imaging Is Associated with Subsequent Cognitive Decline in Alzheimer's Disease. *Alzheimers. Res. Ther.* **2021**, *13*, 196, doi:10.1186/s13195-021-00937-x.
85. Lantero-Rodriguez, J.; Snellman, A.; Benedet, A.L.; Milà-Alomà, M.; Camporesi, E.; Montoliu-Gaya, L.; Ashton, N.J.; Vrillon, A.; Karikari, T.K.; Gispert, J.D.; et al. P-tau235: A Novel Biomarker for Staging Preclinical Alzheimer's Disease. *EMBO Mol. Med.* **2021**, *13*, doi:10.15252/EMMM.202115098.
86. Barthélemy, N.R.; Bateman, R.J.; Hirtz, C.; Marin, P.; Becher, F.; Sato, C.; Gabelle, A.; Lehmann, S. Cerebrospinal Fluid Phospho-Tau T217 Outperforms T181 as a Biomarker for

the Differential Diagnosis of Alzheimer's Disease and PET Amyloid-Positive Patient Identification. *Alzheimer's Res. Ther.* **2020**, *12*, doi:10.1186/S13195-020-00596-4.
87. Cousins, K.A.Q.; Phillips, J.S.; Irwin, D.J.; Lee, E.B.; Wolk, D.A.; Shaw, L.M.; Zetterberg, H.; Blennow, K.; Burke, S.E.; Kinney, N.G.; et al. ATN Incorporating Cerebrospinal Fluid Neurofilament Light Chain Detects Frontotemporal Lobar Degeneration. *Alzheimer's Dement.* **2021**, *17*, 822–830, doi:10.1002/ALZ.12233.
88. Zhang, Y.; Wu, K.M.; Yang, L.; Dong, Q.; Yu, J.T. Tauopathies: New Perspectives and Challenges. *Mol. Neurodegener. 2022 171* **2022**, *17*, 1–29, doi:10.1186/S13024-022-00533-Z.
89. Moscoso, A.; Karikari, T.K.; Grothe, M.J.; Ashton, N.J.; Lantero-Rodriguez, J.; Snellman, A.; Zetterberg, H.; Blennow, K.; Schöll, M. CSF Biomarkers and Plasma P-Tau181 as Predictors of Longitudinal Tau Accumulation: Implications for Clinical Trial Design. *Alzheimer's Dement.* **2022**, doi:10.1002/ALZ.12570.
90. Janelidze, S.; Stomrud, E.; Smith, R.; Palmqvist, S.; Mattsson, N.; Airey, D.C.; Proctor, N.K.; Chai, X.; Shcherbinin, S.; Sims, J.R.; et al. Cerebrospinal Fluid P-Tau217 Performs Better than p-Tau181 as a Biomarker of Alzheimer's Disease. *Nat. Commun.* **2020**, *11*, 1683, doi:10.1038/s41467-020-15436-0.
91. Thijssen, E.; Joie, R. La; Strom, A.; … C.F.-T.L.; 2021, U. Plasma Phosphorylated Tau 217 and Phosphorylated Tau 181 as Biomarkers in Alzheimer's Disease and Frontotemporal Lobar Degeneration: A Retrospective Diagnostic. *Lancet Neurol.* **2021**, *20*, 739–752.
92. Congdon, E.; Sigurdsson, E. Tau-Targeting Therapies for Alzheimer Disease. *Nat. Rev. Neurol.* **2018**, *14*, 399–415.
93. Bittar, A.; Bhatt, N.; Disease, R.K.-N. of; 2020, U. Advances and Considerations in AD Tau-Targeted Immunotherapy. *Neurobiol. Dis.* **2020**, *134*, 104707.
94. Novak, P.; Kovacech, B.; Katina, S.; Schmidt, R.; Scheltens, P.; Kontsekova, E.; Ropele, S.; Fialova, L.; Kramberger, M.; Paulenka-Ivanovova, N.; et al. ADAMANT: A Placebo-Controlled Randomized Phase 2 Study of AADvac1, an Active Immunotherapy against Pathological Tau in Alzheimer's Disease. *Nat. Aging 2021 16* **2021**, *1*, 521–534, doi:10.1038/s43587-021-00070-2.
95. 18-Months Safety Follow-up Study of AADvac1, an Active Tau Vaccine for Alzheimer's Disease (FUNDAMANT) Available online: https://www.clinicaltrials.gov/ct2/show/NCT02031198 (accessed on 4 January 2023).
96. Song, C.; Shi, J.; Zhang, P.; Zhang, Y.; Xu, J.; Zhao, L.; Zhang, R.; Wang, H.; Chen, H. Immunotherapy for Alzheimer's Disease: Targeting β-Amyloid and Beyond. *Transl. Neurodegener.* **2022**, *11*, 1–17, doi:10.1186/S40035-022-00292-3/FIGURES/3.
97. A Study to Evaluate the Safety, Tolerability and Immunogenicity of Tau Targeted Vaccines in Participants With Early Alzheimer's Disease Available online: https://www.clinicaltrials.gov/ct2/show/NCT04445831 (accessed on 4 January 2023).
98. Jadhav, S.; Avila, J.; Schöll, M.; Kovacs, G.G.; Kövari, E.; Skrabana, R.; Evans, L.D.; Kontsekova, E.; Malawska, B.; de Silva, R.; et al. A Walk through Tau Therapeutic Strategies. *Acta Neuropathol. Commun.* **2019**, *7*, 22, doi:10.1186/S40478-019-0664-Z.
99. Mignon, L.; Kordasiewicz, H.; Lane, R.; Smith, A.; Miller, T.; Narayanan, P.; Swayze, E.; Norris, D.; Fitzsimmons, B.; Bennett, F. Design of the First-in-Human Study of IONIS-MAPTRx, a Tau-Lowering Antisense Oligonucleotide, in Patients With Alzheimer Disease

(S2.006). *Neurology* **2018**, *90*.
100. Wischik, C.M.; Bentham, P.; Gauthier, S.; Miller, S.; Kook, K.; Schelter, B.O. Oral Tau Aggregation Inhibitor for Alzheimer's Disease: Design, Progress and Basis for Selection of the 16 Mg/Day Dose in a Phase 3, Randomized, Placebo-Controlled Trial of Hydromethylthionine Mesylate. *J. Prev. Alzheimer's Dis.* **2022**, *9*, 780–790, doi:10.14283/jpad.2022.63.
101. Alvarez, X.A.; Winston, C.N.; Barlow, J.W.; Sarsoza, F.M.; Alvarez, I.; Aleixandre, M.; Linares, C.; García-Fantini, M.; Kastberger, B.; Winter, S.; et al. Modulation of Amyloid-β and Tau in Alzheimer's Disease Plasma Neuronal-Derived Extracellular Vesicles by Cerebrolysin® and Donepezil. *J. Alzheimers. Dis.* **2022**, *90*, 705–717, doi:10.3233/JAD-220575.
102. Teng, E.; Manser, P.T.; Pickthorn, K.; Brunstein, F.; Blendstrup, M.; Bohorquez, S.S.; Wildsmith, K.R.; Toth, B.; Dolton, M.; Ramakrishnan, V.; et al. Safety and Efficacy of Semorinemab in Individuals With Prodromal to Mild Alzheimer Disease: A Randomized Clinical Trial. *JAMA Neurol.* **2022**, *79*, 758–767, doi:10.1001/JAMANEUROL.2022.1375.
103. Easton, A.; Jensen, M.L.; Wang, C.; Hagedorn, P.H.; Li, Y.; Weed, M.; Meredith, J.E.; Guss, V.; Jones, K.; Gill, M.; et al. Identification and Characterization of a MAPT-Targeting Locked Nucleic Acid Antisense Oligonucleotide Therapeutic for Tauopathies. *Mol. Ther. - Nucleic Acids* **2022**, *29*, 625–642, doi:10.1016/J.OMTN.2022.07.027.
104. Polis, B.; Squillario, M.; Gurevich, V.; Srikanth, K.D.; Assa, M.; Samson, A.O. Effects of Chronic Arginase Inhibition with Norvaline on Tau Pathology and Brain Glucose Metabolism in Alzheimer's Disease Mice. *Neurochem. Res.* **2022**, *47*, 1255–1268, doi:10.1007/s11064-021-03519-3.
105. Singer, K.E.; McGlone, E.D.; Collins, S.M.; Wallen, T.E.; Morris, M.C.; Schuster, R.M.; England, L.G.; Robson, M.J.; Goodman, M.D. Propranolol Reduces P-Tau Accumulation and Improves Behavior Outcomes in a Polytrauma Murine Model. *J. Surg. Res.* **2022**, *282*, 183–190, doi:10.1016/j.jss.2022.09.017.
106. Tong, B.C.-K.; Huang, A.S.; Wu, A.J.; Iyaswamy, A.; Ho, O.K.-Y.; Kong, A.H.-Y.; Sreenivasmurthy, S.G.; Zhu, Z.; Su, C.; Liu, J.; et al. Tetrandrine Ameliorates Cognitive Deficits and Mitigates Tau Aggregation in Cell and Animal Models of Tauopathies. *J. Biomed. Sci.* **2022**, *29*, 85, doi:10.1186/s12929-022-00871-6.
107. Bittar, A.; Al-Lahham, R.; Bhatt, N.; Moore, K.; Montalbano, M.; Jerez, C.; Fung, L.; McAllen, S.; Ellsworth, A.; Kayed, R. Passive Immunotherapy Targeting Tau Oligomeric Strains Reverses Tauopathy Phenotypes in Aged Human-Tau Mice in a Mouse Model-Specific Manner. *J. Alzheimer's Dis.* **2022**, *Preprint*, 1–20, doi:10.3233/JAD-220518.
108. Zaki, M.O.; El-Desouky, S.; Elsherbiny, D.A.; Salama, M.; Azab, S.S. Glimepiride Mitigates Tauopathy and Neuroinflammation in P301S Transgenic Mice: Role of AKT/GSK3β Signaling. *Inflammopharmacology* **2022**, *30*, 1871–1890, doi:10.1007/s10787-022-01023-w.
109. Shcherbinin, S.; Evans, C.D.; Lu, M.; Andersen, S.W.; Pontecorvo, M.J.; Willis, B.A.; Gueorguieva, I.; Hauck, P.M.; Brooks, D.A.; Mintun, M.A.; et al. Association of Amyloid Reduction after Donanemab Treatment with Tau Pathology and Clinical Outcomes: The TRAILBLAZER-ALZ Randomized Clinical Trial. *JAMA Neurol.* **2022**, 1DUMMY, doi:10.1001/jamaneurol.2022.2793.

110. Riederer, F. Donanemab in Early Alzheimer's Disease. *J. fur Neurol. Neurochir. und Psychiatr.* **2021**, *22*, 142–143, doi:10.1056/NEJMOA2100708/SUPPL_FILE/NEJMOA2100708_DATA-SHARING.PDF.
111. Ou, W.; Yang, J.; Simanauskaite, J.; Choi, M.; Castellanos, D.M.; Chang, R.; Sun, J.; Jagadeesan, N.; Parfitt, K.D.; Cribbs, D.H.; et al. Biologic TNF-α Inhibitors Reduce Microgliosis, Neuronal Loss, and Tau Phosphorylation in a Transgenic Mouse Model of Tauopathy. *J. Neuroinflammation* **2021**, *18*, doi:10.1186/s12974-021-02332-7.
112. Xia, L.; Pang, Y.; Li, J.; Wu, B.; Du, Y.; Chen, Y.; Luo, M.; Wang, Y.; Dong, Z.; Zhu, L.Q. Dihydroartemisinin Induces O-GlcNAcylation and Improves Cognitive Function in a Mouse Model of Tauopathy. *J. Alzheimer's Dis.* **2021**, *84*, 239–248, doi:10.3233/JAD-210643.
113. Sun, X. ying; Li, L. jie; Dong, Q.X.; Zhu, J.; Huang, Y. ru; Hou, S. jie; Yu, X. lin; Liu, R. tian Rutin Prevents Tau Pathology and Neuroinflammation in a Mouse Model of Alzheimer's Disease. *J. Neuroinflammation* **2021**, *18*, doi:10.1186/s12974-021-02182-3.
114. Anglada-Huguet, M.; Rodrigues, S.; Hochgräfe, K.; Mandelkow, E.; Mandelkow, E.-M. Inhibition of Tau Aggregation with BSc3094 Reduces Tau and Decreases Cognitive Deficits in RTg4510 Mice. *Alzheimer's Dement. (New York, N. Y.)* **2021**, *7*, e12170, doi:10.1002/trc2.12170.
115. Sonawane, S.K.; Chinnathambi, S. Epigallocatechin-3-Gallate Modulates Tau Post-Translational Modifications and Cytoskeletal Network. *Oncotarget* **2021**, *12*, 1083–1099, doi:10.18632/oncotarget.27963.
116. Wang, W.; Zhou, Q.; Jiang, T.; Li, S.; Ye, J.; Zheng, J.; Wang, X.; Liu, Y.; Deng, M.; Ke, D.; et al. A Novel Small-Molecule PROTAC Selectively Promotes Tau Clearance to Improve Cognitive Functions in Alzheimer-like Models. *Theranostics* **2021**, *11*, 5279–5295, doi:10.7150/thno.55680.
117. Neves, A.F.; Camargo, C.; Premer, C.; Hare, J.M.; Baumel, B.S.; Pinto, M. Intravenous Administration of Mesenchymal Stem Cells Reduces Tau Phosphorylation and Inflammation in the 3xTg-AD Mouse Model of Alzheimer's Disease. *Exp. Neurol.* **2021**, *341*, doi:10.1016/J.EXPNEUROL.2021.113706.
118. Dam, T.; Boxer, A.L.; Golbe, L.I.; Höglinger, G.U.; Morris, H.R.; Litvan, I.; Lang, A.E.; Corvol, J.-C.; Aiba, I.; Grundman, M.; et al. Safety and Efficacy of Anti-Tau Monoclonal Antibody Gosuranemab in Progressive Supranuclear Palsy: A Phase 2, Randomized, Placebo-Controlled Trial. *Nat. Med.* **2021**, *27*, 1451–1457, doi:10.1038/s41591-021-01455-x.
119. Rühlmann, C.; Wölk, T.; Blümel, T.; Stahn, L.; Vollmar, B.; Kuhla, A. Long-Term Caloric Restriction in ApoE-Deficient Mice Results in Neuroprotection via Fgf21-Induced AMPK/MTOR Pathway. *Aging (Albany. NY).* **2016**, *8*, 2777–2789, doi:10.18632/AGING.101086.
120. Brownlow, M.L.; Joly-Amado, A.; Azam, S.; Elza, M.; Selenica, M.L.; Pappas, C.; Small, B.; Engelman, R.; Gordon, M.N.; Morgan, D. Partial Rescue of Memory Deficits Induced by Calorie Restriction in a Mouse Model of Tau Deposition. *Behav. Brain Res.* **2014**, *271*, 79–88, doi:10.1016/J.BBR.2014.06.001.
121. Arendt, T.; Stieler, J.T.; Holzer, M. Tau and Tauopathies. *Brain Res. Bull.* **2016**, *126*, 238–292, doi:10.1016/J.BRAINRESBULL.2016.08.018.
122. Wang, J.Z.; Wang, Z.H.; Tian, Q. Tau Hyperphosphorylation Induces Apoptotic Escape and

Triggers Neurodegeneration in Alzheimer's Disease. *Neurosci. Bull. 2014 302* **2014**, *30*, 359–366, doi:10.1007/S12264-013-1415-Y.

123. Andrade-Moraes, C.H.; Oliveira-Pinto, A. V.; Castro-Fonseca, E.; da Silva, C.G.; Guimarães, D.M.; Szczupak, D.; Parente-Bruno, D.R.; Carvalho, L.R.B.; Polichiso, L.; Gomes, B. V.; et al. Cell Number Changes in Alzheimer's Disease Relate to Dementia, Not to Plaques and Tangles. *Brain* **2013**, *136*, 3738–3752, doi:10.1093/BRAIN/AWT273.
124. Zuniga, G.; Levy, S.; Ramirez, P.; Mange, J. De; Gonzalez, E.; Gamez, M.; Frost, B. Tau-Induced Deficits in Nonsense-Mediated MRNA Decay Contribute to Neurodegeneration. *Alzheimer's Dement.* **2022**, doi:10.1002/ALZ.12653.
125. Islam, M.I.; Nagakannan, P.; Shcholok, T.; Contu, F.; Mai, S.; Albensi, B.C.; Del Bigio, M.R.; Wang, J.F.; Sharoar, M.G.; Yan, R.; et al. Regulatory Role of Cathepsin L in Induction of Nuclear Laminopathy in Alzheimer's Disease. *Aging Cell* **2022**, *21*, doi:10.1111/ACEL.13531.
126. Islam, M.I.; Nagakannan, P.; Ogungbola, O.; Djordjevic, J.; Albensi, B.C.; Eftekharpour, E. Thioredoxin System as a Gatekeeper in Caspase-6 Activation and Nuclear Lamina Integrity: Implications for Alzheimer's Disease. *Free Radic. Biol. Med.* **2019**, *134*, 567–580, doi:10.1016/j.freeradbiomed.2019.02.010.
127. Greenberg, S.G.; Davies, P.; Schein, J.D.; Binder, L.I. Hydrofluoric Acid-Treated Tau PHF Proteins Display the Same Biochemical Properties as Normal Tau. *J. Biol. Chem.* **1992**, *267*, 564–569, doi:10.1016/S0021-9258(18)48531-6.
128. Guo, T.; Dakkak, D.; Rodriguez-Martin, T.; Noble, W.; Hanger, D.P. A Pathogenic Tau Fragment Compromises Microtubules, Disrupts Insulin Signaling and Induces the Unfolded Protein Response. *Acta Neuropathol. Commun.* **2019**, *7*, 1–15, doi:10.1186/S40478-018-0651-9/FIGURES/6.
129. Isoform Tau-F of Microtubule-Associated Protein Tau Available online: https://www.uniprot.org/uniprotkb/P10636/entry (accessed on 16 February 2023).
130. Zonderland, J.; Wieringa, P.; L Moroni -; 2019, U. A Quantitative Method to Analyse F-Actin Distribution in Cells. *MethodsX* **2019**, *6*, 2562–2569.
131. Dwane, S.; Durack, E.; Kiely, P.A. Optimising Parameters for the Differentiation of SH-SY5Y Cells to Study Cell Adhesion and Cell Migration. *BMC Res. Notes* **2013**, *6*, doi:10.1186/1756-0500-6-366.
132. Teppola, H.; Sarkanen, J.R.; Jalonen, T.O.; Linne, M.L. Morphological Differentiation Towards Neuronal Phenotype of SH-SY5Y Neuroblastoma Cells by Estradiol, Retinoic Acid and Cholesterol. *Neurochem. Res.* **2016**, *41*, 731–747, doi:10.1007/S11064-015-1743-6.
133. Lotan, R. Retinoids in Cancer Chemoprevention. *FASEB J. Off. Publ. Fed. Am. Soc. Exp. Biol.* **1996**, *10*, 1031–1039, doi:10.1096/fasebj.10.9.8801164.
134. Melino, G.; Thiele, C.J.; Knight, R.A.; Piacentini, M. Retinoids and the Control of Growth/Death Decisions in Human Neuroblastoma Cell Lines. *J. Neurooncol.* **1997**, *31*, 65–83, doi:10.1023/a:1005733430435.
135. Encinas, M.; Iglesias, M.; Liu, Y.; Wang, H.; Muhaisen, A.; Ceña, V.; Gallego, C.; Comella, J.X. Sequential Treatment of SH-SY5Y Cells with Retinoic Acid and Brain-Derived Neurotrophic Factor Gives Rise to Fully Differentiated, Neurotrophic Factor-Dependent, Human Neuron-Like Cells. *J. Neurochem.* **2000**, *75*, 991–1003, doi:10.1046/J.1471-4159.2000.0750991.X.

136. Kimura, T.; Sharma, G.; Ishiguro, K.; Hisanaga, S.I. Phospho-Tau Bar Code: Analysis of Phosphoisotypes of Tau and Its Application to Tauopathy. *Front. Neurosci.* **2018**, *12*, 44, doi:10.3389/FNINS.2018.00044/BIBTEX.
137. Nixon, R.A.; Yang, D.-S. Autophagy Failure in Alzheimer's Disease—Locating the Primary Defect. *Neurobiol. Dis.* **2011**, *43*, 38–45, doi:https://doi.org/10.1016/j.nbd.2011.01.021.
138. Wang, Y.; Krüger, U.; Mandelkow, E.; Mandelkow, E.M. Generation of Tau Aggregates and Clearance by Autophagy in an Inducible Cell Model of Tauopathy. *Neurodegener. Dis.* **2010**, *7*, 103–107, doi:10.1159/000285516.
139. Wang; Mandelkow, E. Degradation of Tau Protein by Autophagy and Proteasomal Pathways. *Biochem. Soc. Trans.* **2012**, *40*, 644–652, doi:10.1042/BST20120071.
140. Lim, F.; Hernández, F.; Lucas, J.J.; Gómez-Ramos, P.; Morán, M.A.; Ávila, J. FTDP-17 Mutations in Tau Transgenic Mice Provoke Lysosomal Abnormalities and Tau Filaments in Forebrain. *Mol. Cell. Neurosci.* **2001**, *18*, 702–714, doi:https://doi.org/10.1006/mcne.2001.1051.
141. Runwal, G.; Stamatakou, E.; Siddiqi, F.H.; Puri, C.; Zhu, Y.; Rubinsztein, D.C. LC3-Positive Structures Are Prominent in Autophagy-Deficient Cells. *Sci. Reports 2019 91* **2019**, *9*, 1–14, doi:10.1038/s41598-019-46657-z.
142. Kuma, A.; Matsui, M.; Mizushima, N. LC3, an Autophagosome Marker, Can Be Incorporated into Protein Aggregates Independent of Autophagy: Caution in the Interpretation of LC3 Localization. *Autophagy* **2007**, *3*, 323–328, doi:10.4161/AUTO.4012.
143. Yoshii, S.R.; Mizushima, N. Monitoring and Measuring Autophagy. *Int. J. Mol. Sci.* **2017**, *18*, doi:10.3390/ijms18091865.
144. Kaushik, S.; Cuervo, A.M. The Coming of Age of Chaperone-Mediated Autophagy. *Nat. Rev. Mol. Cell Biol.* **2018**, *19*, 365–381, doi:10.1038/s41580-018-0001-6.
145. Frost, B.; Bardai, F.H.; Feany, M.B. Lamin Dysfunction Mediates Neurodegeneration in Tauopathies. *Curr. Biol.* **2016**, *26*, 129–136, doi:10.1016/j.cub.2015.11.039.
146. LJ Mah, A El-Osta, T.K. ΓH2AX: A Sensitive Molecular Marker of DNA Damage and Repair. *Leukemia* **2010**, *24*, 679–686.
147. Asada-Utsugi; Megumi; Uemura; Ayaki, et al. Failure of DNA Double-Strand Break Repair by Tau Mediates Alzheimer's Disease Pathology in Vitro. *Commun. Biol.* **2022**, *5*, 358.
148. Zimmer-Bensch, G.; Zempel, H. Dna Methylation in Genetic and Sporadic Forms of Neurodegeneration: Lessons from Alzheimer's, Related Tauopathies and Genetic Tauopathies. *Cells* **2021**, *10*, doi:10.3390/CELLS10113064.
149. Coppieters, N.; Dieriks, B. V; Lill, C.; Faull, R.L.M.; Curtis, M.A.; Dragunow, M. Global Changes in DNA Methylation and Hydroxymethylation in Alzheimer's Disease Human Brain. *Neurobiol. Aging* **2014**, *35*, 1334–1344, doi:10.1016/j.neurobiolaging.2013.11.031.
150. Löffler, T.; Flunkert, S.; Taub, N.; Schofield, E.L.; Ward, M.A.; Windisch, M.; Hutter-Paier, B. Stable Mutated Tau441 Transfected SH-SY5Y Cells as Screening Tool for Alzheimer's Disease Drug Candidates. *J. Mol. Neurosci.* **2012**, *47*, 192–203, doi:10.1007/S12031-012-9716-6.
151. Biedler, J.L.; Helson, L.; Spengler, B.A. Morphology and Growth, Tumorigenicity, and Cytogenetics of Human Neuroblastoma Cells in Continuous Culture. *Cancer Res.* **1973**, *33*, 2643–2652.
152. Kuramoto, T.; Werrbach-Perez, K.; Perez-Polo, J.R.; Haber, B. Membrane Properties of a

Human Neuroblastoma II: Effects of Differentiation. *J. Neurosci. Res.* **1981**, *6*, 441–449, doi:10.1002/jnr.490060402.
153. Adem, A.; Mattsson, M.E.; Nordberg, A.; Påhlman, S. Muscarinic Receptors in Human SH-SY5Y Neuroblastoma Cell Line: Regulation by Phorbol Ester and Retinoic Acid-Induced Differentiation. *Brain Res.* **1987**, *430*, 235–242, doi:10.1016/0165-3806(87)90156-8.
154. Påhlman, S.; Ruusala, A.I.; Abrahamsson, L.; Mattsson, M.E.; Esscher, T. Retinoic Acid-Induced Differentiation of Cultured Human Neuroblastoma Cells: A Comparison with Phorbolester-Induced Differentiation. *Cell Differ.* **1984**, *14*, 135–144, doi:10.1016/0045-6039(84)90038-1.
155. Tosetti, P.; Taglietti, V.; Toselli, M. Functional Changes in Potassium Conductances of the Human Neuroblastoma Cell Line SH-SY5Y during in Vitro Differentiation. *J. Neurophysiol.* **1998**, *79*, 648–658, doi:10.1152/jn.1998.79.2.648.
156. Lopes, F.M.; Schröder, R.; da Frota, M.L.C.J.; Zanotto-Filho, A.; Müller, C.B.; Pires, A.S.; Meurer, R.T.; Colpo, G.D.; Gelain, D.P.; Kapczinski, F.; et al. Comparison between Proliferative and Neuron-like SH-SY5Y Cells as an in Vitro Model for Parkinson Disease Studies. *Brain Res.* **2010**, *1337*, 85–94, doi:10.1016/j.brainres.2010.03.102.
157. Bell, M.; Zempel, H. SH-SY5Y-Derived Neurons: A Human Neuronal Model System for Investigating TAU Sorting and Neuronal Subtype-Specific TAU Vulnerability. *Rev. Neurosci.* **2022**, *33*, 1–15, doi:10.1515/REVNEURO-2020-0152/HTML.
158. Li, X.-C.; Hu, Y.; Wang, Z.-H.; Luo, Y.; Zhang, Y.; Liu, X.-P.; Feng, Q.; Wang, Q.; Ye, K.; Liu, G.-P.; et al. Human Wild-Type Full-Length Tau Accumulation Disrupts Mitochondrial Dynamics and the Functions via Increasing Mitofusins. *Springer* **2016**, doi:10.1038/srep24756.
159. Andorfer, C.; Kress, Y.; Espinoza, M.; De Silva, R.; Tucker, K.L.; Barde, Y.-A.; Duff, K.; Davies, P. Hyperphosphorylation and Aggregation of Tau in Mice Expressing Normal Human Tau Isoforms. *Wiley Online Libr.* **2003**, *86*, 582–590, doi:10.1046/j.1471-4159.2003.01879.x.
160. der Jeugd, A. Van; Ahmed, T.; Burnouf, S.; Belarbi, K.; Hamdame, M.; Grosjean, M.-E.; Humez, S.; Balschun, D.; Blum, D.; Buée, L.; et al. Hippocampal Tauopathy in Tau Transgenic Mice Coincides with Impaired Hippocampus-Dependent Learning and Memory, and Attenuated Late-Phase Long-Term Depression of Synaptic Transmission. *Neurobiol. Learn. Mem.* **2011**, *95*, 296–304, doi:https://doi.org/10.1016/j.nlm.2010.12.005.
161. Khlistunova, I.; Biernat, J.; Wang, Y.; Pickhardt, M.; von Bergen, M.; Gazova, Z.; Mandelkow, E.; Mandelkow, E.-M. Inducible Expression of Tau Repeat Domain in Cell Models of Tauopathy: Aggregation Is Toxic to Cells but Can Be Reversed by Inhibitor Drugs. *J. Biol. Chem.* **2006**, *281*, 1205–1214, doi:10.1074/jbc.M507753200.
162. Bandyopadhyay, B.; Li, G.; Yin, H.; Kuret, J. Tau Aggregation and Toxicity in a Cell Culture Model of Tauopathy. *J. Biol. Chem.* **2007**, *282*, 16454–16464, doi:10.1074/jbc.M700192200.
163. Vogelsberg-Ragaglia, V.; Bruce, J.; Richter-Landsberg, C.; Zhang, B.; Hong, M.; Trojanowski, J.Q.; Lee, V.M. Distinct FTDP-17 Missense Mutations in Tau Produce Tau Aggregates and Other Pathological Phenotypes in Transfected CHO Cells. *Mol. Biol. Cell* **2000**, *11*, 4093–4104, doi:10.1091/mbc.11.12.4093.

164. Guo, J.L.; Lee, V.M.-Y. Seeding of Normal Tau by Pathological Tau Conformers Drives Pathogenesis of Alzheimer-like Tangles. *J. Biol. Chem.* **2011**, *286*, 15317–15331, doi:10.1074/jbc.M110.209296.
165. Nonaka, T.; Watanabe, S.T.; Iwatsubo, T.; Hasegawa, M. Seeded Aggregation and Toxicity of {alpha}-Synuclein and Tau: Cellular Models of Neurodegenerative Diseases. *J. Biol. Chem.* **2010**, *285*, 34885–34898, doi:10.1074/jbc.M110.148460.
166. Lu, M.; Kosik, K.S. Competition for Microtubule-Binding with Dual Expression of Tau Missense and Splice Isoforms. *Mol. Biol. Cell* **2001**, *12*, 171–184, doi:10.1091/mbc.12.1.171.
167. Bondulich, M.K.; Guo, T.; Meehan, C.; Manion, J.; Rodriguez Martin, T.; Mitchell, J.C.; Hortobagyi, T.; Yankova, N.; Stygelbout, V.; Brion, J.P.; et al. Tauopathy Induced by Low Level Expression of a Human Brain-Derived Tau Fragment in Mice Is Rescued by Phenylbutyrate. *Brain* **2016**, doi:10.1093/brain/aww137.
168. Bondulich, M.K.; Guo, T.; Meehan, C.; Manion, J.; Rodriguez Martin, T.; Mitchell, J.C.; Hortobagyi, T.; Yankova, N.; Stygelbout, V.; Brion, J.P.; et al. Tauopathy Induced by Low Level Expression of a Human Brain-Derived Tau Fragment in Mice Is Rescued by Phenylbutyrate. *Brain* **2016**, *139*, 2290–2306, doi:10.1093/brain/aww137.
169. Wray, S.; Saxton, M.; Anderton, B.H.; Hanger, D.P. Direct Analysis of Tau from PSP Brain Identifies New Phosphorylation Sites and a Major Fragment of N-Terminally Cleaved Tau Containing Four Microtubule-Binding Repeats. *J. Neurochem.* **2008**, *105*, 2343–2352, doi:10.1111/j.1471-4159.2008.05321.x.
170. Lyu, C.; Da Vela, S.; Al-Hilaly, Y.; Marshall, K.E.; Thorogate, R.; Svergun, D.; Serpell, L.C.; Pastore, A.; Hanger, D.P. The Disease Associated Tau35 Fragment Has an Increased Propensity to Aggregate Compared to Full-Length Tau. *Front. Mol. Biosci.* **2021**, *8*, doi:10.3389/FMOLB.2021.779240/FULL.
171. Lyu, C.; Pollack, S.J.; Al-Hilaly, Y.K.; Da Vela, S.; Serpell, L.; Svergun, D.; Pastore, A.; Hanger, D.P. Self-Assembly and Cellular Effect of Tau35, a Disease-Associated Tau Fragment. *Alzheimers. Dement.* **2021**, *17*, e052072, doi:10.1002/ALZ.052072.
172. Jiang, L.; Wolozin, B. B A S I C S C I E N C E A N D P A T H O G E N E S I S PODIUM PRESENTATION Oligomeric Tau Disrupts Nuclear Envelope via Binding to Lamin Proteins and Lamin B Receptor. **2021**, doi:10.1002/alz.054521.
173. Montalbano, M.; McAllen, S.; Sengupta, U.; Puangmalai, N.; Bhatt, N.; Ellsworth, A.; Kayed, R. Tau Oligomers Mediate Aggregation of RNA-Binding Proteins Musashi1 and Musashi2 Inducing Lamin Alteration. *Aging Cell* **2019**, *18*, e13035, doi:10.1111/acel.13035.
174. Camozzi, D.; Capanni, C.; Cenni, V.; Mattioli, E.; Columbaro, M.; Squarzoni, S.; Lattanzi, G. Diverse Lamin-Dependent Mechanisms Interact to Control Chromatin Dynamics. *http://dx.doi.org/10.4161/nucl.36289* **2014**, *5*, 427–440, doi:10.4161/NUCL.36289.
175. Frost, B. Alzheimer's Disease: An Acquired Neurodegenerative Laminopathy. *Nucleus* 2016, *7*, 275–283.
176. Maurer, M.; Lammerding, J. The Driving Force: Nuclear Mechanotransduction in Cellular Function, Fate, and Disease. *Annu. Rev. Biomed. Eng.* **2019**, *21*, 443–468, doi:10.1146/annurev-bioeng-060418-052139.
177. Janota, C.; Calero-Cuenca, F.; Gomes, E. The Role of the Cell Nucleus in

Mechanotransduction. *Curr. Opin. Cell Biol.* **2020**, *63*, 204–211.
178. Martino, F.; Perestrelo, A.R.; Vinarský, V.; Pagliari, S.; Forte, G. Cellular Mechanotransduction: From Tension to Function. *Front. Physiol.* **2018**, *9*, doi:10.3389/fphys.2018.00824.
179. Venkatramani, A.; Panda, D. Regulation of Neuronal Microtubule Dynamics by Tau: Implications for Tauopathies. *Int. J. Biol. Macromol.* **2019**, *133*, 473–483, doi:10.1016/j.ijbiomac.2019.04.120.
180. He, H.J.; Wang, X.S.; Pan, R.; Wang, D.L.; Liu, M.N.; He, R.Q. The Proline-Rich Domain of Tau Plays a Role in Interactions with Actin. *BMC Cell Biol.* **2009**, *10*, 81, doi:10.1186/1471-2121-10-81.
181. Fulga, T.; Elson-Schwab, I.; Khurana, V.; … M.S.-N. cell; 2007, U. Abnormal Bundling and Accumulation of F-Actin Mediates Tau-Induced Neuronal Degeneration in Vivo. *Nat. Cell Biol.* **2007**, *9*, 139–148.
182. Guthrie, C.R.; Schellenberg, G.D.; Kraemer, B.C. SUT-2 Potentiates Tau-Induced Neurotoxicity in Caenorhabditis Elegans. *Hum. Mol. Genet.* **2009**, *18*, 1825–1838, doi:10.1093/hmg/ddp099.
183. Bardai, F.H.; Ordonez, D.G.; Bailey, R.M.; Hamm, M.; Lewis, J.; Feany, M.B. Lrrk Promotes Tau Neurotoxicity through Dysregulation of Actin and Mitochondrial Dynamics. *PLoS Biol.* **2018**, *16*, e2006265, doi:10.1371/journal.pbio.2006265.
184. Zhu, X.; Raina, A.K.; Rottkamp, C.A.; Aliev, G.; Perry, G.; Boux, H.; Smith, M.A. Activation and Redistribution of C-Jun N-Terminal Kinase/Stress Activated Protein Kinase in Degenerating Neurons in Alzheimer's Disease. *J. Neurochem.* **2001**, *76*, 435–441, doi:10.1046/j.1471-4159.2001.00046.x.
185. Ferrer, I.; Blanco, R.; Carmona, M.; Puig, B. Phosphorylated Mitogen-Activated Protein Kinase (MAPK/ERK-P), Protein Kinase of 38 KDa (P38-P), Stress-Activated Protein Kinase (SAPK/JNK-P), and Calcium/Calmodulin-Dependent Kinase II (CaM Kinase II) Are Differentially Expressed in Tau Deposits in Neuro. *J. Neural Transm.* **2001**, *108*, 1397–1415, doi:10.1007/s007020100016.
186. Vogel, J.; Anand, V.S.; Ludwig, B.; Nawoschik, S.; Dunlop, J.; Braithwaite, S.P. The JNK Pathway Amplifies and Drives Subcellular Changes in Tau Phosphorylation. *Neuropharmacology* **2009**, *57*, 539–550, doi:10.1016/j.neuropharm.2009.07.021.
187. Ploia, C.; Antoniou, X.; Sclip, A.; Grande, V.; Cardinetti, D.; Colombo, A.; Canu, N.; Benussi, L.; Ghidoni, R.; Forloni, G.; et al. JNK Plays a Key Role in Tau Hyperphosphorylation in Alzheimer's Disease Models. *J. Alzheimers. Dis.* **2011**, *26*, 315–329, doi:10.3233/JAD-2011-110320.
188. Yoshida, H.; Hastie, C.J.; McLauchlan, H.; Cohen, P.; Goedert, M. Phosphorylation of Microtubule-Associated Protein Tau by Isoforms of c-Jun N-Terminal Kinase (JNK). *J. Neurochem.* **2004**, *90*, 352–358, doi:10.1111/j.1471-4159.2004.02479.x.
189. Reynolds, C.H.; Utton, M.A.; Gibb, G.M.; Yates, A.; Anderton, B.H. Stress-Activated Protein Kinase/c-Jun N-Terminal Kinase Phosphorylates Tau Protein. *J. Neurochem.* **1997**, *68*, 1736–1744, doi:10.1046/j.1471-4159.1997.68041736.x.
190. Luna-Muñoz, J.; Chávez-Macías, L.; García-Sierra, F.; Mena, R. Earliest Stages of Tau Conformational Changes Are Related to the Appearance of a Sequence of Specific Phospho-Dependent Tau Epitopes in Alzheimer's Disease. *J. Alzheimers. Dis.* **2007**, *12*,

365–375, doi:10.3233/jad-2007-12410.
191. Grueninger, F.; Bohrmann, B.; Czech, C.; Ballard, T.M.; Frey, J.R.; Weidensteiner, C.; von Kienlin, M.; Ozmen, L. Phosphorylation of Tau at S422 Is Enhanced by Abeta in TauPS2APP Triple Transgenic Mice. *Neurobiol. Dis.* **2010**, *37*, 294–306, doi:10.1016/j.nbd.2009.09.004.
192. Bogoyevitch, M.A.; Boehm, I.; Oakley, A.; Ketterman, A.J.; Barr, R.K. Targeting the JNK MAPK Cascade for Inhibition: Basic Science and Therapeutic Potential. *Biochim. Biophys. Acta* **2004**, *1697*, 89–101, doi:10.1016/j.bbapap.2003.11.016.
193. Song; Zhe; Xue, C.; Wang, H.; Han, S.; Liu, W.; Peng, B.; He, X.; Yin., J. "Overexpression of Tau Impairs Insulin Signaling Through the JNK Pathway." *Stem Cells Regen. Med.* **2019**, 44–53.
194. Martin, L.; Latypova, X.; Wilson, C.M.; Magnaudeix, A.; Perrin, M.-L.; Yardin, C.; Terro, F. Tau Protein Kinases: Involvement in Alzheimer's Disease. *Ageing Res. Rev.* **2013**, *12*, 289–309, doi:10.1016/j.arr.2012.06.003.
195. Tolosa, E.; Litvan, I.; Höglinger, G.U.; Burn, D.; Lees, A.; Andrés, M. V; Gómez-Carrillo, B.; León, T.; Del Ser, T. A Phase 2 Trial of the GSK-3 Inhibitor Tideglusib in Progressive Supranuclear Palsy. *Mov. Disord.* **2014**, *29*, 470–478, doi:10.1002/mds.25824.
196. Noble, W.; Planel, E.; Zehr, C.; Olm, V.; Meyerson, J.; Suleman, F.; Gaynor, K.; Wang, L.; LaFrancois, J.; Feinstein, B.; et al. Inhibition of Glycogen Synthase Kinase-3 by Lithium Correlates with Reduced Tauopathy and Degeneration in Vivo. *Proc. Natl. Acad. Sci. U. S. A.* **2005**, *102*, 6990–6995, doi:10.1073/pnas.0500466102.
197. Yadikar, H.; Torres, I.; Aiello, G.; Kurup, M.; Yang, Z.; Lin, F.; Kobeissy, F.; Yost, R.; Wang, K.K. Screening of Tau Protein Kinase Inhibitors in a Tauopathy-Relevant Cell-Based Model of Tau Hyperphosphorylation and Oligomerization. *PLoS One* **2020**, *15*, e0224952, doi:10.1371/journal.pone.0224952.
198. Sohn, P.D.; Tracy, T.E.; Son, H.I.; Zhou, Y.; Leite, R.E.P.; Miller, B.L.; Seeley, W.W.; Grinberg, L.T.; Gan, L. Acetylated Tau Destabilizes the Cytoskeleton in the Axon Initial Segment and Is Mislocalized to the Somatodendritic Compartment. *Mol. Neurodegener.* **2016**, *11*, doi:10.1186/S13024-016-0109-0.
199. Thomas, E.; Zuniga, G.; Sun, W.; Frost, B.; Elizabeth Ochoa, et al. Awakening the Dark Side: Retrotransposon Activation in Neurodegenerative Disorders. *Curr. Opin. Neurobiol.* **2020**, *61*, 65–72.
200. Ramirez, P.; Zuniga, G.; Sun, W.; Beckmann, A.; Ochoa, E.; DeVos, S.L.; Hyman, B.; Chiu, G.; Roy, E.R.; Cao, W.; et al. Pathogenic Tau Accelerates Aging-Associated Activation of Transposable Elements in the Mouse Central Nervous System. *Prog. Neurobiol.* **2022**, *208*, 102181, doi:10.1016/J.PNEUROBIO.2021.102181.